

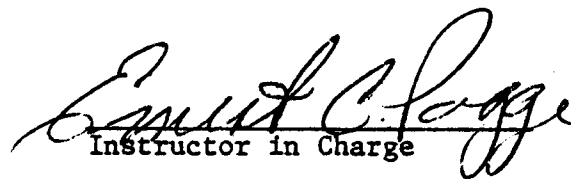
THE DISTRIBUTION AND MECHANISMS OF SALT WATER  
INTRUSION IN THE FRESH WATER AQUIFER AND IN  
RATTLESNAKE CREEK, STAFFORD COUNTY, KANSAS

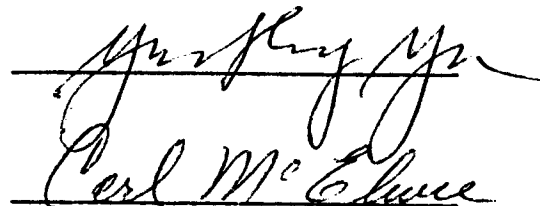
by

Patrick M. Cobb

B.S. in Geophysics, University of Kansas, 1976

Submitted to the Department of Civil  
Engineering and the Faculty of the  
Graduate School of the University of  
Kansas in partial fulfillment of the  
requirements for the degree of Master  
of Water Resources Science.

  
Instructor in Charge

  
\_\_\_\_\_

## TABLE OF CONTENTS

	Page
Table of Contents	ii
List of Figures	v
List of Figures Appearing with Appendices	vii
Chapter 1 -- Introduction	1
Overview	1
The origin of this investigation	2
Previous work	2
The generalized historical surface water quality map	6
The entry of low quality water into Rattlesnake Creek	8
Mechanisms of stream pollution described in the literature	10
Method of investigation	11
Observation well network	11
Collection of samples	12
Quarterly head measurements	13
Chapter 2 -- Geology and hydrology of Stafford County	16
Stratigraphy	16
Bedrock lithology	16
Bedrock configuration	17
The Permian aquifer	19
The Cretaceous aquitard	22
The Pleistocene aquifer	22
Chapter 3 -- The distribution of salt water in the aquifers	26
Preparation of cross section	26
Paleo drainage	27
Clay units	28
Discussion of east-west cross sections	31
Discussion of the north-south cross sections	32
Overview of cross sections	42
Chapter 4 -- Flow of groundwater in Stafford County	44
Potentiometric surfaces	44
Vertical components of flow	49
Hydraulic connection between the aquifers	50
Vertical flownets between recharge and discharge points	52
Isochlor distribution near site V	56
Chapter 5 -- The salt water upconing problem	59
The two fluid system	59
Conditions for the existence of an interface	60
Upconing of a horizontal interface	62

Chapter 6 -- The McWhorter approximation	65
Concepts and assumptions	65
Mathematical equations	67
Graphical solution	69
Application to Rattlesnake Creek problem	70
Determining physical parameters	70
Final transformation of the approximation	73
Chapter 7 -- Results of the McChorter method	76
Explanation of graphical computation	76
Stability of the solution for various densities at certain discharges	77
Chapter 8 -- Numerical simulation of the salt water interface	88
Methods of modeling the interface problem	88
An alternative model to the McWhorter approach	89
The accuracy of the approximation	93
Results of the numerical model study	94
Conclusions	100
Appendix I. Base flow gain in Rattlesnake Creek between Macksville and Zenith, Kansas	102
Appendix II. Lithologic logs	105
Appendix III. Construction of observation well sites	117
Appendix IV. Quarterly water levels and hydrographs	121
Appendix V. A general outline of the principles of the flow of viscuous fluids in porous media	126
Darcy's law	126
Fluid potential	127
Hydraulic conductivity	128
Spatial variation of permeability	130
Generalized Darcy flow	130
Range of validity of Darcy flow	131
The flow of fluids in extensive media	132
Special considerations	133
Flownets and potentiometric surfaces	133
Measuring and comparing hydraulic heads in extensive porous media	134
De termination of the direction of vertical flow between nearby wells	137
Appendix VI. A synopsis of the surficial and subcropping geology in Stafford County, Kansas, with a discussion of the occurrence of halite in the Permian "red beds"	143
Introduction	143
The Permian system	146
Stratigraphy of the Nippewalla	147
Harper sandstone	147
Salt Plain formation	148

Cedar Hills sandstone	148
Flower-pot shale	149
Blaine formation	149
Dog Creek shale	150
Whitehorse sandstone (Custerian Stage)	150
Pre-Nippewalla halite deposition	151
The occurrence of halite in the Nippwealla group	151
Harper - Salt Plain halite	152
The Flower-pot salt units	153
The Blaine salt	154
Atomic energy Commission Test core #5	154
The Harper - Salt Plain - Cedar Hills interval	154
The Flower-pot interval	155
The Blaine interval	155
The Cretaceous system	156
The Cheyenne sandstone	157
The Kiowa formation	157
The Dakota formation	158
The Quaternary system	158
Appendix VII. Development of the McWhorter approximation	161
Introduction	161
Development of the infinite series solution	161
Development of closed form solution	164
Application of boundary conditions	168
Interface position	170
Bibliography	172

## List of Figures

Figure	Title	Page
1	Location map of study area	3
2	Locations and values of historical chloride data used in this study and the traces of the cross sections	4
3	Historical distribution of chloride values on major surface drainages in Stafford County, Kansas	7
4	Partial chemical analyses of water from wells used in this study	14
5	Quality description of water based on specific conductance	15
6	Bedrock contour map of Stafford County and parts of Reno and Rice counties	18
7	Magnitude of laboratory coefficient of permeability for different classes of soils	21
8	Inferred major paleo drainage traces	29
9	Explanation of symbols used in the hydrologic cross sections in the following eight figures	33
10	Cross section C'-A' showing isochlors	34
11	Cross section E'-E showing isochlors	35
12	Cross section D'-D	36
13	Cross section A''-A	37
14	Cross section A-A'	38
15	Cross section B-B'	39
16	Cross section B-B''	40
17	Cross section C-C'	41
18	Potentiometric surface of the upper unconsolidated aquifer, May 1980	45
19	Potentiometric surface of the bedrock aquifer, May 1980	47
20	Indicated direction of vertical flow component across the bedrock surface	48

21	Approximate flow field in uniformly permeable material between the recharge distributed over the free surface and the valley sinks	54
22	Schematic of a water-coning system in a homogeneous medium	63
23	Equilibrium conditions along the axis of a water-coning system	63
24	McWhorter's approximation: flow toward a drain and flow toward an idealized drain	66
25	Geohydrologic cross section at site V on Rattlesnake Creek showing parameters used in the solution of the McWhorter approximation	71
26	Typical graphical solution for McWhorter approximation	79
27	Stable values of $\xi/m$ (unitless)	80
28	Water density versus dissolved chloride @ 24°C for water samples taken October, 1978	81
29	Calculated values for $\xi/m$ for various values of $m$ and the associated discharges	82
30	Idealization of the relative upward deflection of the interfaces bounding waters of uniform and nonuniform density below drains operating in fresh water	85
31	Definition sketch for determining $\sin \theta$ and $\cos \theta$ along the interface; definition sketch for determining the discharge $Q$ ; and schematic of the projection model	91
32	Tabulated values of stable $\xi/m$ obtained from the computer model	95
33	A comparison of $\xi/m$ values predicted by the models used in this study. $Q=1 \text{ ft}^2/\text{day}$ .	97

## List of Figures Appearing with Appendices

Figure	Title	Page
I-1a	Average annual rate of gain; water year 1978, Rattlesnake Creek, Macksville to Zenith, Kansas	104
I-1b	Six-year average rate of gain, Rattlesnake Creek, Macksville to Zenith, Kansas	104
III-1	Schematic of typical observation well nest	120
V-1	Schematic of the density corrected pure water head difference	140
V-2	Relative density of pure water ( $\rho$ ) versus temperature ( $^{\circ}\text{C}$ )	141
V-3	Contrast between calculated and measured pure water head differences of wells completed at different elevations in water	142
VI-1	Detailed stratigraphy most probably occurring in Stafford County	144
VII-1	Schematic for image well approximation in a half plane	162
VII-2	Boundary of a drain of radius $a$	162
VII-3	Image well approximation in the complex plane	164

## ABSTRACT

The portion of the Great Bend Prairie located to the east of U.S. Highway 281 is generally known to be underlain by salt water originating in the Permian bedrock. In cooperation with the Big Bend Groundwater Management District #5, the Kansas Geological Survey is establishing an extensive coarse grid of multiple level observation piezometer sites from which potentiometric head values and water quality samples may be obtained.

In this investigation, potentiometric head values, water quality data, and stratigraphic information collected in Stafford County during June, 1978 through May 1980 are combined with data from a previous study. Potentiometric head data is used to infer the horizontal flow direction in the Permian and Pleistocene aquifers, as well as the vertical direction of flow between the aquifers. The general distribution of salt water is depicted by isochlors on eight hydrologic cross sections, where it is noted that except near gaining streams, especially the Rattlesnake Creek, low quality water is confined to the deeper portions of the Pleistocene aquifer and the Permian aquifer.

The hypothesis of dynamic upconing is advanced to explain the distribution of chloride ions both in and beneath the major effluent streams. Two analytical models were used to test the hypothesis. The results indicated that except for very small values of stream gain and very large density contrasts unstable coning could be expected to occur beneath the major gaining streams. Exact quantities of salt water expected to enter the streams could not be ascertained because of the limitations of the models employed; however, it seems clear that the upconing mechanism can account for the observed salt water contamination.

## ACKNOWLEDGMENTS

I wish to express my thanks to the Kansas Geological Survey and the Big Bend Groundwater Management District #5 for the financial and material support which they provided to this endeavor throughout its duration.

Special thanks go to Dr. Carl McElwee, Geohydrology Section, who guided this work, both in theoretical and practical aspects and devoted much time to editing the text. Thanks also to to Richard Sloan, Manager, and the Board of Directors of the Big Bend Groundwater Management District #5 for the liaison which they provided with the local farmers and the actual foot work of arranging drilling sites. Appreciation is also expressed to Drs. Ernest C. Pogge and Y.S. Yu, both of the Department of Civil Engineering for their guidance in organizing the final report.

Drs. Donald Whittemore and Lawrence Hathaway provided assistance in collecting water samples and performed the analyses of the samples. Melvin Kleinschmidt, driller for the Survey, and his crew have given much field support over the summers, and their efforts are acknowledged.

I also want to thank the staff and students of the Geohydrology Section for the support they have given over the last two years. I want to thank Tom McClain, Anthony Severini, and Al Macfarlane who have given much support in the field and Jane Denne and Pam Watson who have provided editorial and graphical assistance. Finally, I want to thank Kaye Long, Geohydrology Section Secretary, for the long hours of typing and proofing which she has provided in completing this thesis.

Lastly, I wish to thank my parents, Jay and Pauline Cobb, for the encouragement they provided long distance from Boston.

## Chapter 1

### INTRODUCTION

#### Overview

This work is dedicated to improved understanding of the geohydrology of Stafford County, Kansas, especially as it pertains to the sources and distribution of low quality saline waters, long known to exist at depth in the subsurface. In order to accomplish this goal, extensive drilling of permanent multi-level observation wells (piezometers) was undertaken. Three-dimensional water quality data obtained from these wells has been combined with similar data from previous studies; and, from these a general, although necessarily incomplete, multi-dimensional distribution of water quality is inferred on the basis of chloride distribution. Water level data, now being taken on a quarterly basis at the multi piezometer sites are used to estimate the hydraulic connection between the Permian/Cretaceous bedrock and the unconsolidated Pleistocene overburden. An attempt is also made to relate local head gradients to regional flow patterns and thus demonstrate the hydrologic intricacies of the region. Finally, the water quality in Rattlesnake Creek is examined in its relationship to the low quality water distribution in the unconsolidated aquifer. A hydrodynamic upconing model is suggested as the driving mechanism for the entry of low quality water into the creek. Evidence is pointed out which indicates that this mechanism is equally applicable to other streams in the area. Bedrock data from the drill holes is used to update the most recent bedrock map. No attempt is made to interpret the regional stratigraphy.

## The Origin of This Investigation

In order to acquire information to determine the influx of low quality water from the Permian bedrock in the Great Bend Prairie, it was necessary to formulate an extensive drilling program. Since such a project was of great interest to the Big Bend Groundwater Management District #5 (GWMD #5), a cooperative program was established between that agency and the Kansas Geological Survey (KGS). The original plan was to concentrate upon the Cedar Hills Sandstone (suggested by Fader and Stullken, 1978). The final plan was to investigate and collect data for a large part of GWMD #5, and hence, a major portion of the eastern half of the Great Bend Prairie (Fig. 1).

The cooperative plan called for installation of a series of observation wells at sites spread in a regular six-mile square grid pattern over the eastern portion of GWMD #5. Each site was to have a minimum of two wells, one completed in the Permian bedrock, and at least one completed in the unconsolidated material. As of July 1, 1980 11 sites are in progress or have been completed, most in Stafford County, and the remainder just over the Stafford-Reno county line. Figure 2 depicts the location of these sites, as well as all other available historical quality data and the traces of cross sections referred to later in the text. This report is centered on the data collected in Stafford County and constitutes the pilot study for the project.

### Previous Work

This study represents the first attempt to gain a detailed understanding of the sources and distribution of low quality groundwater in

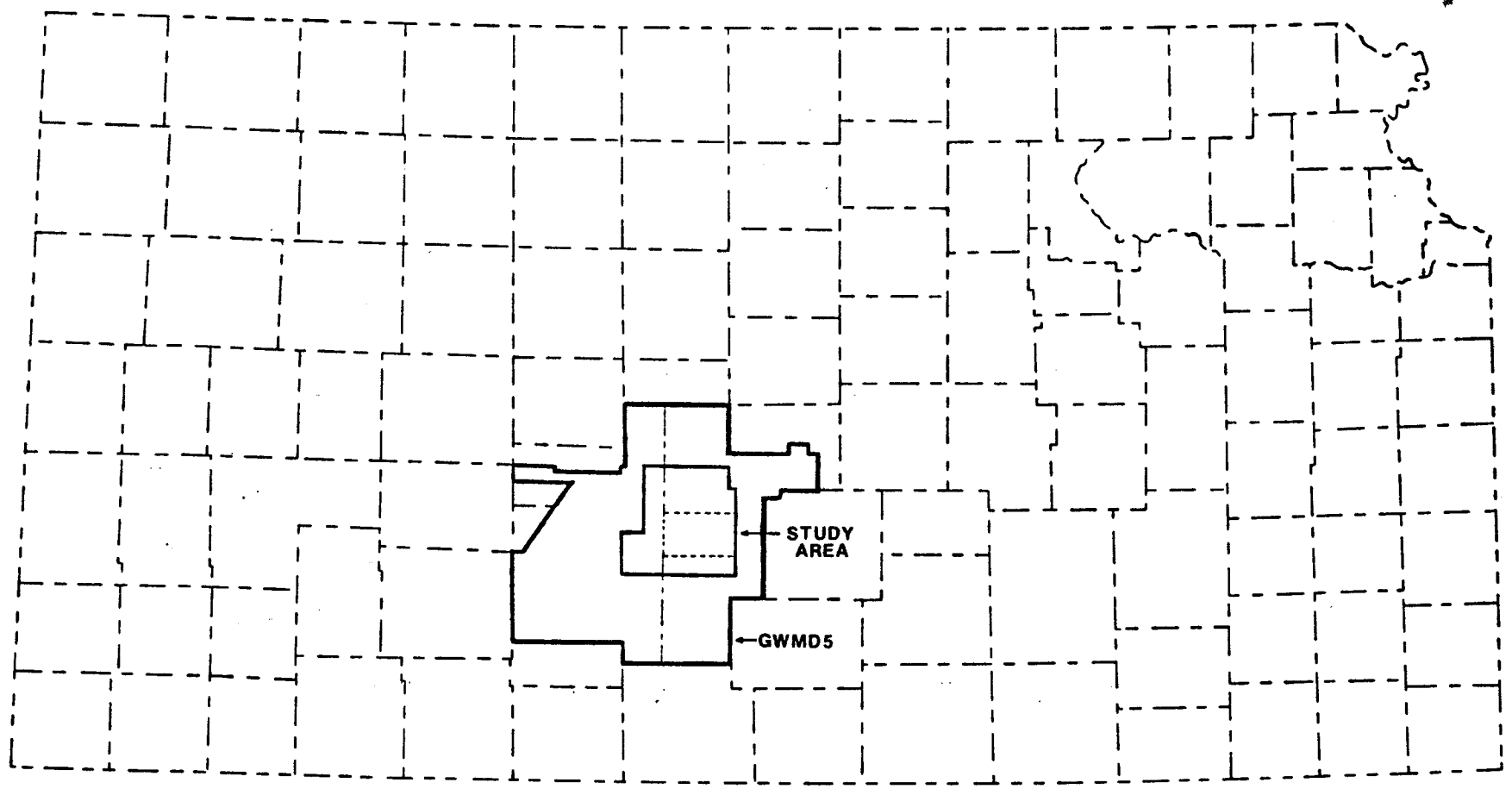
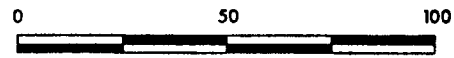
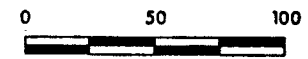


Figure 1. Location Map of Study Area

- boundary or area where major new drilling occurred
- Western Boundary -- Coop Study Area



Scale in miles



Scale in kilometers

Figure 2. Locations of historical chloride data and trace of cross sections for this study.

VII site number of KGS-GWMD#5

⊙ KGS-GWMD#5 1978, 1979

□ Fader and Stullken, 1973

△ Latta, 1942, 1944

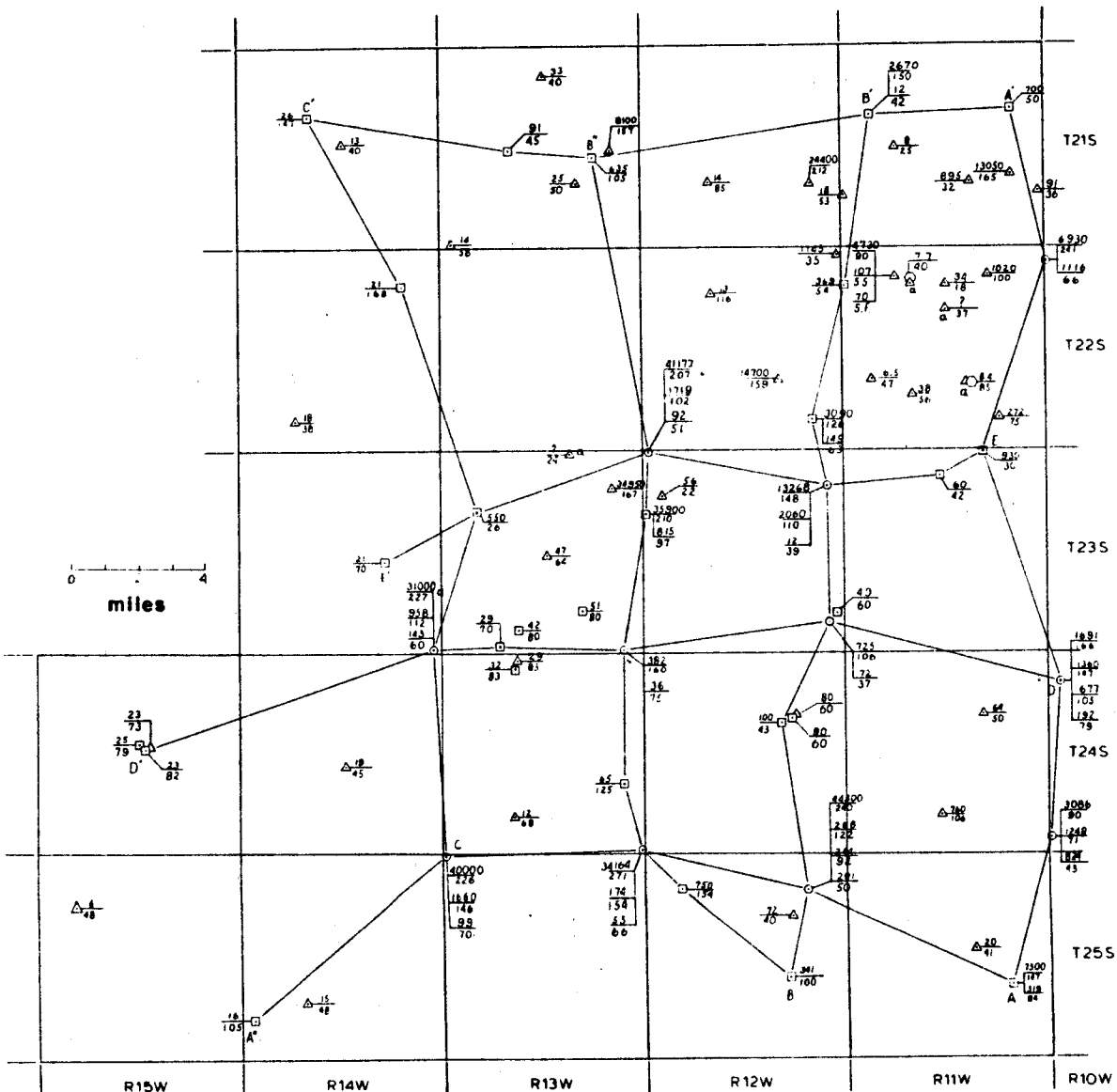
⬡ Hathaway, 1977

⊖ Multiple completion

A — A' Trace of cross section

⊖ chloride (ppm)  
depth (ft)  
single completion

α indicates flowing Artesian well



Stafford County, Kansas. It is a logical progression from previous work carried out in Stafford County and the surrounding region.

The previous work on Stafford County, Kansas was described by Latta (1950). His report is a detailed reconnaissance of the geology, surface hydrology, climatology, and groundwater quality and availability, based on the best information of the time. The geohydrology of the other counties comprising the Great Bend Prairie have been studied over the last 30 years. These investigations are by Latta (1947), McLaughlin (1949), Fent (1950), Bayne (1950), Layton and Berry (1973), and Bayne and Ward (1947).

Fader and Stullken (1978) studied the irrigation situation in the Great Bend Prairie and present a series of maps describing the bedrock topography and the contacts between the subcropping stratigraphic units. A regional water table (December, 1973) and a delineation of the areal distribution of irrigation water quality are described. A regional hydrologic mass balance is also estimated. A separate report was also published (Stullken and Fader, 1976) which includes an inventory of irrigation wells, water quality analyses, and test hole logs. A sparse net of multiple level water samples was collected during the course of that study.

A separate study of irrigation water quality was carried out by Hathaway and others (1978). The results were published in a series of figures depicting the distribution of various irrigation water hazards based on soil and water type combinations.

## The Generalized Historical Surface Water Quality Map

Figure 3 depicts various point chloride values on the major streams in Stafford County. These values have been derived principally in two ways. First, from time averaged values at established observation stations and second, from sampling runs on various streams carried out at many points on the streams over a short period of time. These "seepage runs," as they are termed, are generally conducted to sample base flow only. Stramel (1967) catalogs two seepage runs on Rattlesnake Creek (carried out June 6, 1966 and October 21, 1966) as well as some time series data for various points on that stream, such as the U.S.G.S. Gage Stations at Raymond, Hudson, and Macksville. Latta (1950) catalogs a sampling run along the Rattlesnake Creek and Big Salt Marsh on October 2, 1942. The most recent such survey was conducted by Whittemore (unpublished) in October, 1978.

Other time series data has been collected from Water Resources Data for Kansas (Annual USGS-KGS publication) for Peace Creek and the North Fork of the Ninnescah River which have been collected at irregular intervals over the years. Averages of these data have been plotted on a base map and values of the inferred long-term average chloride concentration are shown on the streams where sufficient data exists. It should be noted here that the chloride values shown in Peace Creek and the North Fork of the Ninnescah River are derived from stations several miles east of the Stafford-Reno County line, and may therefore be higher than actual values on these streams in Stafford County. The product of compiling this information is a generalized historical quality map (Fig. 3) of the major streams in Stafford County. Values of chloride shown in streams on the cross sections are interpolated from this map. Rattle-



snake Creek appears to gain a considerable chloride load after turning to the east in central Stafford County.

Some explanation was not included on Figure 3 due to lack of space. Tabulated here are the Station codes for the gaging stations shown on the map.

H	RSC	near Hudson
HV	RSC	near Haviland
M	RSC	near Macksville
R	RSC	near Raymond
S	NFNR	near Sylvia
SC	PC	Near Sylvia
W	WHC	near St. John
Z	RSC	near Zenith

#### The Entry of Low Quality Water Into Rattlesnake Creek

Historically, there has been a quality problem in the lower reaches of Rattlesnake Creek. Stramel (1967) indicates that the creek water is of good quality to about one mile east of U.S. Highway 281. The Generalized Historical Surface Water Quality Map (see Fig. 3) discussed previously, indicated that the water quality in the creek deteriorates quite rapidly as it turns to the east, after passing the confluence of Wild Horse Creek. Over roughly 5.5 miles of channel the concentration of chloride ions increases from 75 mg/l to about 1,200 mg/l. The map indicates a slight improvement and then deterioration again at Little Salt Marsh. This deterioration continues past Big Salt Marsh. The discharge at Raymond shows a long-term average of 1,200 mg/l chloride ion.

Rattlesnake Creek is described by Latta (1950) as a meandering stream which has reached temporary base level. Its average gradient above St. John is about seven feet per mile, while the gradient below that town is about four feet per mile. Stramel (1967) describes it as a low run-off stream and not flashy as are many Kansas streams. Fader and Stullken (1978) analyzed 11 years of discharge at the Raymond gage, which is near the mouth of Rattlesnake Creek, and computed an estimated mean base flow of  $22.1 \text{ ft}^3/\text{sec}$  or 16,000 acre-ft/year. For this investigation five and one-half years of discharge records were analyzed for the gages at Macksville and Zenith (see Appendix I). The locations of these stations may be found on Figure 3. It was determined that over the 66.2 miles of channel between these sites, the stream gained an average of  $22.86 \text{ ft}^3/\text{sec}$  or 16,550 acre-ft/year. The figures quoted here are averages over the indicated periods of record. The fact that the periods of average are different is of some consequence, and may account for the apparent problem that the change in base flow accumulated between Macksville and Zenith is greater than the average annual base flow at Raymond. The point to be made is that a considerable amount of the base flow is derived in Stafford County.

The literature is not totally consistent in declaring which portions of Rattlesnake Creek are influent or effluent. Stramel (1967) declares that the creek has been "for the most part, a perennial stream." Latta (1950) is more precise, indicating that the creek in Stafford County is above the water table in the upper part of its course and below the water table in the lower part. This is somewhat clarified later when Latta points out that Rattlesnake Creek is perennial from a few miles above St. John to where it turns north at the Little Salt

Marsh; elsewhere it is an intermittent stream. In other words, the creek is an effluent stream in its course through central and east-central Stafford County. In other places, it is at least periodically influent. The analysis for stream gain indicates that between Macksville and Zenith the stream may be influent for short periods of time in the late summer, but for the time this remains an unsubstantiated speculation.

Latta (1950, Plate 1) and Fader and Stullken (1978, Plate 3) both map the potentiometric surface in Stafford County. As was pointed out earlier, these maps are similar even though the data is separated by 30 years. Both these maps depict Rattlesnake Creek as a gaining stream throughout most of its channel in Stafford County. Both maps also agree that the potentiometric contours of the water table converge most drastically upon the stream over the reach from just west of St. John to the vicinity of Hudson. In this reach the stream crosses the subcropping Permian/Cretaceous unconformity and simultaneously undergoes a rapid deterioration of quality.

#### Mechanisms of Stream Pollution Described in the Literature

Latta (1950) does not discuss a mechanism for carrying saltwater from bedrock into Rattlesnake Creek. No discussion of this process occurs in Fader and Stullken (1978). Stramel (1967) also neglects this problem. Whittemore (1978), in discussing variations in river water quality in Kansas streams, alludes to groundwater recharge providing hydrostatic pressure to "flush" out greater amounts of deeper more saline groundwater under the river. Layton and Berry (1973), in discussing salt pollution in South Fork Ninnescah River near Cairo, state

that low quality water is discharged into the lower unconsolidated Holderidge formation which is under hydraulic pressure. Water flows from this formation, into the alluvium and then on into the stream. It is noted that streamflow takes a sharp increase at Cairo.

None of these explanations delve into the exact mechanics of the displacement of the salt water upward and into a stream. Whittemore's mechanism could possibly involve elements of mechanical dispersion and a "piston" type convective displacement. Layton and Berry apparently rely upon dispersive mixing in the lower unconsolidated formation, followed by upward movement due to an over pressure existing in the formation. This water is apparently then flushed into the stream by the normal hydraulic gradient convergent upon the stream. The concern of this investigation is to attempt to relate the chloride distribution near streams indicated in the field reconnaissance and in the historical stream quality data.

#### Method of Investigation

##### Observation Well Network

Field work for this investigation was conducted in the summer and fall of 1978 and 1979. This work consisted principally of constructing the observation wells and sampling them. At each site the first hole was drilled into bedrock. A careful cuttings log was kept of this hole. A gamma ray log was also obtained. If the wall appeared to be stable, an electrical log (spontaneous potential - resistivity) was run in the uncased hole. These data were used to construct a lithologic log for each drill site (Appendix II). The sample log, gamma ray, and electric log data were used to determine completion depths for subsequently

drilled shallow test holes completed in the Pleistocene aquifer. Water samples from the wells completed in the summer of 1978 were collected in October 1978, whereas water samples from the wells completed in the summer of 1979 were collected in November 1979. Quarterly water level measurements were initiated on the wells a few months after completion so that the effects of construction on water levels were minimized.

An average of three wells were constructed per observation site. The typical configuration of screen placement (Appendix III) is to screen the deep well in the Permian bedrock, the second well in the basal unconsolidated material and the third well in the most permeable unit above the basal unit. At two sites (II and III) only two wells were completed (see Figure 2 for site number location). At site II only one permeable unit above the bedrock was noted in the well log. At site III sand bridging caused the screen to be set both in the bedrock and in the unconsolidated. At two other sites (VIII and X), four wells were installed because the drilling log and gamma ray log indicated possible confining layers.

#### Collection of Samples

In the fall of 1978 and 1979 wells drilled during the respective summer months were sampled. These samples were collected under the supervision of Dr. Don Whittemore, Kansas Geological Survey, and analyzed by the Geochemistry Section. On the recommendation of Dr. Larry Hathaway, Kansas Geological Survey, large diameter wells were installed so that electric submersible pumps could be used to sample the formations. Several advantages accrue from this strategy. First, additional flushing of a new well is accomplished, tending to remove considerable

quantities of fine materials from the gravel packs. Secondly, and most important, several casing volumes of water are quickly removable so that the final sample is native formation water not effected by the well installation. Complete analyses were performed on all samples. Figure 4 is a tabulation of portions of the data pertinent to this study. A complete chemical analysis of each well is on file at the Kansas Geological Survey (Hathaway, Whittemore, and Cobb, 1980). In order to impose a meaningful relationship between quality descriptions such as "fresh" or "moderately saline," a table (Fig. 5) is included which assigns quality descriptors to various ranges of Specific Conductivity. Some samples were also checked for specific ion ratios in order to check for oil field brine problems (Whittemore, 1980).

#### Quarterly Head Measurements

Since October 1978, head measurements have been collected for all completed wells on more or less a quarterly basis (Appendix IV). These measurements are recorded as measured in the field, but are converted to freshwater equivalents, as described in Appendix V. Later in the text more discussion will be directed toward this data.

Figure 4 . Partial Well Analyses from Investigation

Well #	Cl <sup>-</sup> (ppm)	Density (gm/ml)	@ Temp (°C)	SpCd (µmho)	@ Temp (°C)	Well #	Cl <sup>-</sup> (ppm)	Density (gm/ml)	A Temp (°C)	SpCd (µmho)	@ Temp (°C)
<sup>1</sup> I-1	13268	1.014	24.0	32700	15.3	<sup>1</sup> VII-1	34164	1.044	24.0	73200	15.2
<sup>1</sup> I-2	2060	1.000	24.0	6160	15.0	<sup>1</sup> VII-2	174	0.999	24.0	1020	15.2
<sup>1</sup> I-3	12	0.997	24.0	400	14.3	<sup>1</sup> VII-3	53	0.998	24.0	648	15.0
<sup>1</sup> II-1	725	0.998	24.0	2820	15.2	<sup>2</sup> VIII-1	44300	1.056	23.4	108000	15.7
<sup>1</sup> II-2	72	0.998	24.0	702	14.4	<sup>2</sup> VIII-2	288	0.999	23.4	1450	15.7
<sup>1</sup> III-1	382	0.998	24.0	1630	15.3	<sup>2</sup> VIII-3	244	0.998	23.4	1290	15.5
<sup>1</sup> III-2	36	0.998	24.0	510	15.2	<sup>2</sup> VIII-4	201	0.999	23.4	1145	14.8
<sup>1</sup> IV-1	31000	1.036	24.0	64000	16.5	<sup>2</sup> IX-1	3086	1.003	23.4	10000	-
<sup>1</sup> IV-2	958	0.999	24.0	3500	16.0	<sup>2</sup> IX-2	1248	1.000	23.4	4460	14.8
<sup>1</sup> IV-3	143	0.998	24.0	975	16.0	<sup>2</sup> IX-3	824	0.999	23.4	3170	14.7
<sup>1</sup> V-1	41477	1.049	24.0	83800	16.0	<sup>2</sup> X-1	1691	1.001	21.8	6000	16.0
<sup>1</sup> V-2	21719	1.026	24.0	52300	15.9	<sup>2</sup> X-2	1360	1.000	22.9	4900	16.1
<sup>1</sup> V-3	92	0.998	24.0	700	15.0	<sup>2</sup> X-3	677	1.000	21.8	2700	15.6
<sup>1</sup> VI-1	40000	1.049	24.0	82500	16.1	<sup>2</sup> X-4	192	0.998	22.9	1020	15.3
<sup>1</sup> VI-2	1661	1.000	24.0	6000	17.0	<sup>2</sup> XI-1	6930	1.008	22.9	21300	15.9
<sup>1</sup> VI-3	99	0.998	24.0	710	15.8	<sup>2</sup> XI-3	1116	1.000	22.8	4000	15.0

1) indicates wells sampled October, 1978

2) indicates wells sampled October-November, 1979

Figure 5 . Quality Description based on Specific Conductance

Quality Description	Specific Conductance ( $\mu\text{mhos}$ at $25^{\circ}\text{C}$ )
Fresh	< 1400
Slightly Saline	1400 - 4000
Moderately Saline	4000 - 14000
Very Saline	14000 - 50000
Briney	> 50000

(after O'Connor, 1971)

## Chapter 2

### GEOLOGY AND HYDROLOGY OF STAFFORD COUNTY

#### Stratigraphy

The generalized geology of Stafford County has been previously described (Latta, 1950). The simplified stratigraphic column employed by Fader and Stullken (1978) is more suited to the needs of the hydrologist, and is used in this discussion when referring to lithologic units. A complete summary of the stratigraphic units in Stafford County, as well as a detailed stratigraphic section, from the Recent Stage of the Quaternary System to the Cimarronian Stage of Lower Permian Series, Permian System (Zeller, 1968) is described in Appendix VI. The principle contributions of the drilling done in this investigation are 1) an addition to the knowledge of the bedrock lithology; and 2) an enhanced interpretation of the bedrock surface configuration.

#### Bedrock Lithology

In an attempt to enhance the identification of formations and formation boundaries prior to drilling and installing test wells for water quality and head studies, a structural cross-section was constructed, for study purposes only, from wire line geophysical logs obtained from the Log Library at the Kansas Geological Survey. This cross section extends from near Kinsley, Kansas to just east of Stafford, Kansas, running along the trace of U.S. 50. Careful examination of the logs show that in Stafford County, between the towns of Macksville and St. John, the lithology of the Cedar Hills Sandstone becomes nearly undifferentiable from the lower Salt Plain - Harper Sandstone

formation complex. Several authors (Fader and Stullken, 1978; Merriam, 1963; Campbell, 1963) show a well defined contact between the Cedar Hills Sandstone and the Salt Plain formation. The evidence gained from examination of oil test logs and test drilling samples does not substantiate the assumption that any unit maintains a uniformly differentiable lithology over large areal extents within the study area.

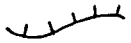
Examination of the lithologic sample logs prepared for each site (Appendix II) indicates that each deep well was completed in fine to very fine grained consolidated material (mudstone or siltstone), generally red or gray. Drill cuttings, but no cores, were recovered from these holes. Virtually no stratification was observed, a feature generally observed in shale. Virtually no clean sandstone of any grain size was identified in the cuttings from the redbed units. If sandstone was drilled through, but was poorly cemented, it is possible that the sand would not be caught in the sample screen. However, the gamma ray and electrical logs do not indicate clean sand bodies of any appreciable thickness in the bedrock. It can be concluded that, if sandstone exists in any large quantity, it is very fine grained and contains large quantities of finer interstitial materials. This has hydrologic implications which will be addressed later.

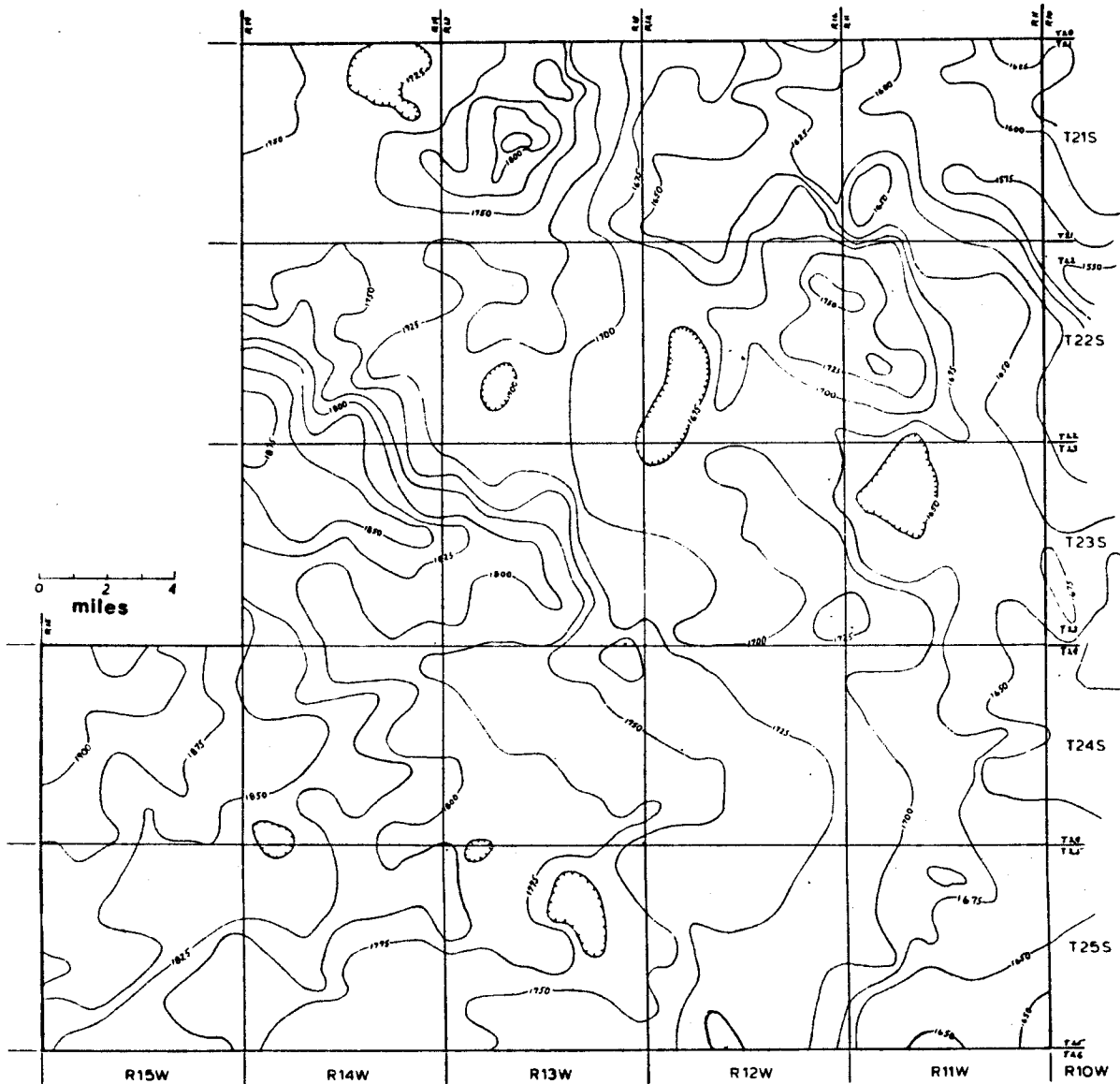
#### Bedrock Configuration

A bedrock map was prepared for Stafford County (Fig. 6). Original data used in the preparation of the bedrock map (Plate 1 in Fader and Stullken, 1978) was obtained from Mr. Lloyd Stullken, USGS, Garden City, Kansas. The Stafford County data were enhanced with the bedrock elevations indicated at the 11 drill sites (see Fig. 2). Elevations were

Figure 6. Bedrock contour map of Stafford County and parts of Rice and Reno counties.

—1800— Contour of equal elevation  
(feet above mean sea level)  
5 foot contour interval

 Indicates depression in bedrock



calculated by locating the drill site on a USGS 7.5-minute topographic map, interpolating the elevation of the land surface from the map, and finally subtracting the indicated depth to bedrock.

The enhanced data was contoured using 25 foot intervals. This results in a more detailed representation of some of the drainage features than is on the Fader and Stullken map. Only a few significant changes resulted from the new data, as most of it was conformal with the previous data. The 1675' closure near sections 30 and 31, T22S, R11W in Figure 6 was interpreted from the bedrock depth at site V (see Fig. 2) and some uncounted data from the original data base. The saddle feature just north of sections 1 and 2, T22S, R13W is interpreted based on site II.

#### The Permian Aquifer

The groundwater system in Stafford County may be described as a system of two aquifers. The deeper aquifer underlying Stafford County is the bedrock aquifer commonly known as the Permian red beds (Swineford, 1955). In eastern Stafford County these units subcrop beneath the unconsolidated Pleistocene deposits, whereas in the western part of the county they are unconformably overlain by the Undifferentiated Lower Cretaceous formation (convenient classification from Fader and Stullken, 1978).

The lack of significant evidence for extensive sandstone units in the Cedar Hills Sandstone found by this author and other investigators who have studied sample logs of the subcropped Permian units (Stullken and Fader, 1976; Latta, 1950) lead to the conclusion that, at least in Stafford County near the Cretaceous-Permian contact, the red beds are hydrologically undifferentiated. Sandstone beds may exist which serve

to improve the permeability, locally, but no substantial evidence exists that in this area large tabular units in the Cedar Hills Sandstone make it a significantly better aquifer than the Salt Plains Formation or the Harper Sandstone. Several more test holes will be drilled in 1980 in the subcrops described as Cedar Hills in Fader and Stullken (1978, Plate 1) which should better define the lithologies. For the remainder of this discussion, the term red beds will mean the Permian aquifer.

No Permian bedrock cores have been obtained or studied from Stafford County as of this writing. Because of this, no laboratory studies have been performed to determine the permeability or storage coefficient of this aquifer (Bear, 1972). The only recourse then is to refer to tables prepared by other researchers (Todd, 1959, for example), which relate particle size or soil type to a laboratory value of the coefficient of permeability. Todd's table (Fig. 7) indicates that the size range of particles retrieved in the cuttings from the Permian units correspond to a "poor aquifer." The range of  $K$  for this group is  $1 \times 10^1$  to  $1 \times 10^{-3}$  (gal/day)/ft<sup>2</sup> or 1.3 - .00013 ft/day. These values are subject to change as variations in the chemical quality of the water produces changes in density and viscosity (see Appendix V). Various methods are available to determine the transmissivity of a "tight" unit from a single well. They are typically described as slug tests. The more simplistic methods (Ferris and Knowles, 1954) will give values of transmissivity while more complex methods (Cooper, Bredehoeft and Papadopoulos, 1967 and 1973) give  $T$  and  $S$  values.

Figure 7 -- Magnitude of laboratory coefficient of permeability for different classes of soils

Soil Class	Clean Gravel	Clean sands; mixtures of clean sand and gravels	Very fine sands; silts; mixtures of sand, silt, and clay; glacial till; stratified clays; etc.	Unweathered clays							
Flow characteristics	Good aquifers		Poor aquifers	Impervious							
	10 <sup>6</sup>	10 <sup>5</sup>	10 <sup>4</sup>	10 <sup>3</sup>	10 <sup>2</sup>	10	1	10 <sup>-1</sup>	10 <sup>-2</sup>	10 <sup>-3</sup>	10 <sup>-4</sup>
	Laboratory coefficient of permeability, K <sub>s</sub> , gal/day/ft <sup>2</sup>										

(from Todd, 1959)

### The Cretaceous Aquitard

The Undifferentiated Lower Cretaceous (Fader and Stullken, 1978) units overlie the Permian red beds in the western part of Stafford County. This unit consists of interbedded sandstones and shales and is generally considered the upper confining layer for the red beds. At site IV in the deep well completed below the Cretaceous formation, the static water level is about one foot above land surface. More evidence will be presented later from well hydrographs which tend to support this view. On the other hand, water quality information from two sites indicate that low quality water, probably from the Cretaceous units, is leaking upward into the Undifferentiated Pleistocene aquifer. This may indicate that there are isolated lenses of low quality water in the Lower Cretaceous. Latta (1950) describes a test hole drilled into the Kiowa Shale in Barton County which flowed salt water (28,300 ppm  $\text{Cl}^-$ ). A test hole at site IV penetrated the Undifferentiated Lower Cretaceous, but no well is screened in that unit. In this investigation the Undifferentiated Lower Cretaceous will not be considered as a significant aquifer. (In the western part of Stafford County where the Cedar Hills Sandstone is better defined, there may be locations where it is hydraulically connected with the Cheyenne Sandstone (Don Ubal, KDH&E, personal communication, 1979). Such occurrences add complexity to the regional aquifer which are not addressable here.)

### The Pleistocene Aquifer

The unconsolidated aquifer, conveniently described as the Undifferentiated Pleistocene deposits (Stullken and Fader, 1976), consists of interbedded gravels, sands, silts, and clays; including all possible

mixtures of these constituents. These deposits are originally due to blanket deposition by meandering streams in the glacial periods of the Pleistocene (Fent, 1950b) and unconformably overlay the Permian and Cretaceous units described above. In many areas of Stafford County these deposits are topped with wind blown sand dunes which have become stabilized and have developed soil profiles (Latta, 1950). Exceptions exist along Rattlesnake Creek and South Fork Ninnescah River where removal of the dunes has occurred.

Examination of the lithologic columns (Appendix II) reveals a great diversity of depositional patterns. There are, however, some dominant characteristics which allow the sites to be grouped in several categories. Well sites near major surface drainage features fall into two categories. Those directly in the active stream valleys tend to have high percentages of sand size and larger particles dominating in the strata above bedrock. Sites I and IX are extremes in this category. Virtually all major traces of silt size particles and smaller are absent. These deposits have probably been reworked by the streams. Such action is suggested by Latta (1950). Sites II, IV, V, and XI are also near streams, but apparently in areas not subject to such thorough reworking as noted above. These sites exhibit about 50% of their unconsolidated thicknesses as sand size and larger particles. Site IV is a notable exception to this observation. It has about 40% sand size and larger particles. These terrace deposits along Rattlesnake Creek have probably not been reworked to quite the extent as the despoits along active streams at other test hole locations.

Sites III, VI, VII, VIII, and X are all distant from major active drainage systems and seem to have a high percentage of fine particles (silt size or less); about 60%. They are probably more representative

of the original older Pleistocene deposits.

Sample logs at most of the sites exhibit to some degree a well defined fairly clean coarse basal sediment in the coarse sand to fine gravel range having thickness ranges from about 30 feet at sites I and XI which are in well defined paleo channels, to about 5 feet at locations II van VIII. These sand and gravel deposits probably correspond to the Nebraskan age deposits described by Fent (1950b). At sites V and IX, these sand and gravel deposits are not found. They were either not deposited, or were deposited and then locally removed at a later time. The cyclical finer and coarser units are described as synchronous with various glacial events (see Appendix VI). The typical lithologic sequence contains two or more clean gravel units which are high yielding aquifers. The intervening beds in general are probably capable of acting as semiconfining units, at least locally, since the areal extent of any single system of cyclical strata is not well defined. O'Connor (personal communication) does not believe any single unit is extensive. The Pleistocene deposits were laid down chiefly in broad meandering streams (Fent, 1950b), rather than in extensive flat lakes (a possible exception being in the salt marsh area) and so could not be expected to have extensive homogeneous deposition. Lateral permeability is probably better developed within any unit than vertical permeability due to laminar deposition by the streams. Hydrographs of shallow and deep wells at these sites (Appendix IV) indicate some rather consistent seasonal variations between potentiometric heads in the unconsolidated units.

In order to obtain an estimate of the order of magnitude of the hydraulic conductivity of the unconsolidated material in Stafford County a pump test was conducted on June 20, 1979 at a well owned by Mr. R.D.

Bookstore of rural St. John, Kansas. The well was located at the center of SW $\frac{1}{4}$  Section 29, T24S, R14W. The test lasted only 357 minutes owing to failure of the pump. The well was 96 feet deep and completely penetrated the Pleistocene aquifer. Drawdown and recovery tests were performed and analysis of data was by the Jacob-Cooper method, Theis Recovery method, and Theis Curve Matching method. A new numerical method of computer curve fitting was also applied (McElwee, 1980). The data for this test and the analyses may be found in Cobb (1979). The hydraulic conductivity was computed to be 72 ft/day and the specific yield to be .025. Had the test continued, the value of specific yield would probably have increased.

## Chapter 3

### THE DISTRIBUTION OF SALT WATER IN THE AQUIFERS

#### Preparation of Cross Sections

The focal point of this investigation is to describe and explain the distribution of salt water in the consolidated and unconsolidated aquifers underlying the Great Bend Prairie in Stafford County. To that end, eight cross sections of the region were prepared: four in the north-south direction and four in the east-west direction. These cross sections portray in as much detail as possible the configurations of the land surface, the phreatic surface of the unconsolidated aquifer, and the bedrock surface. The vertical exaggeration is about 106 times.

The details of the land surface were derived from topographic sheets published by the United States Geological Survey. Stream beds are included, although the dimensions may be slightly exaggerated.

The phreatic surface was derived from Plate 3 of Fader and Stullken (1978). This map portrays the potentiometric surface of the unconsolidated aquifer as of December, 1973. These authors state that "owing to appreciable recharge from the above-normal precipitation in 1973, the potentiometric surface . . . was higher than can be expected in most future years of near- and below-normal precipitation" (p. 8). A map of the water table in Stafford County prepared for the period 1942-1944 (Latta, 1950) shows a configuration which closely resembles the map cited above. This map dates from a period prior to extensive development of irrigation in Stafford County. The criticisms which may legitimately be made of Latta's map are that the measurements were not made over a short span of time and that there is a lack of control in some

locales. However, the close similarity between these maps demonstrates a degree of hydrologic stability in the area.

The bedrock surface was prepared from the bedrock topographic map previously described (Fig. 6). Some of the features depicted are based only on limited data and so may be questionable. However, it is the broad picture of the bedrock which is of principal interest, especially the details of the pre-Quaternary paleo drainage.

The distribution of salt water is depicted by the positions of isochlors portrayed on these cross sections (Figs. 10-17). Figure 9 explains the symbols found on the cross sections. Control is indicated by vertical lines representing sites of known quality analysis. These may be single or multiple level sites. In order to obtain sufficient coverage for these cross sections the multiple level data collected for this investigation (1978, 1979) was combined with certain data from Fader and Stullken (1973). Although there may be legitimate criticism for combining data from three separate (though not broadly spaced) sampling periods, we have chosen to do so here on the grounds that it is the trends of the isochlors which are important in the broad scheme and not the precise values of the isochlors. Data collected by Latta (1950) was almost totally excluded from these cross sections. This was done principally to avoid the above posed objection. The few points of Latta's quality data used were in places where trends already were established.

#### Paleo Drainage

Before discussing the hydrologic cross sections, some discussion of the bedrock topography and the implied paleo drainage is in order.

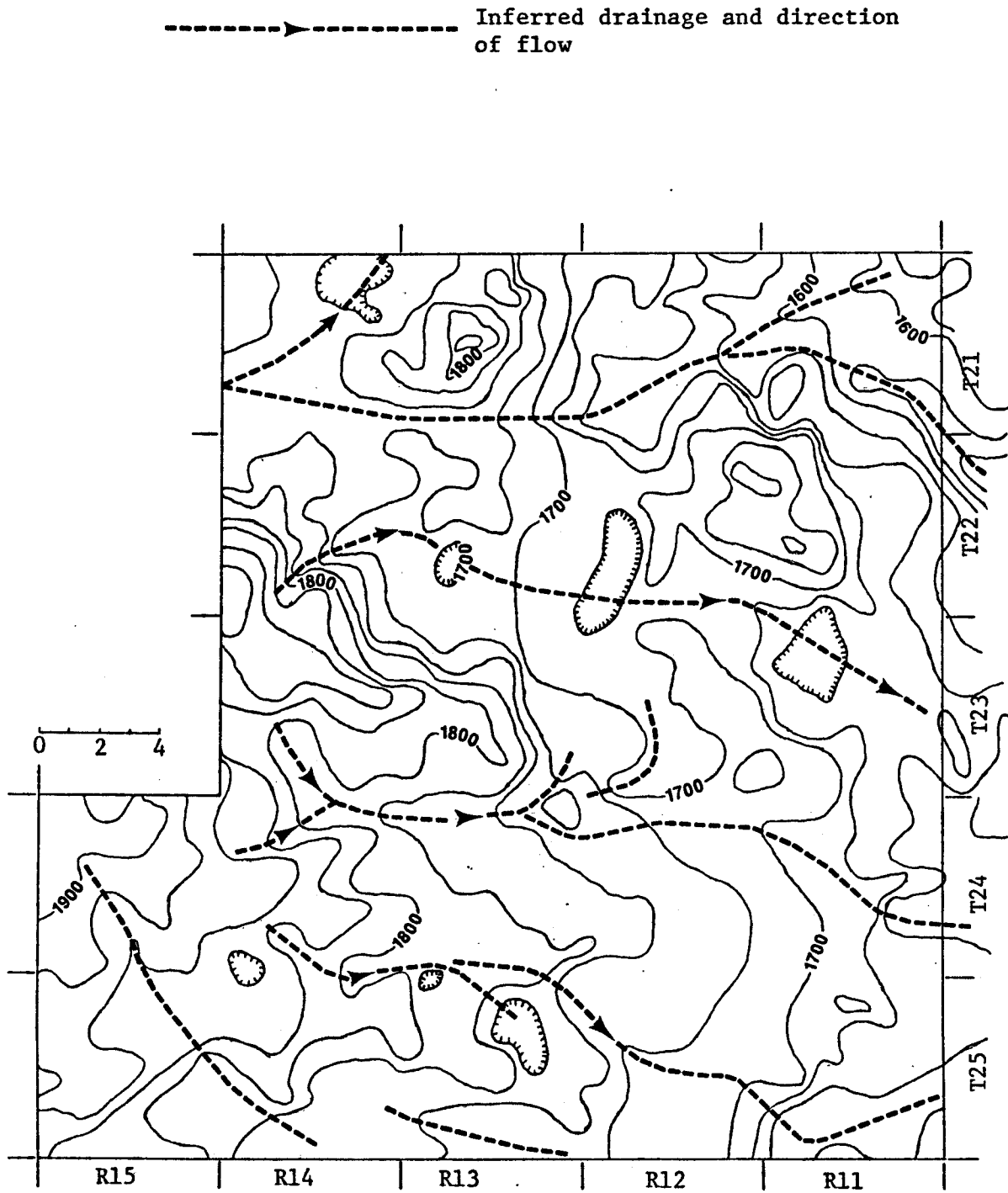
Principal drainage as depicted in Figure 8 appears to trend generally northwest to southeast. In some places lateral channels take on a north-south to northeast-southwest orientation. Bedrock channels are better defined in northern Stafford County. Two principle bedrock channels traverse this area. A deep drainage feature is seen to curve across the northeastern corner of the County, dropping from an elevation of 1,725 feet in the north-central section of the County to one of 1,550 feet as it crosses the County line. A second channel preceeds from the west, through central and east-central Stafford County and then moves off to the southeast. It grades from 1,725 feet to 1,650 feet over this path. This drainage also receives some contribution from the south. This second channel is not as well defined as the drainage to the north. There are two large closed depressions in this southern system.

Channelization is not so pronounced in southern Stafford County. Topography relief tends to be less drastic than in the north. Hence, the drainage tends to occur as broad valleys. Two main channels trending southeast appear to be separated by a broad bedrock high which may be a flow divide between them. Several smaller features occur south of this system, but their extent to the south and east is not defined.

#### Clay Units

The cross sections do not depict the clay dominated strata which occur in the stratigraphy. Occurrence of these units may be important in controlling the distribution of salt water (Fader and Stullken, 1978). Drilling data corroberates this view at certain sites. At sites IV and VI for instance, differences in chloride values of an order of magnitude exist above and below relatively thick units of clay-sand lens

Figure 8. Trace of Paleo Drainage in the Bedrock Surface



complexes. At site V on the otherhand, a 20-foot clay-sand lens complex apparently has little effect upon the distribution of low quality water. Site VIII has a relatively uniform vertical distribution of chlorides, despite the presence of relatively impermeable clays between the screened intervals, while site X shows a factor of four increase in chloride values across sand-clay stratigraphy separating the screened intervals in wells #2 and #4. When interpreting the isochlors on the cross sections, it is probably useful to assume that much of the parallelism which exists in the distribution may be due to the presence of relatively impermeable clay-sand lens systems isolating the larger sand-gravel aquifers from each other. Places where the contours take on large vertical departures from the horizontal are probably places where the more impermeable units are removed or absent, or are not extensive enough to prevent vertical flow of low quality water. Notably, many of these locations are near streams.

Hathaway (1978) believes that the major paleo drainage features may direct better quality water to regions overlying Permian bedrock, flushing out low quality water, and resulting in better water quality than could otherwise be expected. The east-west cross sections discussed next do not necessarily confirm or rebutt this speculation. They do, however, confirm previous statements (Latta, 1950; Fader and Stullken, 1978) that due to density differences, the low quality water tends to collect in these drainage features. Moore (1940) describes an investigation in the Burton Oil Field which indicated that the brine then being placed in pits seeped into the aquifer and rapidly sank to bedrock due to its large density contrast. It is to be expected then that salt water emanating from bedrock should remain near the bedrock surface.

## Discussion of East-West Cross Sections

The east-west cross sections (Figs. 10-13) beginning at the top of the map (Fig. 2) are C'-A', E'-E, D'-D, and A''-A. These sections demonstrate the west-to-east sloping bedrock subcrop and land surface profiles. The approximate Cretaceous-Permian (K/P) unconformity is depicted dipping to the west at a rate of about 10 feet per mile (see Fader and Stullken, Plate 2). The principle features of these east-west cross sections are:

- 1) the appearance of low quality water is not coincident with the position of the Permian-Cretaceous boundary.
- 2) low quality water tends to occur at lower horizons in the unconsolidated formation, especially in the locally occurring depressions. Sections E'-E, C'-A' and A''-A all suggest the 10,000 isochlor is in the vicinity of the bedrock surface. Section D'-D shows a bedrock low between sites II and III which, although not verified by sampling, could contain several thousand milligrams per liter of chloride.
- 3) Section E'-E shows some evidence of salt water rising in the vicinity of meandering Rattlesnake Creek. Other, less dramatic occurrences are suggested on section D'-D near Rattlesnake Creek and on section A''-A near the North Fork Ninnescah River.
- 4) To the west of the first appearance of low quality water, relatively fresh water tends to occur at depths approaching bedrock. East of the first major occurrences, fresh water tends to be confined to the upper 50-100 feet of the aquifer. Fresh artesian water is known to exist at several locations in

the salt marsh area. However, sufficient geohydrologic detail is not known at present to describe the precise mechanism by which this occurs.

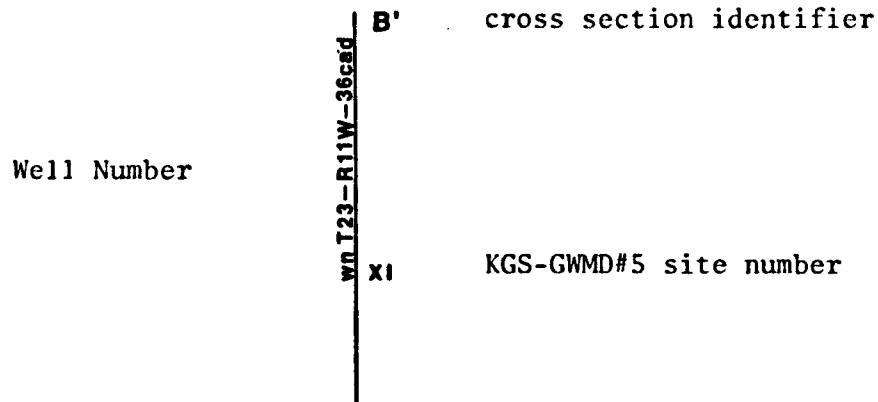
- 5) In certain areas, such as sites II and X (see Fig. 20) which may be recharge features, isochlors are depressed toward bedrock. The unexplored local depression could contain fresher water than expected if the net regional flux has a downward trending component in these areas.
- 6) Water quality tends to deteriorate in the upper 100 feet of the aquifer as it moves to the east. Although the quality of this water is not impressively poor when compared to water occurring lower in the formation, computation of the Sodium Adsorption Ratio indicates it is hazardous for the soil types in the area.

#### Discussion of the North-South Cross Sections

The four north-south trending cross section A-A', B-B', B-B'', and C-C' (Figs. 13-17) show the broad detail of the paleo drainage previously described. The western most cross sections B-B'' and C-C' are the simpler of these situations, while A-A' and B-B' tend to become complicated on the north end due to the presence of the salt marsh geohydrology. The understanding of this area is still limited enough that several areas remain blank and are left to future investigation. The principal features are now discussed:

- 1) The fresh water strata appear to be limited in lateral extent by increasing chloride content as the major surface drainage is approached. Thus, Rattlesnake Creek and, to a lesser

Figure 9. Explanation of symbols used on the hydrologic cross sections in the following eight figures.



- 1600 - elevation above mean sea level
- land surface and bedrock
- December 1973 water table
- ...59... isochlor (ppm Cl<sup>-</sup>)
- |88 point chloride value in well (ppm Cl<sup>-</sup>)
- 889 point chloride value in well not in cross section trace (ppm Cl<sup>-</sup>)
- PC Peace Creek
- NFN North Fork of Ninnescah River
- RSC Rattlesnake Creek
- WHC Wild Horse Creek
- BSM Big Salt Marsh
- LSM Little Salt Marsh
- US 281 U.S. Highway 281
- $\frac{K}{P}$  Permian-Cretaceous uniformity
- 999 Long-Term average chloride value in stream (ppm Cl<sup>-</sup>)

Pages 34 through 41 are oversized illustrations.  
They are in the accompanying envelope.

extent the North Fork of the Ninnescah River, have significant control over the limits of fresh water in the region.

- 2) The natural depression existing beneath Rattlesnake Creek in section B-B" (Fig. 15) appears to be contributing low quality water upward into the Rattlesnake Creek. The extremely high values of the isochlors may be due to locally higher permeability in the Cedar Hills Sandstone, or simply to the inability of the salt water to leave the lowest part of the channel as it is discharged. Other sections show similar upturning of the isochlors, but the magnitude of these is not so great.
- 3) On sections A-A' and B-B' (Figs. 14 and 15), the northern end is dominated by the Big and Little Salt Marshes. Latta indicates that these are regions of natural groundwater discharge. He also indicates that salt water leaves this area and flows eastward to pollute Peace Creek in Reno County. Rattlesnake Creek increases its salt load as it passes the Big Salt Marsh. Instances of fresh to moderately fresh flowing artesian water are also known. These facts, along with the apparently complex distribution of chloride point values document the complicated hydrologic system operating locally here. More work should be directed to this problem in the future.

#### Overview of Cross Sections

Fresh water occurs in the higher elevations of the unconsolidated aquifer in Stafford County. It tends to occur in long lenses bounded on the north and south by low quality water along the major streams. To the west the aquifer tends to be an extensive source of high quality

water, whereas to the east gradual degradation finally results in water which is uniformly low in quality, but not necessarily to the degree seen on some of the streams. To the northeast the system is dominated by the salt marshes. Much more high quality water exists to the northwest than anywhere else in the County.

Salt water probably emanates from much of the Permian subcrop, as well as from the eastern Cretaceous subcrop, although in relatively small quantities. A point beneath Rattlesnake Creek, near a natural depression coincident with the Cedar Hills Sandstone may be a location of enhanced sandstone permeability where abnormally large volumes of low quality water may emanate. In general, the water found beneath the streams in Stafford County is not of the degree of salinity noted at site V.

In general, water in the low areas of the bedrock tends to be the lowest quality water locally. A few places where this principle is violated occurs where isochlors are deflected downward by regional recharge features.

In conclusion, the lowest quality water in the upper unconsolidated aquifer tends to occur near and in the major surface drainage in the area. This is a feature noted not only in Stafford County, but throughout the eastern part of the Great Bend Prairie (see Layton and Berry, 1973). In following chapters we propose to examine this phenomena in detail and offer a hydrodynamic explanation for it.

## Chapter 4

### FLOW OF GROUNDWATER IN STAFFORD COUNTY

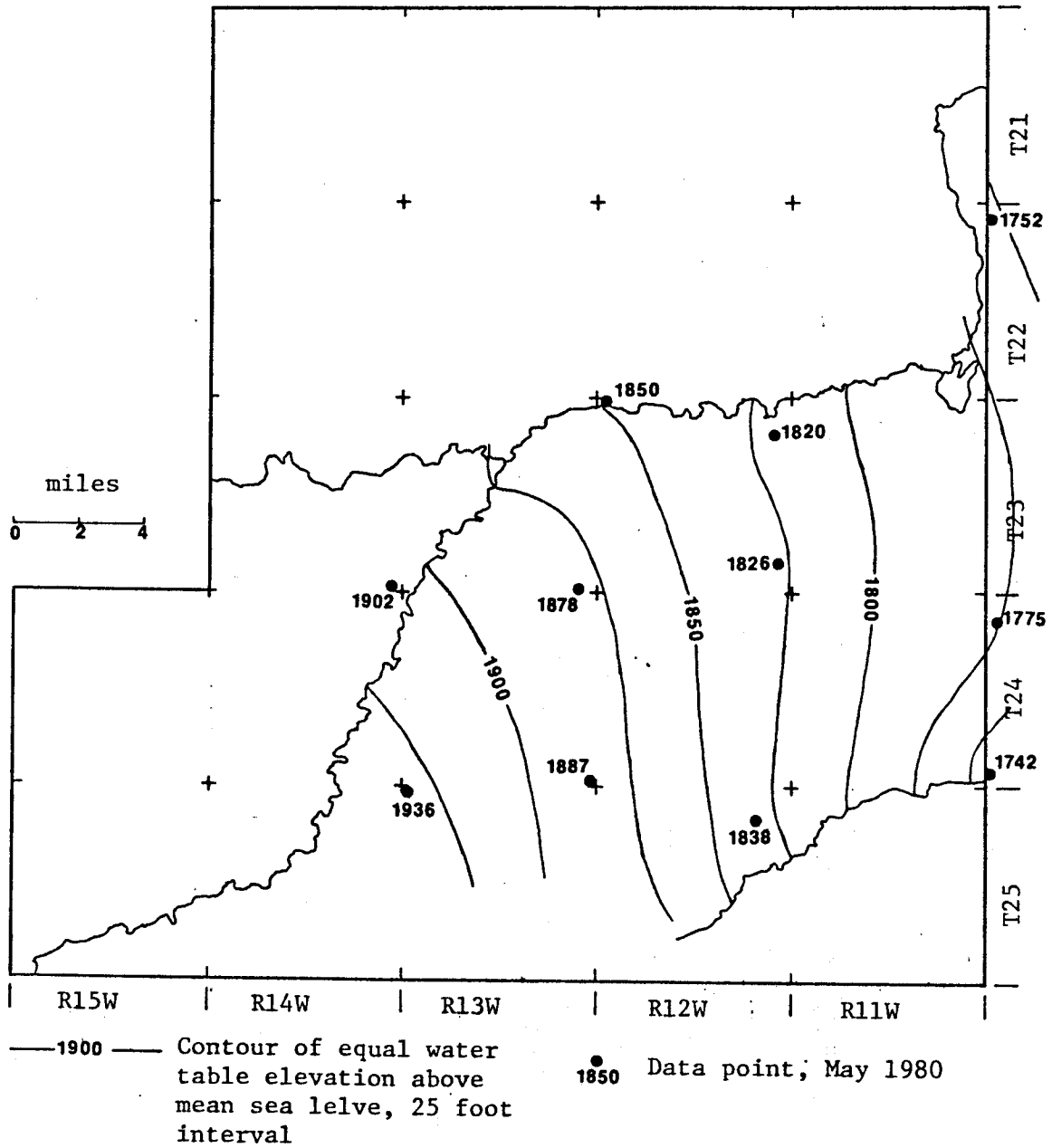
#### Potentiometric Surfaces

The theory of flownets (see Appendix V) is useful in studying the motion of groundwater. Hydrological maps are useful in depicting the areal motion of a system. The underlying assumption in hydrologic mapping is that the flow in the aquifer is essentially horizontal and, therefore, the equipotential surfaces are approximately vertical; thus, vertical components of flow are ignored. In confined aquifers these assumptions constitute the "hydraulic approach," while when dealing with a phreatic aquifer they are known as the "Dupuit assumptions" (Bear, 1980).

Examination of the lithologic columns (see Appendix II) for the drilling sites reveal that in most locations the hydrology of the unconsolidated deposits constitutes a multiple aquifer system. The deepest well is considered to be completed in the bedrock. The well of intermediate depth is considered to be completed in the lower unconsolidated aquifer. The shallow well is considered to be completed in the upper unconsolidated aquifer. At site XI, the shallow well is in the upper unconsolidated aquifer (the site is incomplete). At site II no well was completed in the lower unconsolidated. At site III the screen intended for bedrock became trapped in the lower unconsolidated and was thus screened in both units. This site therefore cannot differentiate conditions in bedrock and the lower unconsolidated aquifer.

The potentiometric surface of the upper unconsolidated aquifer for May 1980 is shown in Figure 18, between Rattlesnake Creek and South Fork

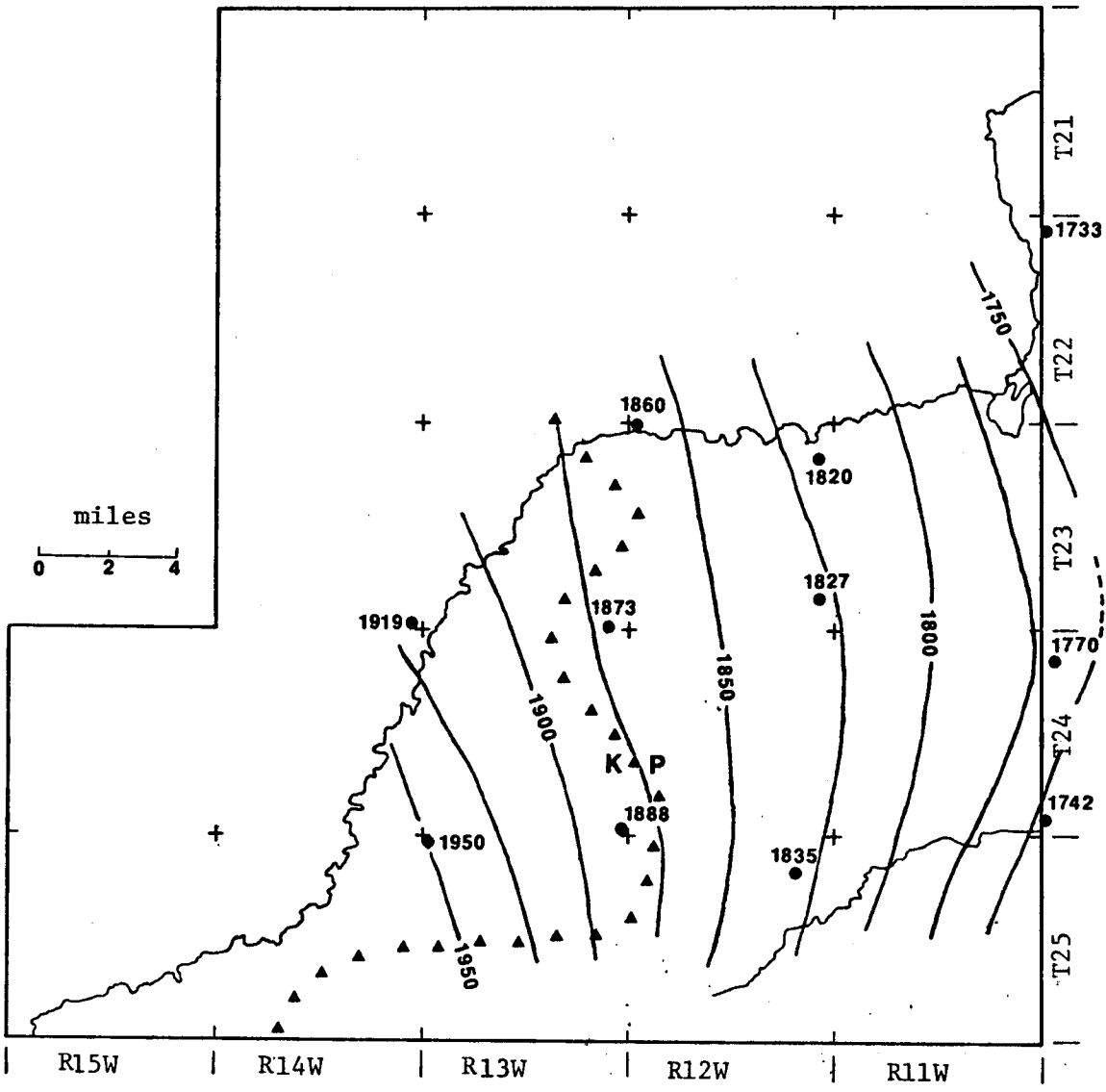
Figure 18. The Potentiometric Surface of the Upper Unconsolidated Aquifer  
May 1980



Ninnescah River using the appropriate head data from Appendix IV. These are heads corrected to a pure water standard (see Appendix V). Contour points along the streams were derived from the 1973 potentiometric map of Fader and Stullken (1978, Plate 3). Comparing the 1980 potentiometric surface with the 1973 potentiometric surface shows that the patterns of the equipotentials are very similar. This indicates that recharge tends to maintain the upper aquifer in an approximate steady state over long periods. The general movement of groundwater is to the east and is effluent to the streams.

A potentiometric map (Fig. 19) was also constructed for the bedrock aquifer for May 1980 from head data for each well screened in the Permian bedrock at each site, corrected to pure water density. At site III, the deep well is actually screened in the unconsolidated aquifer and the bedrock aquifer, but is included as approximate data. Some sites have wells completed at shallow depth in the bedrock. Examination of the hydrographs indicate small differences in corrected heads between wells 1 and 2 at these sites. These data are assumed correct for the purposes of Figure 19. Comparison of Figure 18 with Figure 19 shows a general similarity in the direction of flow in these systems. It must be noted, however, that Figure 18 ignores the effect on hydraulic head which is due to the differences in the elevation of measuring points in a fluid whose density varies spatially. If this correction is significant relative to the head difference due strictly to differences in elevations, then Figure 18 would need to be re-evaluated. In effect, this correct invalidates the assumed vertical equipotentials implied on Figure 18. Noticeable differences in the two tend to occur at major drainages. In many cases this appears to be due to deformation of the

Figure 19. The Potentiometric Surface of the Bedrock Aquifer, May 1980

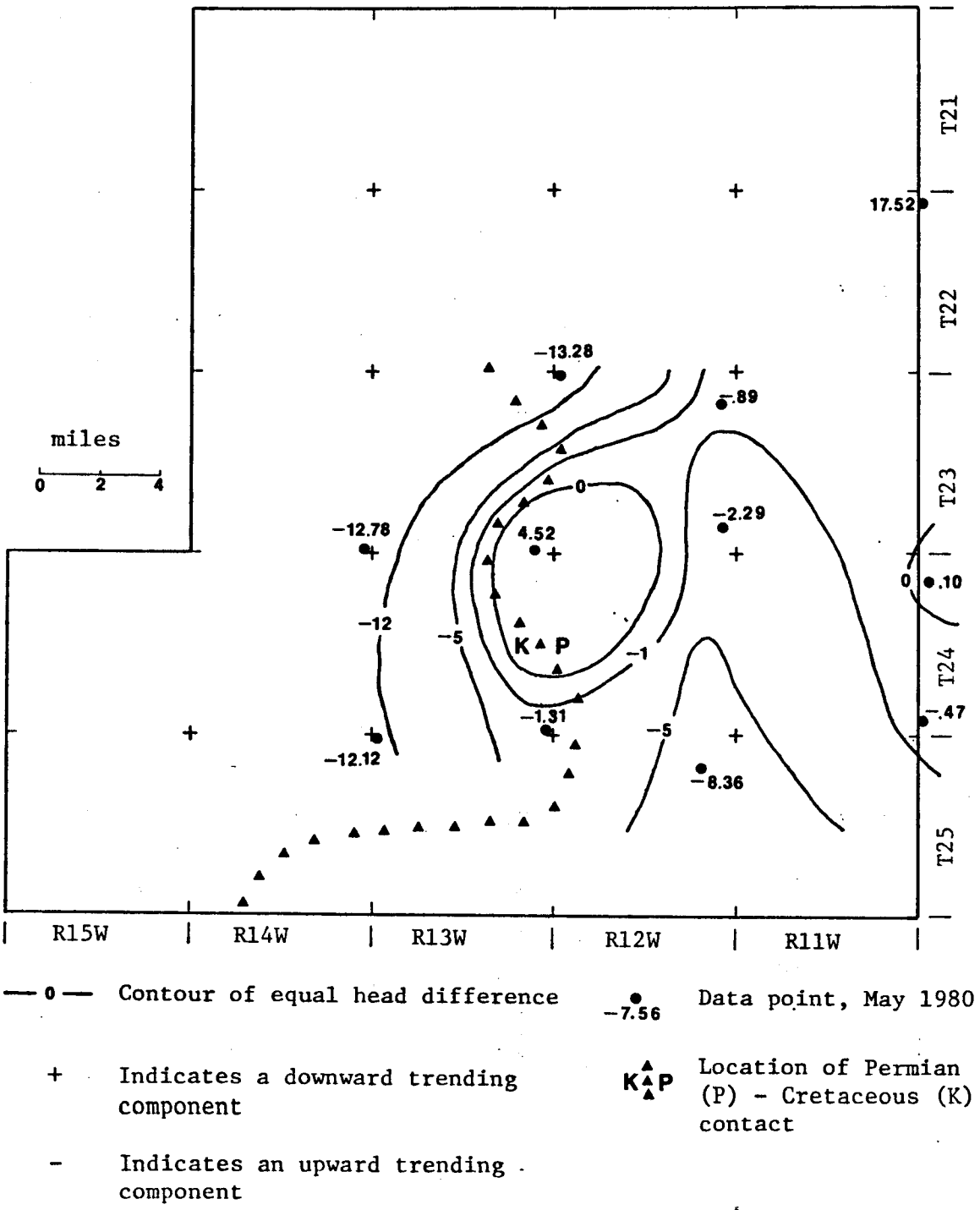


—1900— Contour of equal water table elevation above mean sea level

● Data point, May 1980  
1868

▲▲▲ Location of Permian (P)-Cretaceous (K) contact

Figure 20. Indicated Direction of Vertical Head Difference Across the Bedrock Surface.



free surface contours near major drainage, while the bedrock flownet does not seem to be effected in a similar manner. Due to a lack of great detail of the bedrock flownet near streams, this feature may be an artifact, rather than a real occurrence.

#### Vertical Components of Flow

A third illustration, Figure 20, was prepared by taking the difference between the pure water heads in the deep and intermediate wells and correcting for the head differences created by completing wells at different depths in water of variable density (see Appendix V). This data was plotted at the site location and lines of equal head difference were constructed. Negative contours are regions where the heads will tend to move water upward into the unconsolidated aquifer, while positive contours denote areas of tendency to flow into the bedrock aquifer. Zero contours are lines along which no flow tends to occur. Thus, it is possible to depict a large central feature of downward circulation and a surrounding area of upward circulation. A smaller recharge feature exists to the east on the county line. At site X there seems to be a correlation between improved water quality in the bedrock and indicated downward motion of groundwater. At site II, the bedrock water quality is better than at X, even though the direction of flow is indicated as upward. At site III the problem with the well screen may completely invalidate the comparison of water quality and apparent flow direction. Perhaps what is being measured here is actually circulation only in the unconsolidated. Site XI, near the top of the map shows an extremely negative value. This large difference in head may occur because of a perched condition of the fresh water due to impermeable beds in the

unconsolidated aquifer. An additional source of head difference is a coarse channel gravel just above the bedrock at this site which may act as a sink and relieve some of the pressure in the bedrock. Site XI is too far away from other controls to accurately establish its hydrologic relationship to the more distant wells. It is noteworthy that many of the largest negative values occur west of the Cretaceous-Permian (K/P) unconformity. The Cretaceous (Kiowa) shale is generally regarded as an aquitard, which could maintain the large negative head differences at sites IV and VI. This would be accompanied by a low vertical flux due to reduced permeability. The large negative value at site V is in an area where the Permian is in direct contact with the unconsolidated units. If the Permian permeability is sufficiently great, significant salt water flow could occur here.

The contours shown in Figure 20 simply indicate the general direction of the vertical flow component (see Appendix V). The magnitude of the flow is controlled by the distribution of hydraulic conductivity over the area. The features depicted in Figure 20 appear to define circulation features in and between the aquifers.

#### Hydraulic Connection Between the Aquifers

Comparison of the various well hydrographs at each site indicate that there is some degree of synchronous head change between the aquifers. Hydrographs from sites I, II, V, IX, X, and XI indicate that all wells register nearly synchronous changes in head of about the same magnitude. The wells completed in the Permian (#1 wells) are all completed at relatively shallow depths; less than 35 feet from the bedrock surface to the center of the cased interval. These effects are espe-

cially noticeable for readings in January 1980 and May 1980. The records show that, over time, the absolute values of the head differences maintained between the consolidated aquifer (well #1) and unconsolidated aquifer (well #2) at sites V, X, and XI are considerably greater than those differences at sites I, II, and IX. At this time, no studies of the barometric efficiency of the Permian aquifer have been conducted. The head changes noted in this study appear to correlate with the annual pumpage from and recharge to the aquifer.

Sites IV, VI, VII, and XIII all have the deep well completed at depths ranging from 73 feet to 114 feet into bedrock. The changes in head between consolidated and unconsolidated aquifer are only moderately synchronous and seldom of equivalent amplitude. Sites IV and VI are in areas overlain by the Kiowa Shale, generally described as a confining bed, and they show the least influence from changes in storage in the overlying aquifers. Sites VII and VIII show a somewhat better synchronization of head changes, but again, the similarity of amplitude is absent.

Site III is not discussed here due to the fact that the screen is not confined to one aquifer, but is divided between the consolidated and unconsolidated.

A hypothesis which might explain these hydrographs is put forth here. Suppose that the red beds are under confined pressure beneath the overlying Cretaceous units west of the subcrop area. Suppose also that the fluid in this aquifer is of low quality having a density greater than fresh water. Now there is operating in the overlying unconsolidated aquifer a circulation system on at least a subregional scale in which the fresh and poor quality waters are mixing. If the Permian

formations in the subcrop area are weathered in their upper zones so that the permeability and competency are altered, and the degree of this alteration decreases with increasing depth, then changes in the overburden (fresh water in storage) would be transmitted in a decreasing fashion with depth. The lower permeability and higher bearing strength of the unweathered bedrock aquifer material at depth would allow much less variation of head. Conversely, as the bedrock surface is approached greater permeability and diminished bearing strength let overburden changes become rapidly translated into pressure head changes. This qualitatively explains the varying response of the #1 well to water level changes in the shallow wells on the basis of depth drilled into the Permian.

This hypothesis also implies the interaction of two flow systems, which could account for a water quality gradient in the bedrock. The flow in the unconsolidated aquifer could penetrate into the weathered Permian system until it is damped out by decreasing permeability. In doing so, the fresh flow system could dilute and remove low quality fluid moving up from the totally confined sub-Cretaceous Permian units. This hypothesis cannot be defended here in a rigorous fashion. There may be, and probably are, other explanations. A mathematical formulation would seem quite formidable as would the data collection necessary to validate the requisite assumptions. This will have to remain a tantalizing question for now.

#### Vertical Flownets Between Recharge and Discharge Points

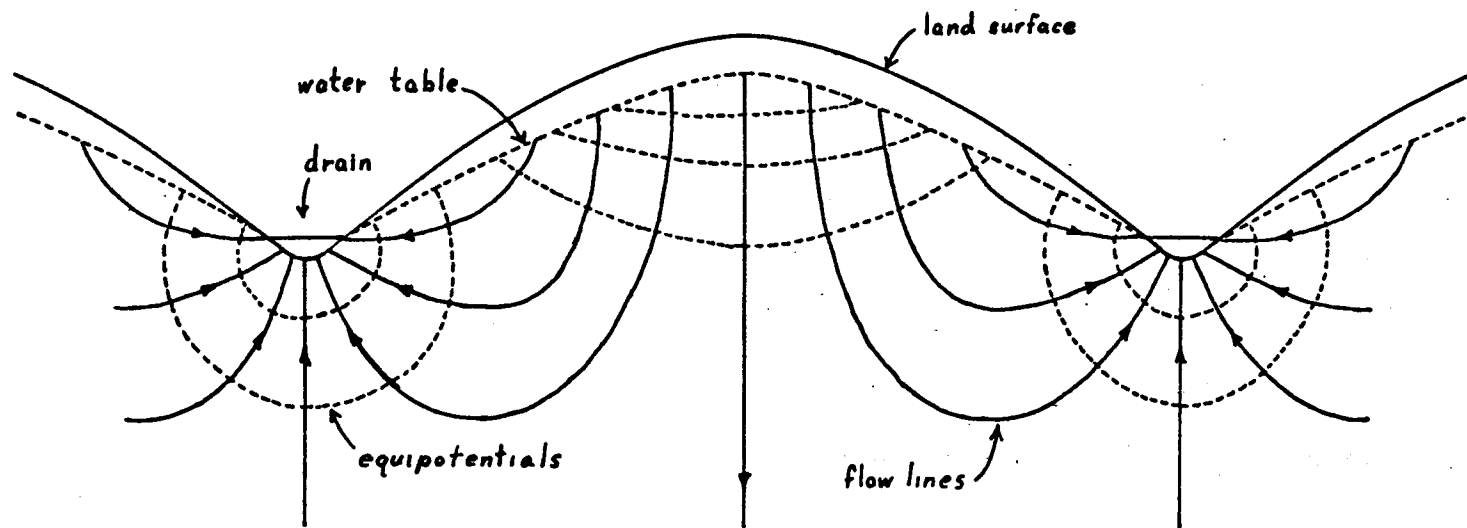
Hubbert (1940), in discussing the topic of flow near the water table, sets out the basic groundwork for the study of regional flow

systems. This was inspired by the then prevalent theory that large portions of the groundwater in storage did not move. Figure 20 depicts the regional flownet proposed by Hubbert in which recharge water enters the water table at regions of high hydraulic potential and is discharged into streams which are at a lower potential. This is essentially a source-sink system in which mass is conserved and in which distribution of flow occurs in agreement with the laws of thermodynamics. Hence, in a regional system involving a single fluid in an isotropic, homogeneous flow system, we see that considerable flow can enter a drainage feature from below.

At the peak of each local high in Figure 21, there is a vertical flow line directed downward. Freeze and Cherry (1979) term this a groundwater divide. Directly beneath each stream is another vertical flow line; directed vertically upward in this case. These vertical flow lines constitute impermeable boundaries, since by definition no flow can cross over flow lines. Hence, they serve to form along with the (assumed) impervious bottom and the phreatic surface, a well defined hydrodynamic system. Freeze and Cherry term a hypothetical boundary separating recharge areas from discharge areas as the hinge line. In the recharge area all flows should show a downward component of motion, while on the discharge side of the hinge line all flow lines should demonstrate a vertical component.

With the preceeding discussion in mind, some data collected for this investigation will now be summarized which suggests a portion of the study area conforms (to a degree) to the basic regional flownet theory. Examination of section B-B' suggests a low rolling prairie profile (Dominico, 1972) consisting of a central topographic high

Figure 21 . Approximate flow field in uniformly permeable material between the recharge distributed over the free surface and the valley sinks.



after Hubbert, 1940

bounded by major drainage on both sides. These streams are the North Fork of Ninnescah River (NFNR) and Rattlesnake Creek (RSC). To the north a similar profile is defined between RSC and the Arkansas River. Also to the south of NFNR another cycle is completed by the South Fork of Ninnescah River. The system depicted in this cross section is therefore only a part of a larger regional system. Toth (1963) discusses the development of regional systems in detail.

The general trace of the water table in cross section B-B' reflects a subdued replica of the topography, a general feature recognized by Toth (1963). In the central portion of the topographic highs on both sides of RSC the water tables approach zero slope. Examination of well hydrographs from sites III and V suggest the areas of recharge and discharge which might be expected in this type of physiography. At site III the pure water heads, corrected for differences in screen elevations, show an invariant downward vertical motion, since  $h_2 > h_1$ . On the other hand, at site V the pure water corrected as before, heads always show a vertically upward motion since  $h_1 > h_2 > h_3$ . Information is not available to fill the gap between these wells, but the general pattern is obvious. Differences in geology might cause subregional systems to develop (Freeze and Cherry, 1979), but these would still only be masked over the regional system. A well drilled near the groundwater divide north of site V would probably corroborate this conclusion. Thus, it is demonstrated that RSC is the regional drain for a portion of a prairie profile system and is, therefore, the point of lowest hydraulic potential in that region. Hubbert (1940) points out that no stagnate bodies of water can exist in the subsurface of such a system "unless it

be a body of water, such as salt water, which is physically different from that flowing."

#### Isochlor Distribution Near Site V

Cross section E'-E (Fig. 10) and B-B'' (Fig. 15) are coincident at site V. Three wells are completed at this site. Well #1 is completed in the Permian bedrock. The total cased depth is 207 feet, with the center of the screened interval at 196 feet, 15 feet into the bedrock. Wells #2 and #3 are completed in the unconsolidated aquifer, with the centers of their screened interval at 97 feet and 46 feet respectively. On cross section B-B'' close control is offered by a double test site (Fader and Stullken, 1978) at T23R12 Section 7ccc. The deep test hole was drilled into the red beds with a total depth of 210 feet while the shallow test was drilled to 97 feet. The long-term quality of RSC on this cross section (B-B'') is defined by the value of 1,000 mg/l chloride ion (see Figures 2 and 3). The chloride concentrations at the various sampling levels suggest a system of isochlors which are highest near NE/4, NW/4, NW/4 Section 6, T23R12 and apparently taper back toward bedrock as they recede away from that location to the north and south.

In cross section E'-E, the view is roughly parallel to the channel of RSC and the creek meanders back and forth across the land surface profile line. The position of the isochlors to the west was not certain due to lack of control. The choice of the 20,000 isochlor intercepting the Cretaceous/Permian unconformity is purely arbitrary. The isochlor gradient west of site V may be much more severe than depicted here, depending upon the hydraulic conductivity of the Kiowa Shale. The relative short reach of stream over which quality deterioration occurs might

suggest a steeper gradient in the isochlors, but on the other hand there is sufficient low quality water known to exist in the Kiowa Shale (Latta, 1950) to produce the distribution of chloride shown here if sufficient head differential and hydraulic conductivity are available to permit it to flow. To the east, distribution control is afforded by site I. Isochlors are interpreted as following the bedrock off to the east. The isochlors are difficult to interpret beneath the meanders of the stream.

The positions of the isochlors are probably not quite as simple as depicted here due to variations in geology. Thus, the presence of 91 mg/l chloride ions at site V, well #1 may be due to isolation of the better quality water by clay. The lithologic log of site V does not substantiate this, however. In fact, the rapid change of quality between wells #2 and #3 suggests the possibility of an interface or at least a relatively thin zone of dispersion.

The evidence thus far presented, the high rate of gain along the stream in this area, the shape and distribution of the isochlors, the rapid change in quality at site V with no apparent stratigraphic control, are all suggestive of the phenomena of dynamic coning of salt water (Muskat, 1935). It remains to be shown that: 1) the flow of fresh groundwater into RSC is sufficient to cause upconing of waters of comparable density to the low quality waters encountered in test drilling, and 2) whether or not this coning is stable or unstable. It might be further asked what rates of gain could occur which would reduce the possibility of this phenomena; what water densities could be expected to be stable?

In this investigation sufficient data was not collected to permit estimation of the effects of dispersion. Therefore, distinction between "upconing" of only moderately low quality water ( $1.001 \geq \rho \geq 1.005$ ) is possibly not differentiable from water in a dispersion zone being carried into the stream. Furthermore, a stable cone of high density water may exist, but its diffusion front could supply the low quality water needed to reduce stream quality, especially if the cone is changing position (Bear, 1972, 1980). Therefore, this investigation can only seek to deal in gross phenomena, and must ignore the fine detail.

## Chapter 5

### THE SALT WATER UPCONING PROBLEM

#### The Two Fluid System

If two or more fluids exist as a system, their relationship may range from being miscible in all proportions like water and alcohol, to being totally immiscible like water and oil. Where they are totally immiscible, these fluids will be separated by a discrete surface, and where miscible they will be separated by a zone of dispersion (Hubbert, 1940). In practice, the zone of dispersion is often thin enough relative to the aquifer thickness to be treated by the abrupt interface approximation. This permits the interface to be treated as a material surface, much as the phreatic surface (Bear, 1980). Hubbert points out that between miscible fluids, such as fresh water and salt water, surface tensions are lacking and, hence, no capillary effects are possible except between the fluids and the matrix grains. This assumption is not true for immiscible or partially immiscible fluids where surface tensions can be maintained between the various fluids as well as the matrix material. Thus, there is added a capillary effect to the existing pressure term in the fluid potential which is discussed below. In most groundwater problems, capillary effects of a fluid-fluid or a fluid-matrix nature are generally ignored. It is also standard practice to ignore the viscosity differences among the various fluids in groundwater work. Verruyt (1980) has recently demonstrated that the velocity distribution along a vertical interface at  $t=0$  is dependent upon  $(\mu_1 + \mu_2)/2$  where  $\mu_i$  is the viscosity of each fluid. Thus, small viscosity differences are justifiably ignored.

Since the system of flow involves two fluids, each fluid must have its own potential field (see Appendix V); the values at any point in either region are given by:

$$5-1) \quad \phi_1 = gz + \frac{p}{\rho_1} \quad \left(\text{units of } \frac{L^2}{T^2} \text{ or energy per unit mass of fluid}\right)$$

and

$$5-2) \quad \phi_2 = gz + \frac{p}{\rho_2}$$

#### Conditions for the Existence of an Interface

For a material interface to exist, Hubbert (1940) points out three physical phenomena which must exist. First, each fluid must tend to be driven back into its own realm. Therefore, the potential of each fluid must increase in the domain of the other. Hence:

$$5-3) \quad \left(\frac{\partial \phi_2}{\partial n_1}\right)_1 > 0$$

$$5-4) \quad \left(\frac{\partial \phi_1}{\partial n_2}\right)_2 > 0$$

Second, the fluid pressure must be single valued at the interface.

Third, the normal component of flow of each fluid at the interface must be zero, i.e.,

$$5-5) \quad \left(\frac{\partial \phi_1}{\partial n_1}\right)_1 = \left(\frac{\partial \phi_2}{\partial n_2}\right)_2 = 0$$

Hubbert (1940) has shown that equations 5-1 through 5-5 imply conditions only satisfied when the lighter fluid overlies the heavier fluid.

The behavior of the interface in relation to the conditions of flow along the interface may be derived by first eliminating  $p$  between equations 5-1 and 5-2, solving for  $z$ , and differentiating with respect to  $S$ , the path along the interface. The result is

$$5-6) \quad \sin \alpha = \frac{\partial z}{\partial S} = \frac{1}{g} \left( \frac{\rho_1}{\rho_2 - \rho_1} \cdot \frac{q_{1s}}{\sigma_1} - \frac{\rho_2}{\rho_2 - \rho_1} \cdot \frac{q_{2s}}{\sigma_2} \right) \quad \text{where}$$

$$q_{1s} = \sigma_1 \frac{\partial \phi_1}{\partial s} \quad \text{and} \quad q_{2s} = \sigma_2 \frac{\partial \phi_2}{\partial s}$$

$\alpha$  is angle of slope measured positively upward in the direction of  $S$ , and  $q_{1s}$  and  $q_{2s}$  are the flow components of fluids 1 and 2 in direction  $s$ . Definitions of  $\sigma$  may be found in Appendix V.

If neither fluid is in motion  $\sin \alpha = 0$ , implying a horizontal interface. If the heavy fluid ( $\rho_2$ ) is assumed to be static, equation 5-6 reduces to

$$5-7) \quad \sin \alpha = \frac{1}{g} \cdot \frac{\rho_1}{\rho_2 - \rho_1} \cdot \frac{q_{1s}}{\sigma_1} = \frac{1}{g} \cdot \frac{\rho_1}{\rho_2 - \rho_1} \cdot \frac{\partial \phi_1}{\partial s}$$

As  $q_{1s}$  increases the interface rises in the direction of flow.

The elevation of any point on the interface may be determined by eliminating  $p$  from equations 5-1 and 5-2 and solving for  $z$ :

$$5-8) \quad z = \frac{1}{g} \left( \frac{\rho_2}{\rho_2 - \rho_1} \cdot \phi_2 - \frac{\rho_1}{\rho_2 - \rho_1} \cdot \phi_1 \right)$$

From equation 5-8 it is obvious that for a static fluid 2  $\phi_2$  is constant, and therefore  $z$ , the elevation of the interface, is dependent upon the value of  $\phi_1$  at any point on the interface.

## Upconing of a Horizontal Interface

For the sake of simplicity let it be assumed that a body of fresh water overlies a body of salt water and that these bodies are separated by a horizontal interface. Now suppose that a sink starts to operate in the fresh water at some distance above the interface. The flow which begins to be directed toward the sink implies that a change is occurring in the potential field of fluid 1. Equations 5-7 and 5-8 depict the behavior of the interface as the field values change. As the values of  $\phi_1$  decrease along the interface, flow develops tangentially along the interface in the direction of decreasing  $\phi_1$ . The interface will rise in the direction of flow as predicted by equation 5-7. Equation 5-8 corroborates this result. As  $\phi_1$  decreases on the interface the second term on the right hand side of equation 5-8 decreases in value and  $z$  increases.

The question not answered by equations 5-7 and 5-8 is whether or not the rise of the interface can continue to the upper limit implied by 5-8 without the salt water entering the sink. A stable interface will mean an interface which is at steady state for a given density of salt water and a sink of a given strength. An unstable cone is one which has broken through to the sink. Muskat (1937) addressed the problem by considering the effects of a change in fluid pressure at a point on an oil-water interface, where the water was considered to be in hydrostatic equilibrium (see Fig. 22). Thus at any point  $P(r,z)$  on the interface:

$$5-9) \quad P(r,z) + \gamma_w gy = P_b$$

where  $P(r,z)$  is the fluid pressure,  $\gamma_w$  the specific weight of water,  $y$  is height of interface above original level, and  $P_b$  is the formation

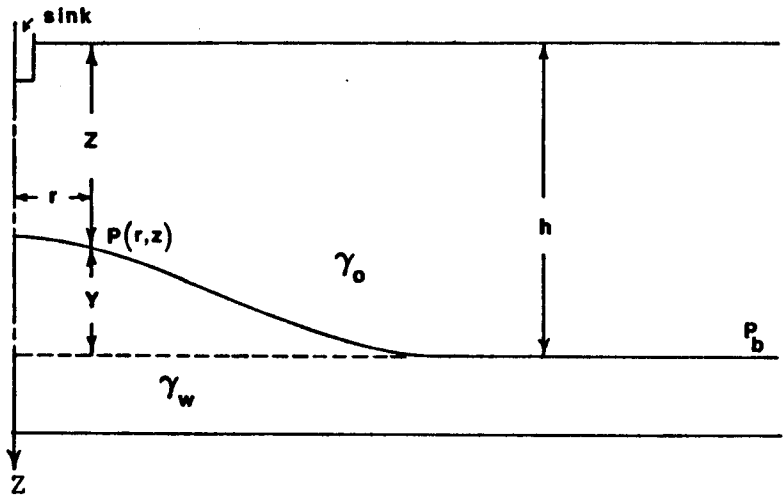


Figure 22. Schematic of a water-coning system in a homogeneous medium

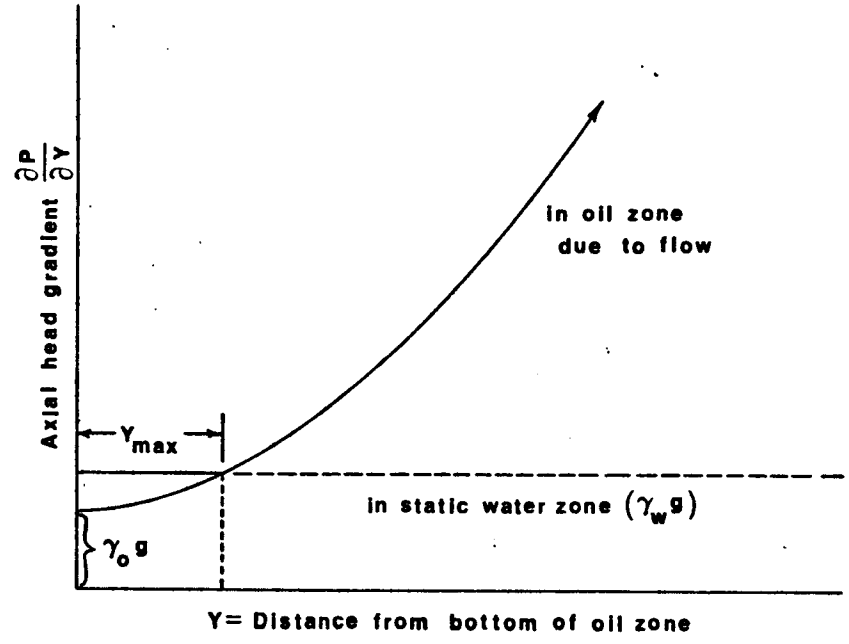


Fig. 23 Equilibrium conditions along the axis of a water-coning system.

(Fig. 22 and 23 after Muskat, 1937)

pressure of the oil at the level of the undisturbed interface. Equation 5-9 represents the necessary condition for the cone to remain in a static condition below the oil zone while flow occurs in the latter. Physically it means that if at some point  $P(r,z)$  the drop in pressure below the reservoir pressure at that level is equal to the differential hydrostatic head

$$\Delta P(r,z) = gy(\gamma_w - \gamma_o)$$

a water column rising to that height  $y$  will be in static equilibrium. The convergent flow in the oil zone towards the well results in a head gradient which increases rapidly as the well is approached. In the water zone, however, there is a constant hydrostatic head. Figure 23 shows the relationship of these curves. Muskat points out that beyond the intersection of the gradient curves, no stable cone can exist and any slight change in formation pressure beyond that dictated by the intersection will result in direct movement of water to the sink. This phenomenon is termed unstable upconing.

The physical situation for salt water overlain by fresh water is not significantly different except for the presence of a zone of transition which has developed due to hydrodynamic dispersion. Bear (1980) points out that as the salt water cone rises this zone widens, and, hence, salt water of some lesser concentration may enter the sink even if the calculated sharp interface achieves a stable height. In the following discussions, the assumption of a sharp interface will be used.

## Chapter 6

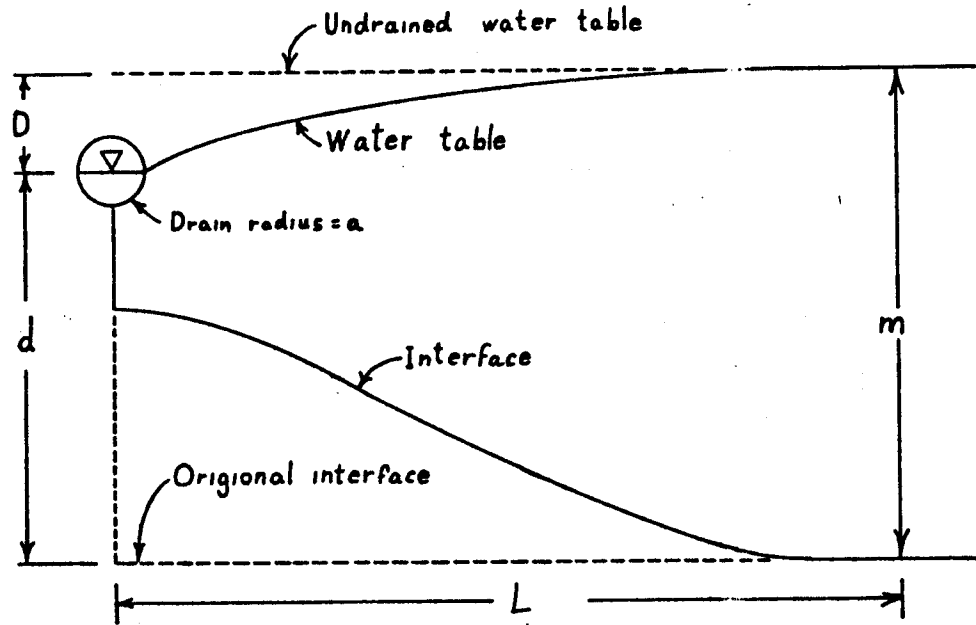
### THE McWHORTER APPROXIMATION

#### Concepts and Assumptions

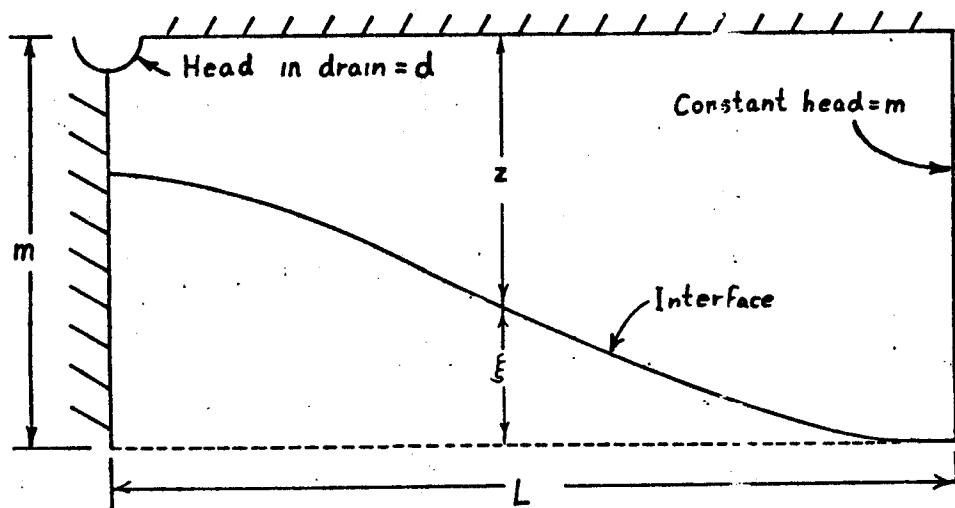
In order to predict the hydrodynamic upconing effect of tile drains placed in known fresh water aquifers underlain by salt water, McWhorter (1972) devised an analytical solution to the problem. For the purposes of this study, it was felt that, except for the actual modification of the land surface, the physical situation near a horizontal tile drain approximates the drainage of an aquifer by the base flow contribution to an effluent stream such as Rattlesnake Creek (RSC) (Fig. 24a).

In McWhorter's depiction of flow toward a drain, the drain of radius  $a$  is centered a distance  $D$  below a water table, in a fresh water system of thickness  $m$ , defined by the free surface and the undisturbed interface. The system is to reach a steady state, with the free surface in the drain being a distance  $d$  above the undisturbed interface and a constant head at  $x=L$  providing the fluid to the system. The interface is assumed to be stable. The approximations in transferring the concept to the natural stream are the assumptions of drain size and of actual maintenance of the constant head boundary at distance  $x=L$ . If a large body of subsurface storage is available this constant head condition may be approximated for short time periods. If recharge is sufficient to supply just the discharge prescribed by the gradient to the stream, this condition may be prolonged. In reality, no aquifer is absolutely steady state and no such approximation would be long valid. A hypothetical drain size was calculated based on Low Flow Stream Measurements provided by the USGS.

Figure 24. McWorter's Approximation



a. Flow toward a drain



b. Idealized flow toward a drain.

(after McWhorter, 1972)

In order to cast the problem into a form more convenient for analysis, McWhorter recognized that in most instances of interest  $D \ll d$  and hence "the contribution to the drain discharge due to flow above the elevation is small compared to that from below the drain." This essentially reduces the problem to that of a confined aquifer of thickness  $m$  (see Fig. 24b) drained by a line sink of constant strength at  $x=0, z=0$  ( $x$  measured positive to the right and  $z$  measured positively downward, relative to the location of the sink). A solution to the upcoming problem is obtained by assuming that the interface does not effect the distribution of head in the fresh water region. This is essentially the same approximation invoked by Muskat and Wyckoff (1935) in their study of the upcoming problem in oil reservoirs. In order for this assumption to approximate reality the change in elevation of the cone must remain small. Muskat (1937) indicates in regard to this approximation, the quantitative details will be effected, but the general features of the critical height of the cone are still valid. McWhorter points out that his approximation predicts a higher discharge than could actually be expected for any particular position of the interface.

#### Mathematical Equations

McWhorter (1972) derived an approximate distribution for head in a system defined by Figure 24b using the method of images (Appendix VII). The unperturbed fresh water head distribution is approximately:

$$6-1) \quad H_1(x, z) = \frac{Q}{2\pi K_f} \cdot \ln \left\{ \cosh \frac{\pi x}{m} - \cos \frac{\pi z}{m} \right\} + \text{constant}$$

He points out that for this distribution, if  $L \geq d$ ,  $H_f = m$  at  $x=L$ . Subject to the boundary conditions  $H_f = m$  at  $x=L$  and  $H_f = d$  on  $x^2 + z^2 = a^2$  (see Appendix VII for details) it is shown that the discharge to the drain is given by

$$6-2) \quad Q = 2\pi K_f (m-d) \left/ \ln \left\{ \frac{\cosh \frac{\pi L}{m} - 1}{\cosh \frac{\pi a}{m} - 1} \right\} \right.$$

and the head distribution by

$$6-3) \quad H_f = \frac{Q}{2\pi K_f} \cdot \ln \left\{ \frac{\cosh \frac{\pi x}{m} - \cos \frac{\pi z}{m}}{\cosh \frac{\pi L}{m} - 1} \right\} + m$$

Finally, the position of the perturbed interface, relative to its original position is given by

$$6-4) \quad \xi = \frac{\gamma_f}{\Delta\gamma} (m - H_f^1), \quad \Delta\gamma = \gamma_s - \gamma_f$$

Using the relationship  $z = m - \xi$  derived from Figure 24b, equation 6-3 may be recast to the form

$$6-5) \quad H_f^1 = \frac{Q}{2\pi K_f} \cdot \ln \left\{ \frac{\cosh \frac{\pi x}{m} - \cos \pi \left(1 - \frac{\xi}{m}\right)}{\cosh \frac{\pi L}{m} - 1} \right\} + m$$

on the interface. Simultaneous solution of equations 6-4 and 6-5 are used to determine the position of the interface  $\xi$  and the free surface  $H_f^1$ . McWhorter (1972) used these equations to derive the maximum safe installation depth  $D$  for a tile drain to avoid upconing for a given discharge. The equations were used in a slightly different strategy for this investigation.

### Graphical Solution

In order to easily determine the stability of a cone of saline water, a graphical solution of equations 6-4 and 6-5 is convenient. Some preliminary simplification is possible on equation 6-5. As McWhorter points out, stability of the cone at the point directly beneath the stream implies stability of the entire cone. Thus, solution at  $x=0$  is an appropriate indicator for the system. Since  $\cosh 0=1$ , equation 6-5 reduces to:

$$6-6) \quad H_f^i = \frac{Q}{2\pi K_f} \cdot \ln \left\{ \frac{1 - \cos \pi \left(1 - \frac{\xi}{m}\right)}{\cosh \frac{\pi L}{m} - 1} \right\} + m$$

Now equation 6-4 can easily be manipulated to the form:

$$6-7) \quad \frac{H_f^i - d}{m - d} = 1 - \left( \frac{m}{m-d} \right) \left( \frac{\Delta \gamma}{\gamma_f} \right) \left( \frac{\xi}{m} \right)$$

McWhorter then indicates that after substitution of equation 6-2 into equation 6-6, some algebraic manipulation leads to

$$6-8) \quad \frac{H_f^i - d}{m - d} = 1 - \left[ \ln \left\{ \frac{1 - \cos \pi \left(1 - \frac{\xi}{m}\right)}{\cosh \frac{\pi L}{m} - 1} \right\} \right] / \left[ \ln \left\{ \frac{\cosh \frac{\pi a}{m} - 1}{\cosh \frac{\pi L}{m} - 1} \right\} \right]$$

Equations 6-7 and 6-8 are dimensionless functions in terms of  $H_f^i$  and  $\xi$  for any set of physical parameters  $a$ ,  $m$ ,  $d$ ,  $\gamma_s$ ,  $\gamma_f$ , and  $L$ . For a graphical solution, using the argument  $\xi/m$ , solving 6-8 for a set of physical parameters gives a single curve. Solution of equation 6-7 for a range of  $\gamma_s$  again using  $\xi/m$  as argument, produces a family of straight lines which may intersect the locus of equation 6-8. The possible solutions

are (McWhorter, 1972): no intersection which implies unstable upconing, a tangent to the curve which implies the critical height for the cone, a non-tangent intersection which implies a stable cone height. This last situation offers one ambiguity in that two points of intersection may occur for the larger values of  $\xi/m$  where the radius of curvature decreases. Muskat and Wyckoff (1935) point out that in this case, choice of the correct root is dictated by the requirement that the stable free surface represent the lowest potential energy, a condition which is satisfied by the lower cone. More discussion of the solution will occur when the actual physical problem of RSC is addressed.

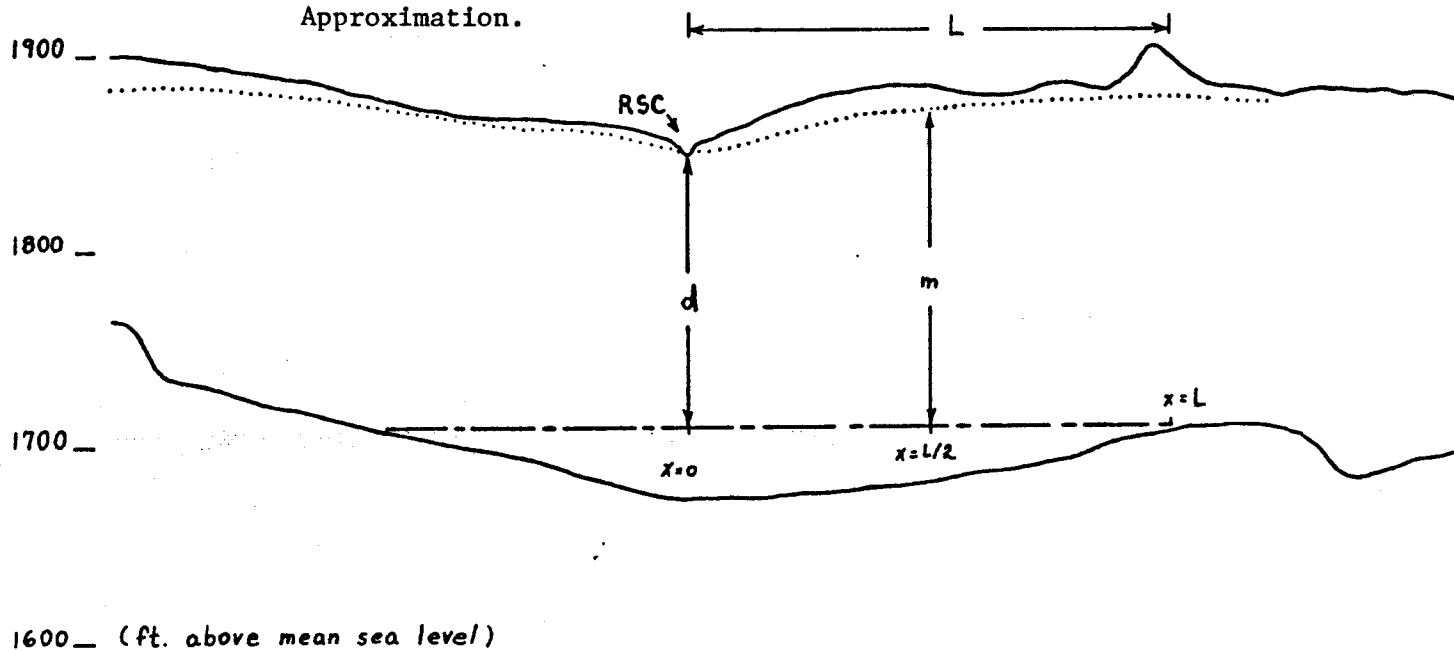
#### Application to Rattlesnake Creek Problem

##### Determining Physical Parameters

The problem was addressed by assuming that a particular free surface represented a more-or-less steady condition. The December 1973 potentiometric surface in Fader and Stullken (1978, Plate 3), which was used because of its availability, seems to fit this requirement, for it closely resembles the 1942-44 potentiometric map of Latta (1950). Cross section B-B" was used for the purpose of evaluating several of the required parameters for the McWhorter model. The part of that cross section used for the parameter estimation is reproduced as Figure 25.

The approximation of the semi-circular drain radius required to simulate the natural drainage posed a problem. In its base flow regime the stream tends to be broad and shallow. As flow increases, the depth tends to increase. The principal assumption used here, and no empirical evidence is given in support, is that the radius of the stream must be sufficient to carry the average stream flow at a velocity not unreason-

Figure 25 . Geohydrologic Cross Section at Site V on Rattlesnake Creek  
 Showing Parameters used in the Solution of the McWhorter  
 Approximation.



..... December 1973 Potentiometric surf.  
 --- Salt Water Interface  
 ——— Bedrock and Land Surface



able for the conditions of the stream. United States Geological Survey discharge records for water year 1978 indicate that the average discharge at Macksville (19 years of record) was 37.2 cfs. The average at Zenith (5.5 years of record) was 95.4 cfs. The average discharge along the stream was 66.3 cfs. Flow measurement records made near Zenith on October 5, 1977 showed a velocity of 1 ft/sec for a discharge of 29 cfs. Similar measurements made on June 8, 1978 show a velocity of 1.7 ft/sec for a discharge of 196 cfs. Noting that average stream velocity is relatively invariant over a range of discharges from  $3 \times 10^1$  to  $2 \times 10^2$  cfs, we will assume an average stream velocity of one ft/sec as not unreasonable. This implies a channel cross section of  $66.3 \text{ ft}^2$  to carry the average discharge at an average velocity of 1.0 ft/sec. Solving

$$a = r = \left( \frac{2A}{\pi} \right)^{1/2}$$

gives a drain radius of 6.48 ft. This value was used throughout the computational portion of this investigation.

The value of L was determined from Figure 25 as the average of the measured distances from the center of the RSC channel to where the potentiometric surface approached tangency with the horizontal. This value was determined to be 4.8 miles (25,344 ft). L was considered to remain constant for all discharges (i.e., horizontal portions of the cross sectional water table were assumed to remain horizontal as storage changed.

The parameter d was the measured distance from the channel to the position of the undisturbed interface. For the solutions presented in this investigation the stream free surface was considered to remain relatively constant in elevation while the water table was allowed to

move freely to accommodate simulated variations in storage-discharge. The undisturbed elevation of the interface was, for lack of any other control, assumed to be controlled by the prominence on the right side of Figure 25. This gives a value to  $d$  of 142 feet.

The value of  $m$  was computed at  $x=L/2$  to be 161 feet. At  $x=L$ ,  $m=168$  feet. In order to satisfy the McWhorter approximation the aquifer thickness at  $x=L$  is  $m$  and the head there is also  $m$ . The potential at the drain can be arbitrarily set. Therefore, the thickness  $m$  was approximated at  $x=L/2$ , to avoid over-estimating the effective thickness. This then implied that  $H_f^1(L)=m$  also. There are probably other options for making this approximation, but this particular one is thought to be conservative. Thus,  $m$  is assumed to be 161 feet for the starting data.

From pump test data (Cobb, 1979), the hydraulic conductivity was estimated to be 72 ft/day. This test was conducted in western Stafford County and may not accurately reflect local conditions.

Based on analysis of bedrock and unconsolidated aquifer wells, a range of salt water densities was chosen for test values. A range  $1.050 \leq \gamma_s \leq 1.005$  was studied.

#### Final Transformation of the Approximation

Physical conditions in a natural drainage system of the scale of the RSC basin are such that  $L \gg m \gg a$ . This allows some simplification of the final equations to be made.

First, recall that in its exponential form

$$\cosh x = \frac{e^x + e^{-x}}{2}$$

Now consider equation (ii), and note that the term

$$\ln\left(\cosh \frac{\pi L}{m} - 1\right)$$

may be reduced in the following fashion.

$$\begin{aligned} \ln\left(\cosh \frac{\pi L}{m} - 1\right) &\simeq \ln\left(\cosh \frac{\pi L}{m}\right), L \gg m \\ &\simeq \ln\left[\left(e^{\frac{\pi L}{m}} + e^{-\frac{\pi L}{m}}\right)/2\right] \end{aligned}$$

For large L,  $e^{-\frac{\pi L}{m}} \rightarrow 0$ . This leaves

$$\ln\left(\cosh \frac{\pi L}{m} - 1\right) = \frac{\pi L}{m} - \ln 2.$$

Equation 6-2 now becomes

$$Q \simeq 2\pi K_f(m-d) / \left[ \frac{\pi L}{m} - \ln 2 - \ln\left(\cosh \frac{\pi a}{m} - 1\right) \right]$$

or, since for the condition  $L \gg m \gg a$  allows ignoring the log terms

$$6-9) \quad Q \simeq 2K_f m \left(\frac{m-d}{L}\right)$$

which approximates the discharge of a confined aquifer to a stream for both sides.

Equation 6-8 must also be modified to reflect the orders of magnitude of the system parameters. Similar approximations applied to that equation yield

$$6-10) \quad \frac{H_1 - d}{m - d} \simeq 1 - \frac{\ln\left[1 - \cos \pi\left(1 - \frac{L}{m}\right)\right] - \frac{\pi L}{m} + \ln 2}{\ln\left(\cosh \frac{\pi a}{m} - 1\right) - \frac{\pi L}{m} + \ln 2}$$

Equations 6-7 and 6-10 were solved graphically with the aid of a few simple programs on an HP25 calculator. The results will be discussed, as well as the effects of varying certain parameters in the next chapter.

## Chapter 7

### RESULTS OF THE McWHORTER METHOD

#### Explanation of Graphical Computation

In order to construct the solution graphs for solving the transformed McWhorter equations 6-7 and 6-10, two sets of tables were computed for each discharge. The general scheme is first explained, and the specific solutions are then outlined.

Equation 6-10 was solved first. Physical quantities, explained earlier, were used and the equation was solved over a range of the independent variable  $\xi/m$

$$.05 \leq \xi/m \leq .95$$

On occasion the range was widened to .99 in order to verify the shape of the function near the  $\xi/m$  axis. This computation produced a single curve along which  $\frac{H_f^1 - d}{m-d}$  is in an inverse relationship to  $\xi/m$ . Next, equation 6-7 was solved for values of  $m$  and  $d$  over ranges of  $\xi/m$  and  $\Delta\gamma$ .  $\gamma_f$  was always assumed equal to unity in this study. The ranges were as above for  $\xi/m$  and for  $\Delta\gamma$

$$.005 \leq \Delta\gamma \leq .05$$

These computations produced a family of straight lines whose intersections were considered indications of stability; unstable solutions were considered to be those for which no intersections occurred. Sets of computations were performed for a range of stream gains, the highest gain being that predicted using equation 6-9, and then obtaining smaller

discharges by reducing  $m$ . This is equivalent to assuming that the head in the stream is relatively unchanged, while the water table varies over time. Figure 26 is a typical solution graph for the McWhorter Approximation. This particular solution is for  $Q=3 \text{ ft}^2/\text{day}$ .

#### Stability of the Solution for Various Densities at Certain Discharges

The occurrence of a stable solution to the modified McWhorter equations does not prove the existence of a stable cone beneath a stream. However, it reinforces that model if a certain density water can be theoretically shown to be stable at an elevation similar to that measured in the field. To an extent, the discharge at which this match occurs is flexible as McWhorter points out that his equations tend to over predict discharge. Thus, it would not be unreasonable to expect to match an historical isochlor with a stable density at a measured discharge somewhat less than that predicted by the McWhorter equations. To some extent, it is possible to do this by changing the slope of the free surface to reduce the discharge, or to raise the elevation of the undisturbed interface. In this study changes of discharge have been produced by changes of slope, rather than by increasing the initial elevation of the interface. The existence of an historical set of measurements corroborates the initial slope of the free surface (Fader and Stullken, 1978, Plate 3), but no evidence is available to corroborate the original, undisturbed interface. Furthermore, the isochlors are taken from data which is asynchronous to the water table. Later, some computer work will be presented to attempt to confirm the modeling by analytical solution.

The failure to predict a stable cone does not invalidate the work of this investigation, but rather indicates the sensitivity of the salt water to dynamic upconing caused even by small values of discharge to the stream.

Solutions were computed for various discharges, ranging from 17.39 ft<sup>2</sup>/day to 1 ft<sup>2</sup>/day. The larger value was derived from the situation depicted in Figure 25, while the remaining values were generated by reducing the value of  $m$  at  $x=L/2$ . The solution graphs all had features similar to Figure 26, differing only in details of exact curve shape and positions of intersecting lines. The most salient feature of these solution graphs was that for any given density contrast  $\Delta\gamma$ , stability tended to increase as stream gain  $Q$  was decreased. This implies that  $\xi/m$  became smaller for the various  $\Delta\gamma$  values. Figure 27 is a table of all computed stable values of  $\xi/m$  over the values of  $\Delta\gamma$  and  $Q$  indicated.

Figure 28 is a plot of the native water density,  $\gamma_n$ , versus the dissolved chlorides (ppm  $\text{Cl}^-$ ) @ 24°C. The collection temperature of the water was in the range of 19°C-21°C, so that these density -  $\text{Cl}^-$  relationships are slightly low. This curve is a generalization, as may be seen by noting that some of the density values are not depicted as single valued with respect to chloride concentration. This may simply be due to rounding error, or it may be due to variation in other dissolved constituents. The open triangles plotted on the density/ chloride graph are the isochlor values from cross section B-B". Their density/chloride ratios are read as A: 1.01/10000 and B: 1.025/22000.

The values of  $\xi$  for the crests of the 10000 and 22000 isochlors were measured from cross section B-B" using the undisturbed interface position depicted in Figure 25 as the datum. Values of  $m$  corresponding

Figure 26. Typical graphic solution for the McWhorter approximation.

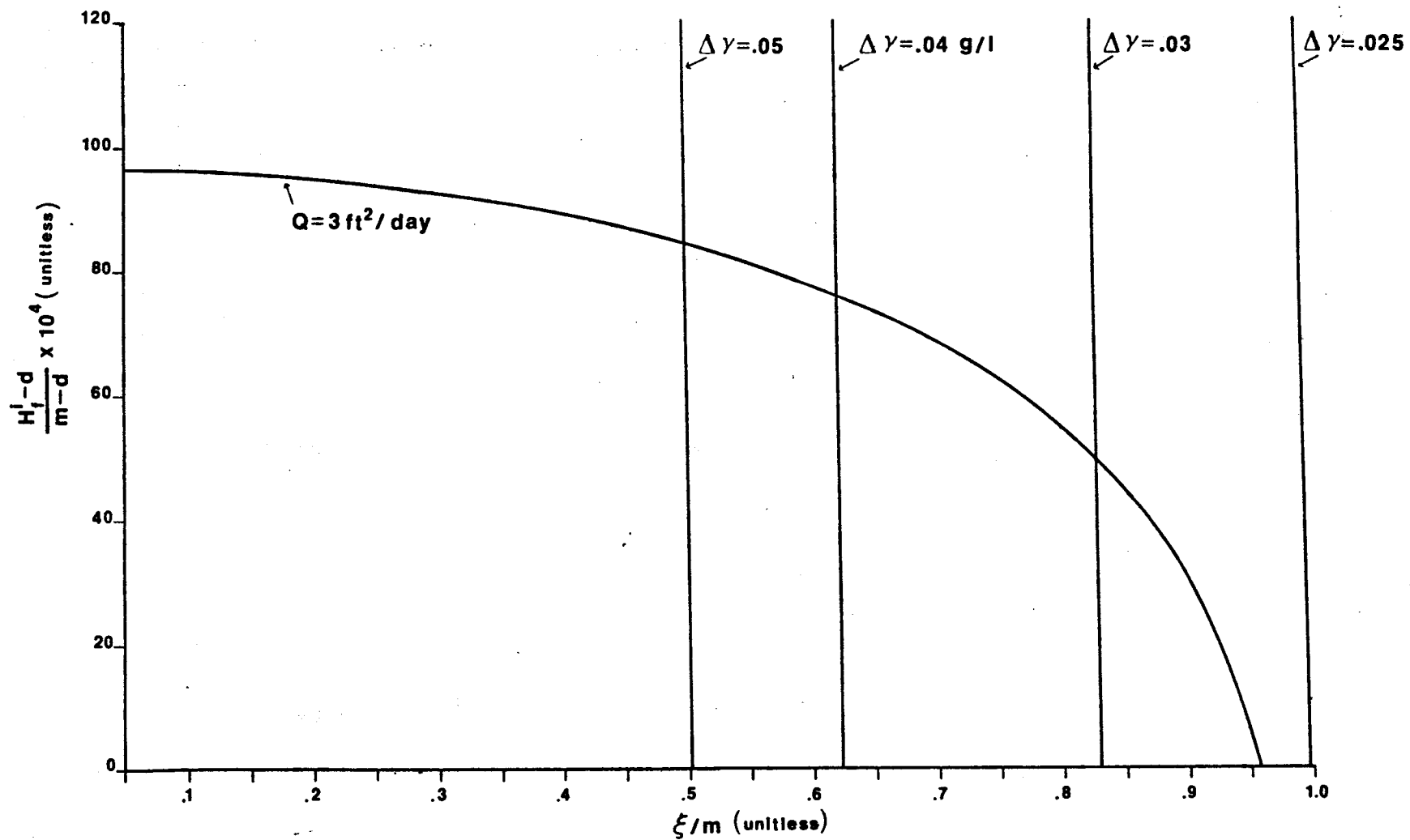


Figure 27 . Stable Values of  $\xi/m$  (unitless)

nc : not computed

U : unstable

Q ft <sup>3</sup> /d	m ft.	$\Delta\gamma$ (g/ml)													
		.005	.007	.008	.009	.010	.015	.018	.020	.025	.030	.035	.040	.045	.050
17.39	161.0	U	nc	nc	nc	nc	nc	nc	nc	nc	nc	nc	nc	nc	U
8.63	152.0	nc	nc	nc	nc	nc	nc	nc	nc	nc	nc	nc	nc	nc	nc
4.0	146.8	nc	nc	nc	nc	nc	nc	nc	nc	nc	U	0.946	0.818	0.725	0.654
3.0	145.6	nc	nc	nc	nc	nc	nc	nc	nc	U	0.825	nc	0.618	nc	0.495
2.0	144.4	nc	nc	nc	nc	nc	U	0.935	0.840	nc	0.558	nc	0.418	nc	0.335
1.0	143.0	nc	U	0.872	0.773	0.695	0.463	0.385	0.347	0.280	0.230	nc	nc	nc	0.139

Figure 28. Water Density vs. Dissolved Chloride @ 24°C

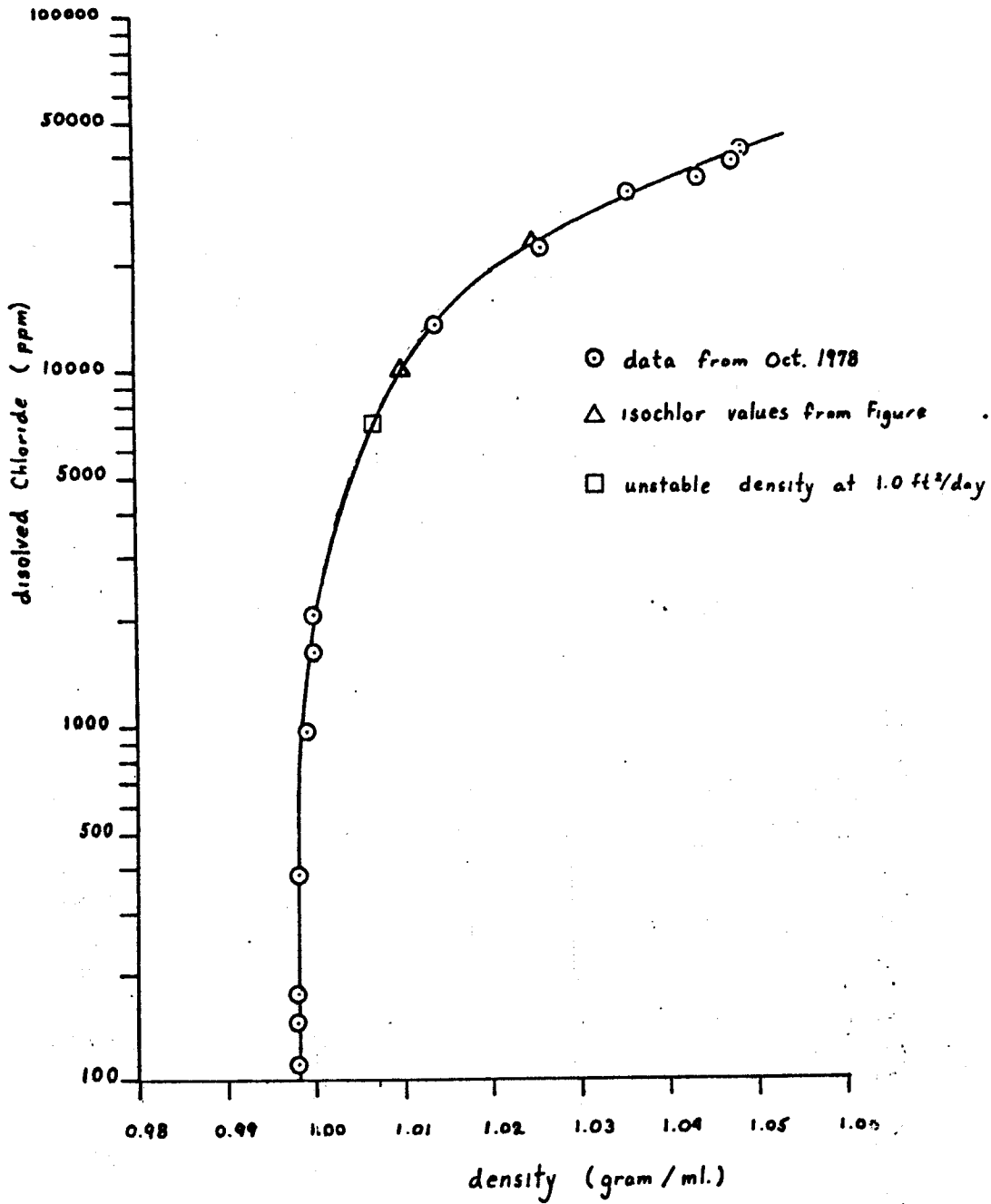


Figure 29. Calculated  $\xi/m$  for various values of  $m$  and the associated discharges.

A. 10000 isochlor

$\xi$ (ft)	$m$ (ft)	$Q_2$ (ft <sup>2</sup> / day)	$\xi/m$
60.0	143.0	1.0	.420
	144.4	2.0	.416
	145.6	3.0	.412
	146.8	4.0	.409
	152.0	8.6	.395
	161.0	17.39	.373

$\Delta\gamma \approx 0.010$

B. 22000 isochlor

$\xi$ (ft)	$m$ (ft)	$Q_2$ (ft <sup>2</sup> / day)	$\xi/m$
38.0	143.0	1.0	.266
	144.4	2.0	.263
	145.6	3.0	.261
	146.8	4.0	.259
	152.0	8.6	.250
	161.0	17.39	.236

$\Delta\gamma \approx 0.025$

to the stream gain rates used in this study were used to compute  $\xi/m$  values. These values are tabulated in Figure 29. Examination of these results indicate that the dependence of  $\xi/m$  on  $Q$  is fairly weak, making it difficult to formulate precise statements about which derived stream gain produces the best fit of  $\xi/m$  to the McWhorter solutions. For a density contrast of .025 ( $\xi/m_B$ ) in Figure 29 and  $\xi/m$  in Figure 27 have their best agreement at  $Q=1 \text{ ft}^2/\text{day}$ . For a  $\Delta\gamma$  of .010,  $\xi/m_A$  and  $\xi/m$  agree most closely for  $1 \text{ ft}^2/\text{day}$  also. It could be argued here that best agreement between the tables is actually at  $\Delta\gamma=.015$  for  $Q=1 \text{ ft}^2/\text{day}$ . The chloride values used here are of a much higher degree of certainty than the values of  $\xi$  or  $m$ . Therefore, comparison is made between  $\xi/m$  values computed for known densities. To attempt to derive  $\Delta\gamma$  values by comparing  $\xi/m$  values between Figures 27 and 29 places unwarranted weight on the accuracy of  $\xi$  and  $m$ .

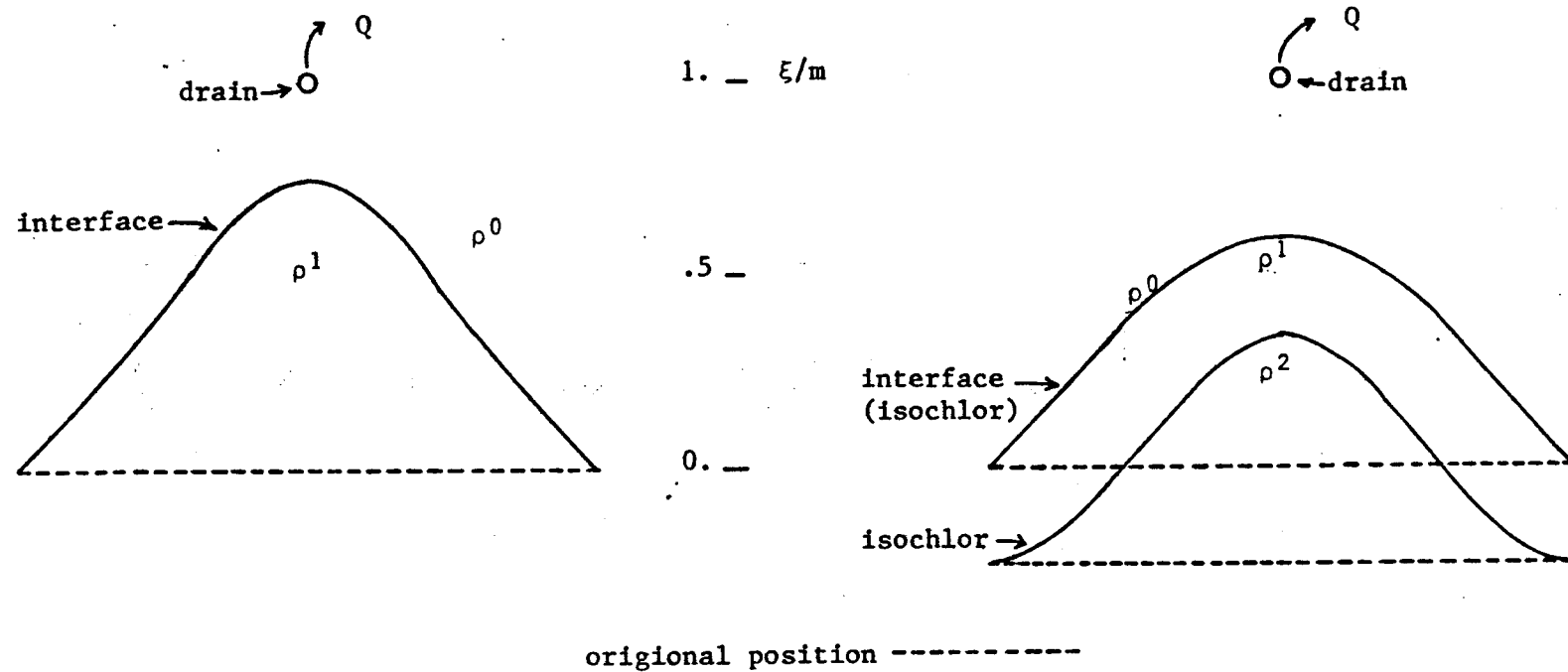
The apparent depression of the 10,000 mg/l isochlor below its predicted position ( $\xi/m_B=0.420$  as compared to  $\xi/m=0.695$  in Figure 16) has several possible interpretations, some of which lend their weight to the verification of a stable cone of salt water. A simplistic observation is that the apparent displacement is an error in interpolation. This explanation is not readily acceptable, given the degree of control in this area. Another possibility is that stratigraphy is controlling the position of the isochlor. The lithologic column at site V indicates a complex of clay and sand lenses whose tortuosity could retard the ability of the salt water to move upward.

A more sophisticated explanation for the depression could be postulated on the basis of Muskat (1937). Since the system being dealt with is actually not of a single density, the question arises as to how a variable density system should react to upconing. An implicit assump-

tion of computing the position of an isochlor is that it is also a stream line as well as a boundary of a uniformly dense body of fluid. Now in reality the system we are dealing with is of variable density. For the moment let us assume that a system of discrete layers of densities  $\rho_0$ ,  $\rho_1$ , and  $\rho_2$  exists in static equilibrium; such that  $\rho_2 > \rho_1 > \rho_0$ , and  $\rho_0$  is fresh water. Now a sink begins to discharge at rate  $Q$  from the fresh water. In response to the disturbance of hydrostatic pressure in the system, the salt water upcones to restore the hydrostatic pressure. The question arises: would a system of  $\rho_0$ ,  $\rho_1$ ,  $\rho_1 > \rho_0$  behave the same as the three fluid system. From an elementary viewpoint, it appears that the two fluid system would result in a larger value of  $(\xi/m)\rho_1$  than would the three fluid system (see Fig. 30). This reasoning is based upon the assumption that the average density of fluid between the undisturbed interface and the disturbed interface is greater in the three fluid system than in the two fluid system, and, hence, that the crest in the two fluid system is higher than in the three fluid system. It is implicitly assumed that as upconing develops, at least some of the upconing fluid flow is derived at some distance below the original interface. This assumes that the mass of the column is basic to restoring the pressure balance. The proof of this hypothesis is not offered here. However, the hypothesis is offered as an explanation for the depressed 10,000 mg/l isochlor.

Finally, the depression of the 10,000 isochlor towards the 22,000 isochlor may be evidence of a zone of dispersion between a cone, defined by the 22,000 isochlor, and the fresh water (Bear, 1972). If this is so, it is apparent that even if a stable cone of dense salt water exists beneath the stream, enough mass of salt is able to escape by dispersion

Figure 30 . Idealization of the Relative Upward Deflection of the Interfaces Bounding Waters of Uniform and Nonuniform Density Below Drains Operating in Fresh Water.



$\rho^0$  : fresh water

$\rho^1$  : water of density 1

$\rho^2$  : water of density 2 ( $\rho^2 > \rho^1 > \rho^0$ )

phenomena to keep salt entering the stream in some quantity. Referring to Figure 29, and noting that water of  $\Delta\gamma=.007$  may have as much as 7000 ppm dissolved chloride ions, it is seen that the unstable water has enough chloride content, even after seven fold dilution, to equal the long-term historical value of 1000 ppm in RSC.

An apparent paradox remains to be discussed. This relates to the discrepancy of discharges predicted by the measured dimensions on section B-B" and the discharge predicted by the stability curves. As noted earlier, the various sets of data used to construct the sections are not synchronous. The discharge of  $17.38 \text{ ft}^2/\text{day}$  is based upon a December 1973 water table, while the apparent stable 22000 isochlor is based on October 1978 data, a period over which base flow could change appreciably. The average base flow gain over the Macksville-Zenith reach is computed to be  $5.56 \text{ ft}^2/\text{day}$ . This is only a third of the December 1973 gain, and 5 times the gain predicted by the stable isochlor solution. This paradox can only be resolved by a more detailed study in which all necessary information is determined more or less simultaneously. This information should include the phreatic surface configuration, the stream quality, the stream flow, the water quality in the various wells and the local hydraulic conductivity. One parameter which is difficult to access, but critical to the solution in that  $m$  and  $\xi/m$  depend upon it, is the position of the "undisturbed interface." If the salt water discharge of the Permian could be determined, a good estimate of this parameter could be gained from a steady state interface model.

At this point, the analysis of the McWhorter approximation is essentially complete. The analytical solution seems to indicate the possibility for some development of a stable cone at low values of

aquifer discharge. There would appear to be associated with this system a dispersion zone which would continue to supply salt water to the stream. As aquifer discharge increases the possibility of stability decreases. The crucial, but as yet unanswered question is what portion of the stream gain is salt water and to what extent is it diluted as it enters the stream. There is also the question of whether or not the salt water discharge from bedrock could keep pace during these high periods of aquifer discharge. Such a situation might justify the explanation of flushing. These questions would seem to require more information than is presently available. In summary, it is stated here that the RSC apparently received salt from dispersion above a stable cone at low aquifer discharges and by unstable upconing during periods of high stream gain.

## NUMERICAL SIMULATION OF THE SALT WATER INTERFACE

## Methods of Modeling the Interface Problem

The precise mathematical statement of the dynamic behavior of an interface between salt water and fresh water results in a pair of non-linear partial differential (PD) equations in terms of  $\phi_f$  and  $\phi_s$  (see Bear, 1980). Even numerical methods experience difficulties achieving a solution in this case. The common method used to overcome this problem is to use vertically averaged heads in the two fluid bodies equivalent to the Dupuit-Forchheimer assumptions (Bear, 1980). Shamir and Dagan (1971) published the pioneering work in solving a vertically averaged numerical solution. A more recent solution for the two-dimensional case has been published by Mercer and others (1980).

The problem of stable or unstable upconing beneath a gaining stream was addressed in the previous chapter by use of an analytical approximation achieved by reducing an image well model to closed form through application of complex variables. An alternative method of investigating the stability or instability of waters of specified densities under specified values of stream gain is desirable. The assumption that the upconing salt water does not effect the distribution of fresh water potentials will obviously cause some discrepancy between real and approximate cone stability conditions. The only way to actually do away with this restriction would be to model the nonlinear PD equations referred to above. A simpler method would involve the vertically averaged potentials. This method has its own problem, for although it assumes a free surface for the fresh water and accounts for the effect

of the rising cone on the distribution of fresh water equipotentials, it actually redefines the potential field and ignores the radial convergence of the equipotentials toward the sink. Thus, the results of the McWhorter approximation are not directly comparable to the results of the vertically averaged schemes. The two sets of results may be useful, however, in defining the probable range of water density and stream gain for cone stability. A range of the heights for those cones determined to be stable should also result. The scope of this chapter is then to outline an alternate upconing model, to state the results of this model, to compare the results to the McWhorter results, and finally to demonstrate the result of the present model if it is assumed the upconing doesn't affect the fresh water potential.

#### An Alternative Model to the McWhorter Approach

The model outlined here is a numerical solution of analytical flow equations reduced to a computer algorithm. The model was designed by Dr. Carl McElwee of the Kansas Geological Survey. The principal features of the model are as follows. It assumes a static body of salt water overlain by a dynamic body of fresh water in which the equipotentials are vertical. Horizontal flow is assumed to originate from a point defined by a constant fresh head and a constant salt water interface height and proceed toward a hypothetical drain location. The fresh water flow field is assumed to be effected by the rise of the salt water interface. The solution of the algorithm produces a piecewise continuous profile in the case of a stable cone, but is much less well defined for the case of instability.

The theory of this algorithm is based upon the work of Hubbert (1940) in which he shows that the angle  $\theta$  of the interface above the horizontal datum is related to the relative velocities of the two fluids separated by the interface:

$$8-1) \quad \sin \theta \approx \frac{\partial Z_i}{\partial S} = (\gamma_1 - \gamma_2)^{-1} \left[ \gamma_1 \frac{\partial h_1^i}{\partial S} - \gamma_2 \frac{\partial h_2^i}{\partial S} \right]$$

Under the conditions that  $\gamma_2 > \gamma_1$  and that  $h_1^i$  and  $h_2^i$  are the fresh and salt heads at the  $i^{\text{th}}$  point on the interface. In general both fresh and salt waters are in motion. Application of the chain rule to the derivatives of  $h_1^i$  and  $h_2^i$  yield

$$8-2) \quad \sin \theta = (\gamma_1 - \gamma_2)^{-1} \left[ \gamma_1 \frac{\partial h_1^i}{\partial X} \cdot \frac{\partial X}{\partial S} - \gamma_2 \frac{\partial h_2^i}{\partial X} \cdot \frac{\partial X}{\partial S} \right]$$

Observing from Figure 31a that  $\frac{\partial X}{\partial S} = \cos \theta$  and dividing out this factor yields

$$8-3) \quad \tan \theta = \frac{\sin \theta}{\cos \theta} = \frac{\partial Z_i}{\partial S} \cdot \frac{\partial S}{\partial X} = (\gamma_1 - \gamma_2)^{-1} \left[ \gamma_1 \frac{\partial h_1^i}{\partial X} - \gamma_2 \frac{\partial h_2^i}{\partial X} \right]$$

At this point a static salt water condition is assumed which implies that  $\frac{\partial h_2^i}{\partial X} = 0$  and that

$$8-4) \quad \tan \theta \approx (\gamma_1 - \gamma_2)^{-1} \left[ \gamma_1 \frac{\partial h_1^i}{\partial X} \right]$$



This is an excellent assumption when the system is in steady state.

Referring to Figure 31b it is seen that at any point  $i$  the flow of the fresh water is defined by

$$8-5) \quad Q = -K_f b \frac{\partial h}{\partial x}$$

where  $Q$  = the discharge per unit width of aquifer,

$K_f$  = the fresh water hydraulic conductivity,

$b$  = the thickness of aquifer bounded by a salt water interface and free surface,

$\frac{\partial h}{\partial x}$  = the hydraulic gradient

Rearranging equation 8-5 yields:

$$8-6) \quad \frac{\partial h}{\partial x} = - \frac{Q}{K_f b}$$

and finally, after substituting equation 8-6 into equation 8-4

$$8-7) \quad \tan \theta = \frac{\gamma_1}{\gamma_2 - \gamma_1} \left( \frac{Q}{K_f b} \right)$$

The model operates by projecting forward in space the positions of the free surface and the interface from the  $i^{\text{th}}$  node to the  $(i+1)^{\text{th}}$  node. The total number of nodes is  $L/\Delta x + 1$ , where  $L$  is the distance from a hypothetical constant head boundary to a hypothetical drain (which if a real stream, would also constitute a constant head if seasonal fluctuations are not considered). The method of projection is simply

$$8-8) \quad h^{i+1} = h^i + \left( \frac{\partial h}{\partial x} \right)_i \Delta x = \left( \frac{\partial h}{\partial x} \right)_i = - \frac{Q}{K_f b_i}$$

$$8-9) \quad z^{i+1} = z^i + \tan \theta^i \Delta x, \quad \tan \theta^i = \frac{\gamma_1}{\gamma_1 - \gamma_2} \left( \frac{\partial h}{\partial x} \right)_i$$

$$8-10) \quad b_{i+1} = h^{i+1} - z^{i+1}$$

where  $h$  denotes the height of the free surface,  $z$  denotes the height of the interface and  $\Delta x = L/n$ ,  $n$  being an arbitrary integer.

Computations proceed from node 1, where  $h^1$ ,  $z^1$ ,  $b_1$ ,  $Q$ , and  $K_f \gamma_1$  and  $\gamma_2$  are all known quantities, and move forward toward the  $n+1$  node (see Fig. 31c).

#### The Accuracy of the Approximation

Since the forward projection scheme depends principally upon the accuracy of the estimation of  $\left( \frac{\partial h}{\partial x} \right)_i$ , choice of  $\Delta x$  is the single most crucial factor in achieving the desired degree of accuracy. It is obvious that the value of  $\Delta x$  becomes more important as the discharge point ( $n+1$ <sup>th</sup> node) is approached, since  $\theta$  is increasing and  $\tan \theta$  is also increasing. Prior to running the set of parameters previously used in the McWhorter approximation, a test was made to determine the best value for  $\Delta x$  in terms of improvement of result versus number of nodes. Runs were made for  $\gamma_2 = 1.018$  and  $Q = -.5 \text{ ft}^2/\text{day}$  (equivalent to  $q = -1.0$  for the McWhorter model, since this approximation is only over half of the aquifer). The number of nodes for the four runs were 26, 51, 101, and

201; L remaining constant at all time. The values of the ratio of  $(z_{n+1} - z_1)$  to  $b_1$  ( $\xi/m$  for McWhorter model) for the node configuration were .75, .77, .79, and .80 respectively. The value which seemed to give the most improvement in the specified ratio was  $n=101$ . This value was utilized for all succeeding runs. As Q is increased and/or  $\gamma_2$  is decreased, cone height will increase and a greater number of nodes may yield a better solution. This speculation was not verified, however. A test was made to determine if unstable solutions could be made to become stable by increasing the number of nodes n. No great improvement was noted, a fact which supports the assumption that the model can actually differentiate stability from instability, and that these conditions are not simply artifacts of the approximation. For the purposes of the numerical projection model, an unstable cone is one which rises to meet the free surface, although not necessarily at the  $n+1^{\text{th}}$  node.

#### Results of the Numerical Model Study

The numerical model described previously was used to simulate a flow system in the same geological cross section as used for the McWhorter approximation (see Fig. 25, Chpt. 6). A similar range of water density differences was utilized. The suite of stream gain rates per foot of channel was identical except for the inclusion of the value  $5.73 \text{ ft}^2/\text{day}$ , a value which represents the historical average gain between Macksville and Zenith referred to earlier. As may be seen by examining the table in Figure 32, the range of stable cone height values is greatly diminished in comparison to the predictions of the McWhorter model. Only for extremely low values of stream gain (Q) and relative large values of density contrast ( $\Delta\gamma$ ), can stable cones be expected to

Figure 32. Tabulated values of  $\xi/m$  from the computer model.

Q ft <sup>2</sup> /d	m ft	$\Delta\gamma$ (gm/ml)								
		.008	.010	.015	.018	.020	.025	.030	.040	.050
1	143.0	U	U	U	.792	.628	.443	.348	---	.191
2	144.4	---	---	---	---	---	---	U	.619	.437
3	145.6	---	---	---	---	---	---	---	---	U
4	146.8	---	---	---	---	---	---	---	---	U
5.73	149.1	---	---	---	---	---	---	---	---	U
8.63	152.7	---	---	---	---	---	---	---	---	U
17.4	162.9	---	---	---	---	---	---	---	---	U

--- = no calculations

U = unstable

be found according to this numerical model. Furthermore, the heights of the stable interfaces are generally 10% to 20% higher than the McWhorter predictions, when both models predict stability.

As  $Q$  is increased the stability of the interfaces decreases much more rapidly for the numerical approximation than for McWhorter's approximation. This is a result of the numerical model's consideration of the influence of the rising cone on the distribution of the fresh water equipotentials. In order to demonstrate that this is so, the numerical solution was modified so that changes in  $b$  due to changes in the interface height were not carried forward in space; i.e.,  $b_i = h_i - z_1$  rather than  $= (h_i - z_1)$ . This is equivalent to using the Dupuit discharge formula to determine the potential distribution and  $\frac{\partial h}{\partial x}$  over a discrete set of nodes with spacing  $\Delta x$ . Row D in Figure 33 is a tabulation of the results of this modified numerical approximation. All values being compared in Figure 33 are for  $Q=1 \text{ ft}^2/\text{day}$ . Stability is extended considerably over row B which is the unmodified numerical model, but not to the same extent as row A which is the solution set from the McWhorter approximation. This does not demonstrate the only differences between the McWhorter approximation and the numerical approximation. Two other differences include assumptions about conditions of confinement and the fact that each model assumes a different equipotential distribution, especially near the drain location. The numerical model was also modified to run as a confined system ( $b_i = b_1$ ) ignoring the effect of the rising salt water on the equipotential distribution. Row C is the tabulation of the results of this model run for  $Q=1.0 \text{ ft}^2/\text{day}$ . Note that the difference between rows C and D is minimal; but the smaller  $\xi/m$  values of row C indicates that the confined

Figure 33. A comparison of  $\xi/m$  values predicted by the models used in this study.  $Q=1 \text{ ft}^2/\text{day}$

Model	$\Delta\gamma \text{ (gm/ml)}$									
	.007	.008	.009	.010	.015	.018	.020	.025	.030	.050
A	U	.87	.77	.69	.46	.38	.35	.28	.23	.14
B	---	---	---	---	U	.792	.638	.443	.348	.191
C	---	U	.954	.859	.573	.478	.429	.344	.286	.172
D	---	U	.957	.861	.574	.478	.430	.344	.287	.172

A = McWhorter's confined approximation

B = Computer model, unconfined, upconing effects potential distribution

C = Computer model, confined, upconing not effecting potential distribution

D = Computer model, unconfined, upconing not effecting potential distribution

model is more stable. As  $Q$  is increased the unconfined model results (D) should become unstable at a faster rate than the confined numerical model results (C). This is due to the fact that in the confined model,  $(b_i = b_1)$  will yield a more slowly changing potential distribution than  $b_i = h_i - z_1$  used in the unconfined model. Both models would still be more stable than the model used to produce B since they do not consider the effect of the upconing upon the potential distribution in the fresh water.

The principle remaining uncertainty in this study is the reconciliation of the values of  $Q$  and  $\Delta\gamma$  where the approximations do not agree. To a large extent the differences in model assumptions just enumerated account for the differences in the results. In Chapter 7 an attempt was made to establish a meaningful relationship between the isochlors in Figure 15 (cross section B-B") and the model results. This comparison was based on the assumption that the isochlors represented stream lines separating moving and static fluids. In the case of the unstable interface, salt water is actually moving into the sink or stream, and it is clear that isochlors and stream lines will not generally coincide. Examination of the hydrographs of site V (Appendix IV), corrected to fresh water and for differences of elevation, indicates a vertical component of flow. Hence, the condition of instability of the salt water body may exist. Thus, the results of the numerical computer model are not inconsistent with actual field data. Close attention to Figures 31 and 34 indicates that except for very small rates of gain, only the larger density contrasts may hope to be stable. This is especially true for gains of  $4 \text{ ft}^2/\text{day}$  and greater, a range which encompasses the historical gain noted earlier. Thus, it may be reasonably, but not unequiv-

ocally, stated that the mechanisms of unstable hydrodynamic upconing of salt water contributes significantly to the degradation of stream quality in areas where stream gains are relatively high and salt water is available.

## CONCLUSIONS

By conducting a drilling program and utilizing previous data, the generalized distribution of poor quality water was determined based upon mapping of water samples analyzed for chloride ion in parts per million. In general, except near major gaining streams, the poor quality water remained near bedrock.

In order to account for the presence of low quality water beneath and within the major gaining streams, the mechanism of dynamic upconing of static salt water beneath a fresh water flow field was hypothesized. Two models were used to compare the historical heights of isochlors above a hypothetical level, undisturbed interface. The McWhorter approximation predicted approximately the correct stable cone height for water with a density of 1.025, but over-predicted the elevation of water with a density of 1.010. This discrepancy suggested that variable density water would not behave as predicted by the McWhorter approximation. A numerical solution of an alternate analytical approximation, based on the Dupuit assumptions and Hubbert's equation relating fresh water -salt water velocities and density contrast to the slope of the interface cone, was prepared and run with the same data as the McWhorter approximation. It predicted instability of interfaces for nearly all values of  $Q$  and  $\Delta\gamma$ . Historical hydrographs at the test site show a vertical velocity in all tested parts of the aquifer which indicates that the salt water is in motion. Thus, instability of the salt water is a possibility.

There is an apparent contradiction here in that one model predicts stability while the other predicts instability of the salt water inter-

face. This problem is resolved by noting that the predicted stability was for  $Q$  of  $1 \text{ ft}^2/\text{day}$  and recalling that the McWhorter equation over-predicts discharge values for stable cone configurations due to ignoring effects of the cone upon the fresh water potential, which were shown not to be insignificant. Coupling these facts with the results of the numerical approximation and the experimentally derived average annual gain of  $5.73 \text{ ft}^2/\text{day}$  for the reach of RSC being studied, it can be concluded that except for very small rates of gain and large density contrasts, salt water will tend to upcone unstably and enter the gaining reach of RSC.

That the above conclusion is not incontestable is fully realized. This study needs to be repeated using time synchronous data for all parameters and more sophisticated modeling techniques which can at least account for variations in permeability and a fully two-dimensional flow field. This would permit better assessment of the stability-instability problem; and if unstable, it would allow computation of the actual flow of salt water into the stream.

Other streams in the Great Bend Prairie demonstrate a similar set of circumstances - a high gaining reach corresponding to a rapid increase in dissolved solids. These streams should be investigated from the standpoint of the upconing problem. A management technique is suggested by this approach: by consumptive use, reduce the gain of the streams due to lowering the free surface of the aquifer. The unanswered questions posed by this approach are: 1) would upconing be stabilized to the extent that the reduced fresh water inflow would be able to maintain acceptable quality standards, and 2) would the salt water not removed by upconing become a problem elsewhere in the aquifer system.

Appendix I. Base Flow Gain in Rattlesnake Creek Between Macksville  
and Zenith, Kansas

In order to estimate the order of magnitude of base flow gain by Rattlesnake Creek in Stafford County, flow records were examined for the period from 29 May 1973 through 30 September 1978. The stations for which record was obtained were (07142300) near Macksville and (07142575) near Zenith. These stations are maintained by the U.S. Geological Survey, and occur at mile 87.5 and 19.3 respectively on Rattlesnake Creek, encompassing a reach of 66.2 miles of channel. The analyzed data consisted of average daily discharges expressed in cubic feet per second. The data are published in Water Resources for Kansas, water years 1973-1978.

In order to conduct the analysis, a composite hydrograph was constructed for each year with both stream discharge curves on the same graph. Straight line approximations of the base flow were approximated over discrete, but variable, periods of time. Since the discharge curves are relatively flat most of the fall, winter and spring, this could be fairly easily done. During the summer and large storm events, the process was more difficult. Attempts were made to pick the recession curves and determine the base flow component by polygonal integration (Linsley, et. al., 1975). These records were examined by Dr. Ernest Pogge of the Kansas Water Resources Institute, Lawrence. He indicated that the estimates of the recession flows were probably overestimated, but that the other estimates were probably reasonable.

An average daily gain rate of 22.86 cfs over the Macksville-Zenith reach was estimated. This may be expressed as 5.73 cubic feet of water

gained per day per foot of channel length. The following table is a summary of the reduced data and computation of the above figures. The gain was computed for the days during which gain was noted and then divided by the period of record to give average daily rate of gain. As an example, tabulation of Water Year 1978 is reproduced here (see Figure I-1).

Figure I-1. Average Annual Rate of Gain; Water Year 1978

Rattlesnake Creek, Macksville to Zenith, Kansas

$\Delta t$ days	$f_m$ cfs	$f_z$ cfs	$\Delta f$ cfs	$\Delta t \cdot \Delta f$ cfs · day
24	16	31	+15	360
58	18	36	+18	1044
62	20	43	+23	1426
92	25	56	+31	2852
26	35	62	+27	702
5	43	66	+23	115
33	32	41	+9	297
11	12	18	+6	66

311 days ————— totals ————— 6862 cfs · day

average daily rate of gain over period of record:  $6862/365 = 18.8$  cfs

$f_m$ : average daily base flow component at Macksville

$f_z$ : " " " " " " Zenith

$\Delta f = f_z - f_m$ : average daily rate of change in base flow over the reach

Six Year Average Rate of Gain

Water Year	$\Delta t \cdot \Delta f$ total per year	$\frac{\Delta t \cdot \Delta f}{365}$
1973	1331	10.73
1974	12630.5	34.60
1975	7910.5	21.67
1976	5045	13.28
1977	5551	15.21
1978	6862	18.8
Average		22.86 cfs

The average five year rate of gain over the 66.2 reach is 22.86 cfs.

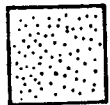
This figure may also be expressed as 0.35 cfs/mile.

Total daily flux is computed as  
 $(0.35 \text{ ft}^3/\text{sec}) \cdot (86400 \text{ sec/day}) =$   
 $3024 \text{ ft}^3/\text{day} \cdot \text{mile}$   
 or: 5.73  $\text{ft}^3/\text{day} \cdot \text{foot}$

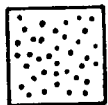
Yearly average gain: 16550 AF

## Appendix II. Lithologic Logs

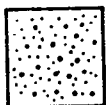
### Lithologies



--Sand



--Gravel



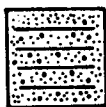
--Sand & gravel



--Clay - silt



--Sandy clay - silt



-- Sand and/or gravel  
with clay lenses



--Siltstone/mudstone



--Shale

1 well number

well screen

1200 depth below L.S. (feet)

S.C. = specific conductivity ( $\mu\text{mho/cm}$ )

T. = temperature ( $^{\circ}\text{C}$ )

L.S. = land surface (feet above mean sea level)

B.R. = bedrock

T.D. = total depth

q = quartz

qa = quartz arkose

b = brown

r = red

y = yellow

g = gray

o = orange

bl = black

t = tan

bu = blue

ss = sandstone

gr = green

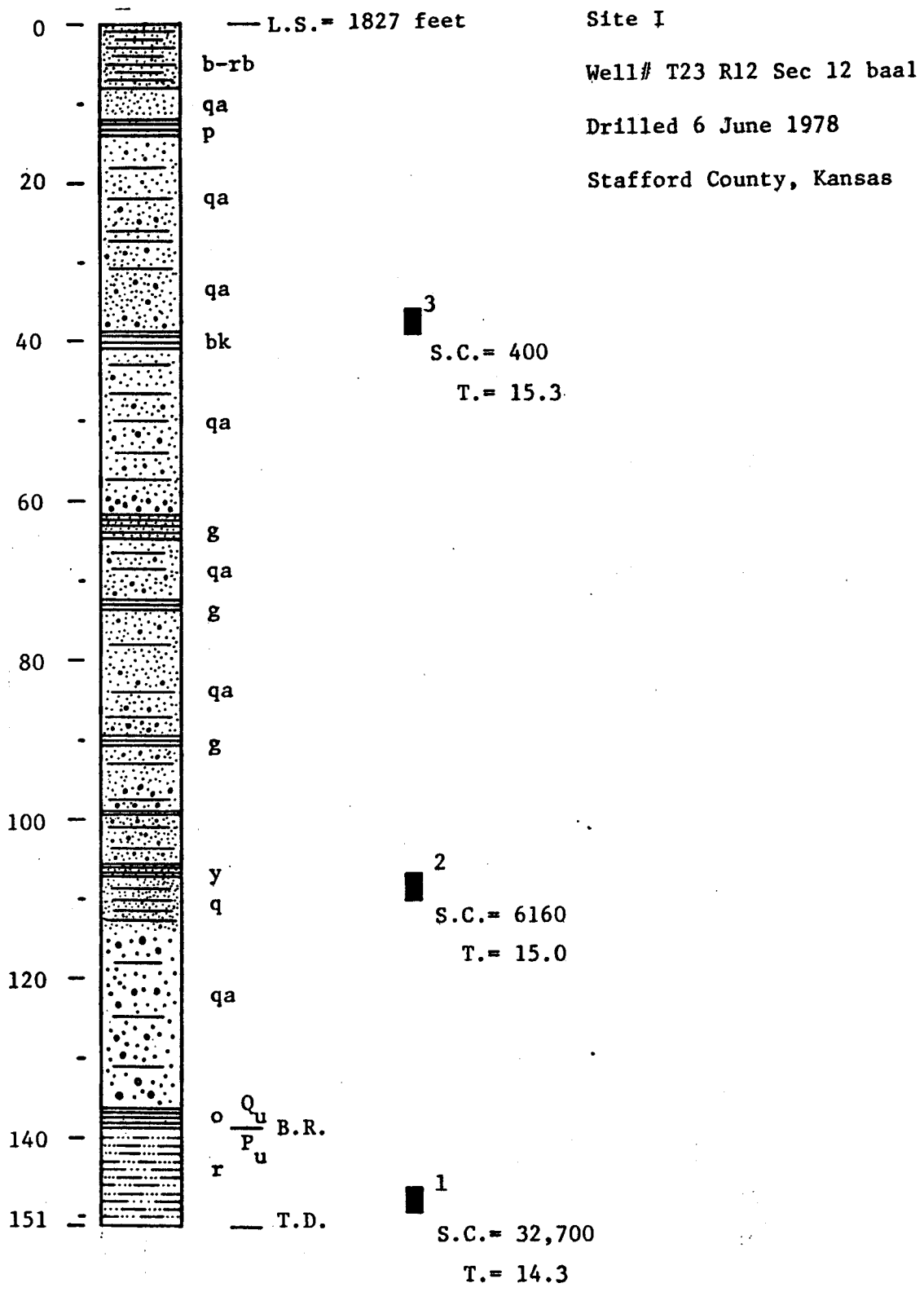
p = pink

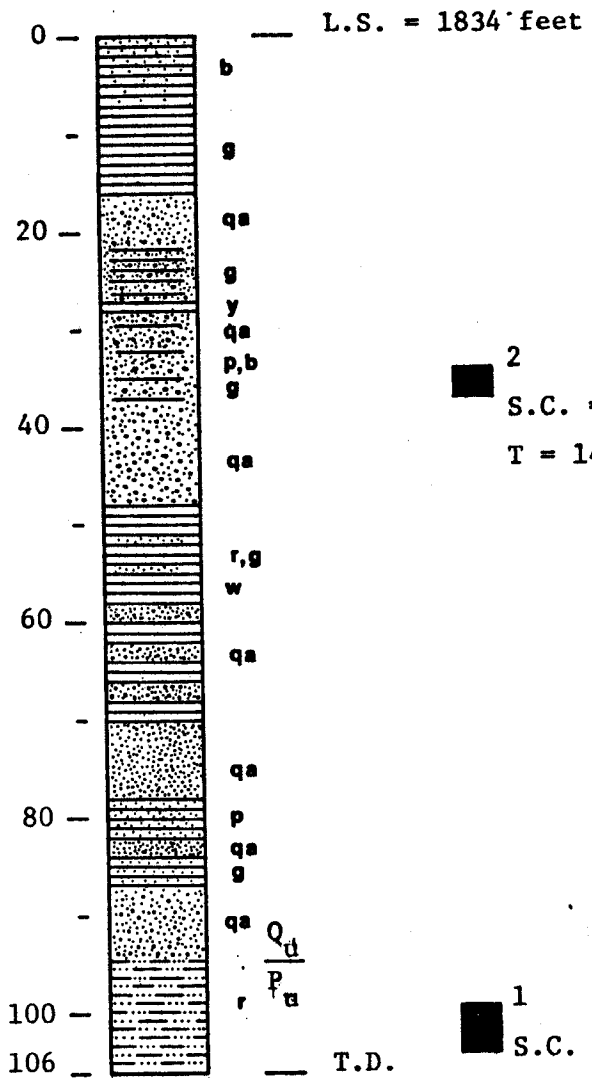
w = white

dk = dark

lt = light

gyp = gypsum





Site II  
 Well# T23 R12 Sec 36 ab  
 Drilled 13 June 1978  
 Stafford County, Kansas

2  
 S.C. = 702  
 T = 14.4

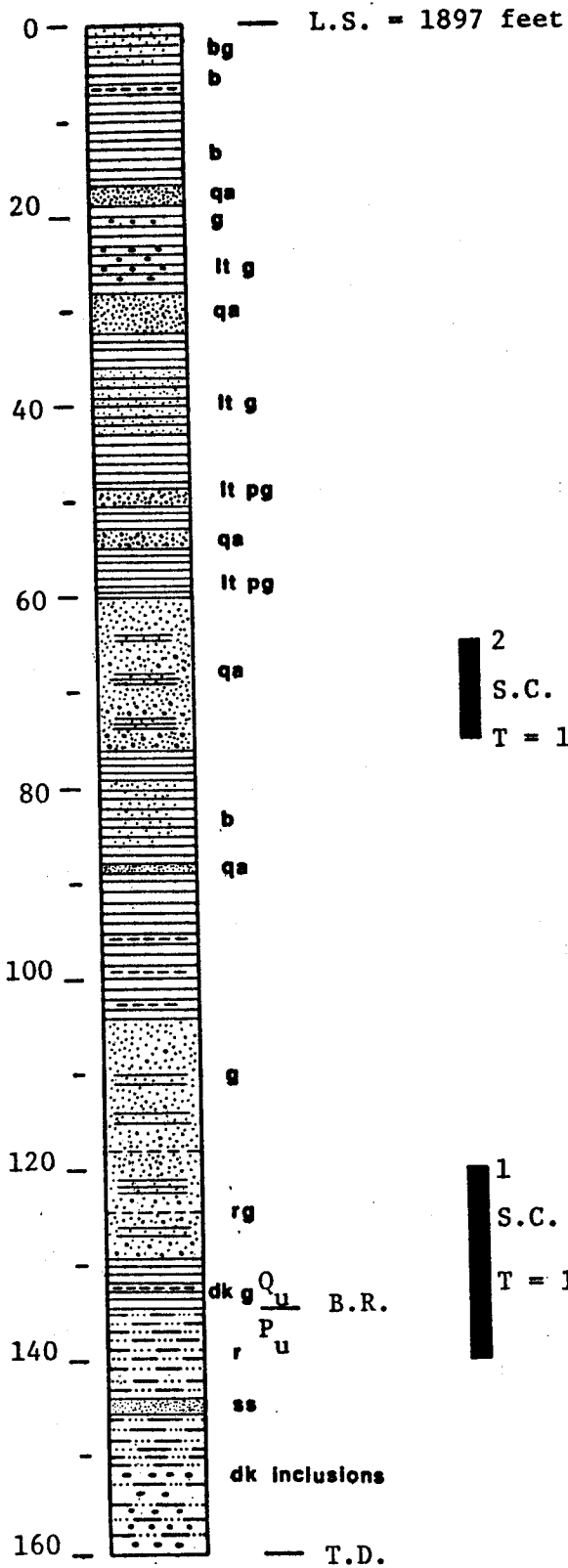
1  
 S.C. = 2820  
 T = 15.2

Site III

Well# T23 R13 Sec 36 dccl

Drilled 15 June 1978

Stafford County, Kansas



----- caliche

..... cementations

2

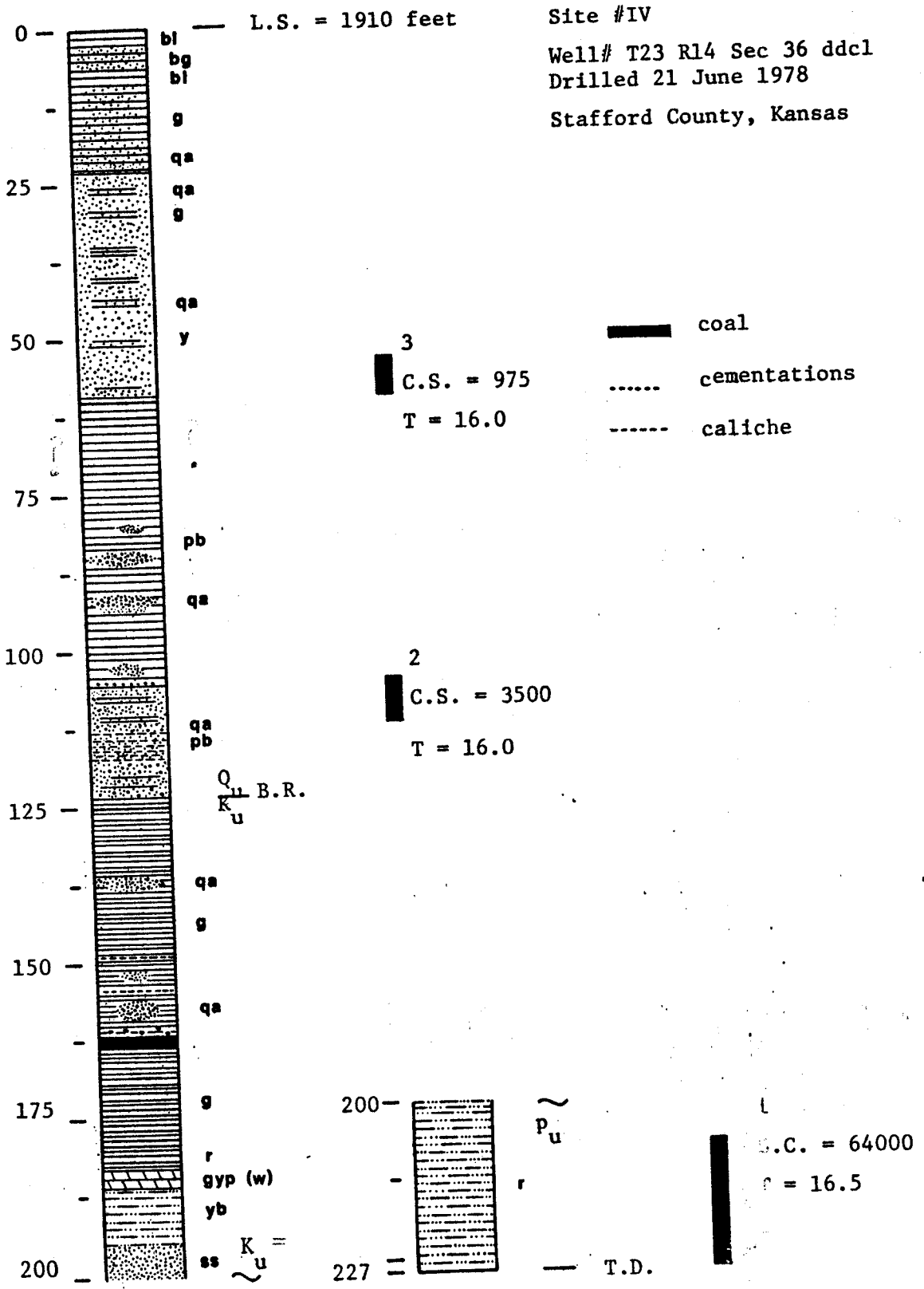
S.C. = 510

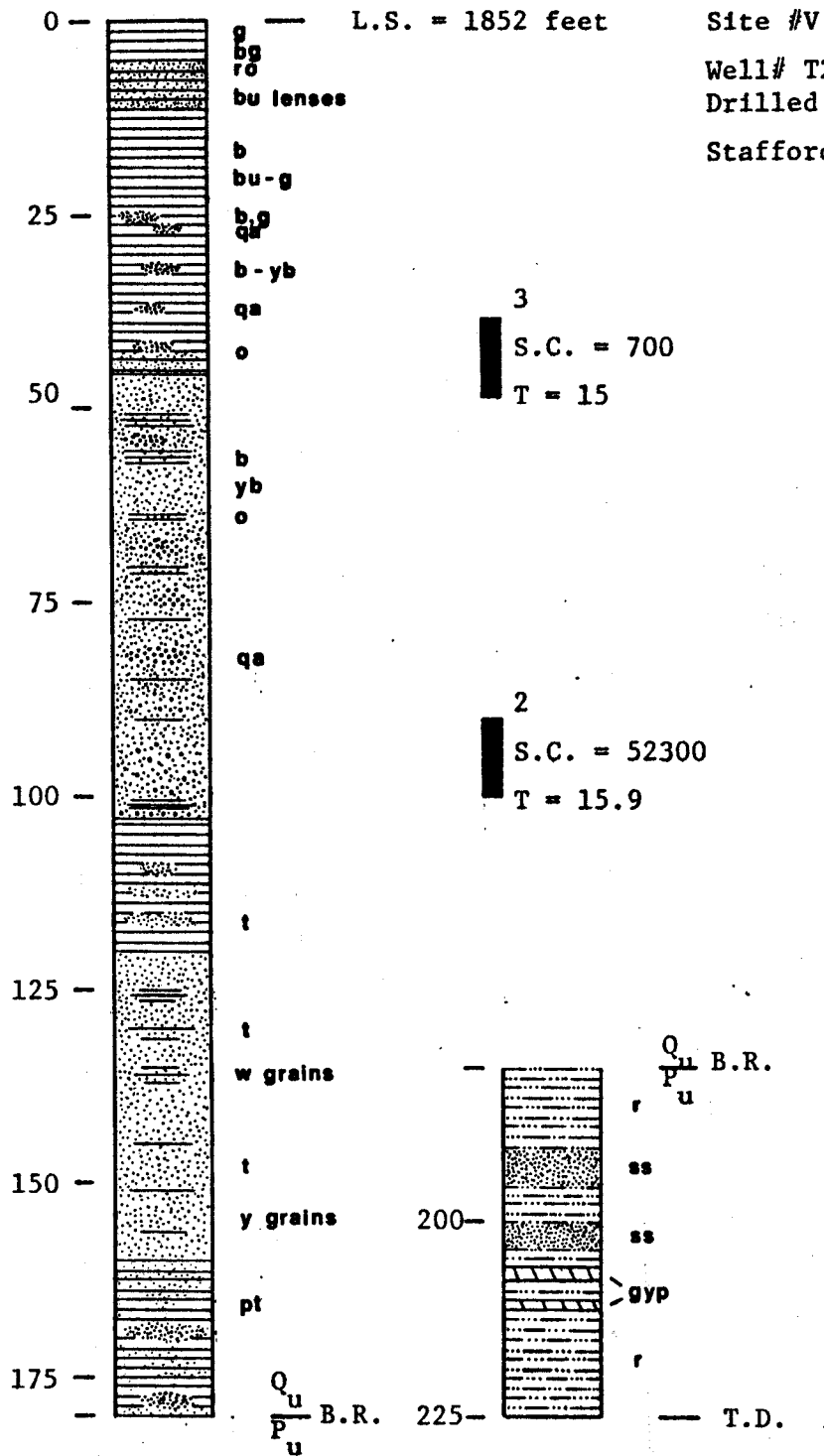
T = 15.2

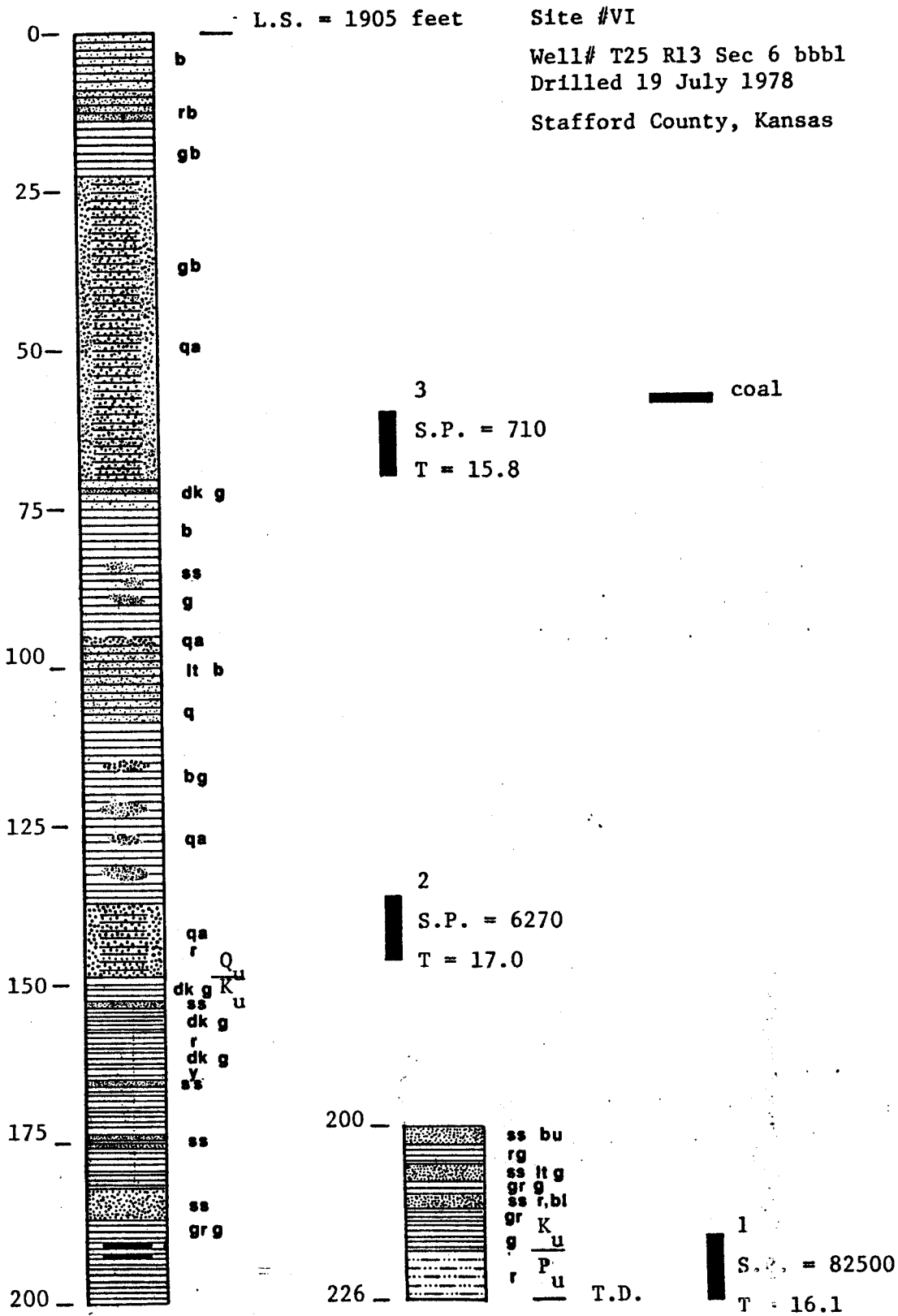
1

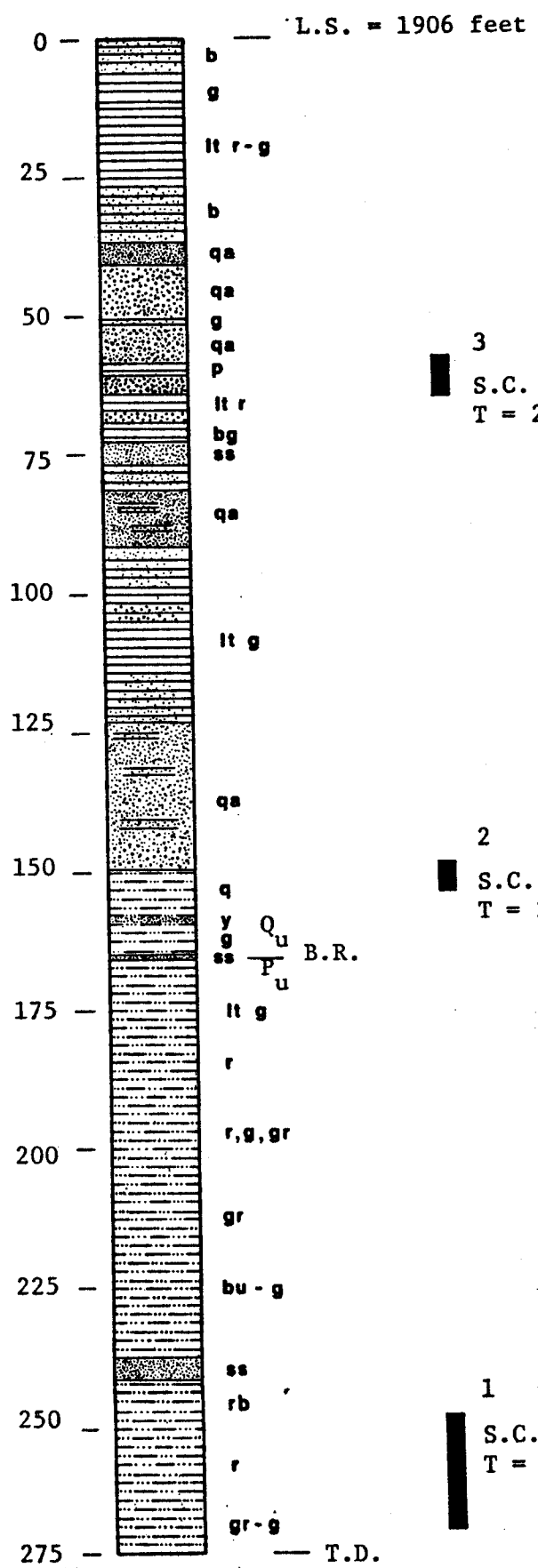
S.C. = 1630

T = 15.3









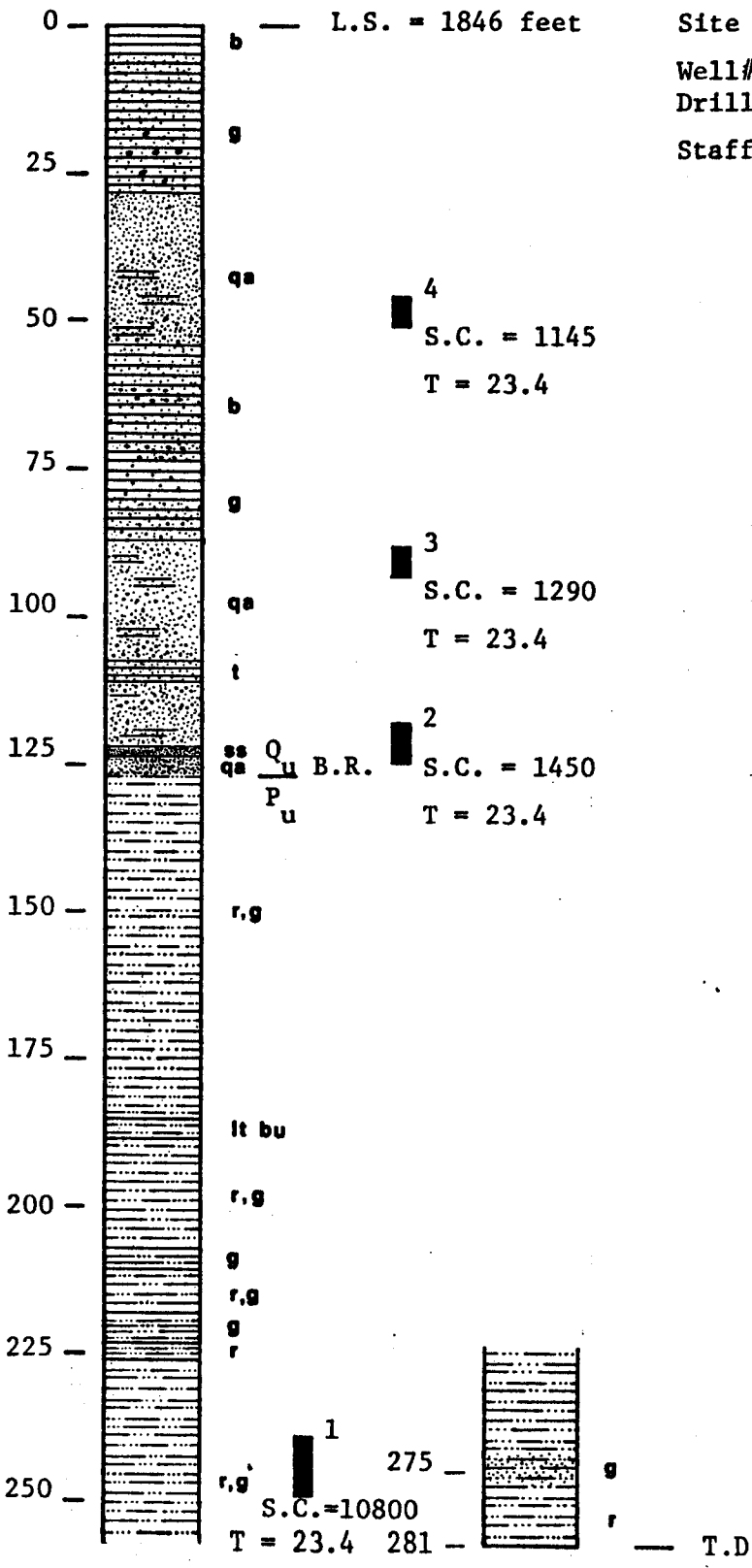
Site #VII  
 Well# T24 R13 Sec 36 ddd1  
 Drilled 1 August 1978  
 Stafford County, Kansas

3  
 S.C. = 648  
 T = 24

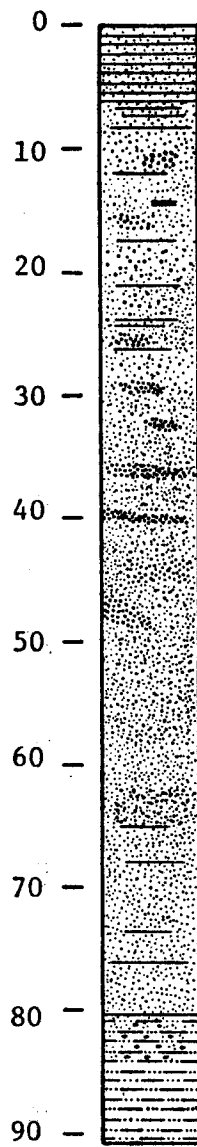
2  
 S.C. = 1020  
 T = 24

1  
 S.C. = 73200  
 T = 24

Qu  
 Pu B.R.



Site VIII  
 Well# T25 R14 Sec 11 aal  
 Drilled 14 August 1978  
 Stafford County, Kansas



— L.S. = 1750 feet

Site #IX  
 Well# T24 R10 Sec 31 cbcl  
 Drilled 25 July 1979  
 Stafford County, Kansas

qa (b)

qa (r)

qa

qa

qa

3  
 S.C. = 3170  
 T = 23.4

..... cementations

2  
 S.C. = 4460  
 T = 23.4

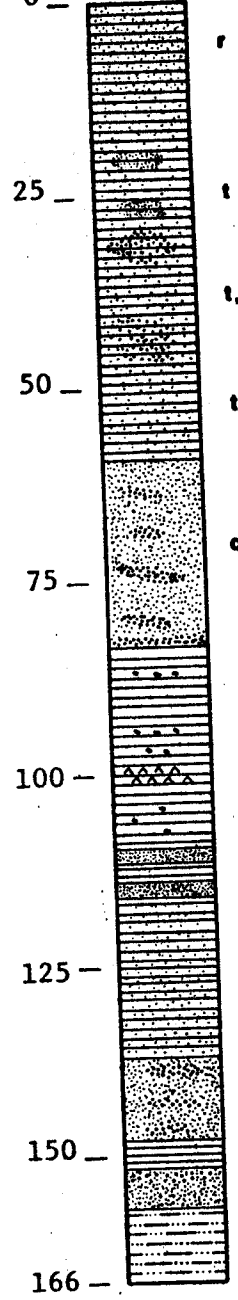
Qu B.R.  
 Pu

1  
 S.C. = 10000  
 T = 23.4

— T.D.

0 — L.S. = 1790 feet

Site #X  
Well# T24 R10 Sec 6 dccl  
Drilled 2 August 1979  
Reno County, Kansas



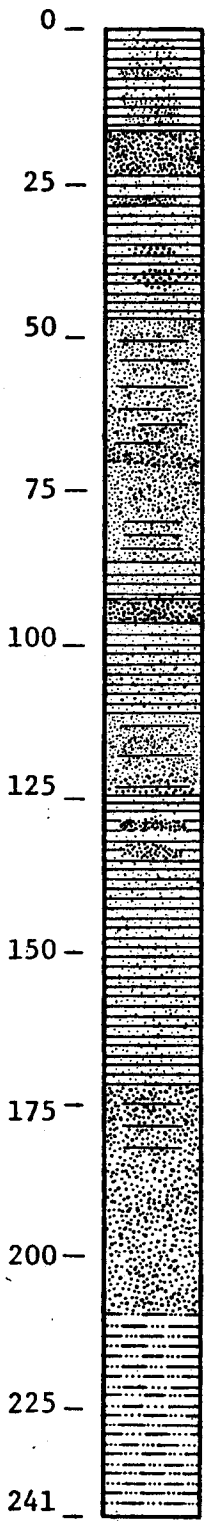
4  
 ■ S.C.=1020 ^^^^^ shells  
 T = 22.9

3  
 ■ S.C. = 2700  
 T = 21.8

2  
 ■ S.C. = 4900  
 T = 22.9

1  
 ■ S.C. = 6000  
 T = 21.8

Qu  
 Pu  
 B.R.  
 — T.D.



L.S. = 1763 feet

Site #XI

Well# T22 R10 Sec 6 cbb1

Drilled 16 August 1979

Reno County, Kansas

3  
 S.C. = 4000  
 T = 22.9

2 not drilled

$\frac{Q_u}{P_u}$  B.R.

1  
 S.C. = 21300  
 T = 22.9

### Appendix III. Construction of Observation Well Sites

All bore holes were drilled with a Failing 1250 hydraulic rotary drilling rig. In the 1978 drilling season only eight inch bits were available. This led to difficulties in the installation of the five inch PVC screen and casing used to complete the wells. The difficulties arose in part due to the limited clearance when casing was being installed in the eight inch holes and the fact that the holes were not always straight. Added complications occurred because the subsurface clay layers tended to deform around the hole, thus interfering with the casing as it was put into the ground. Consequently, the casing had to be driven past these obstructions on many occasions. This was generally accomplished without incident, except at one location, when a casing was shattered and the hole had to be plugged and abandoned. From another consideration, the collapse of the clay was beneficial, for it enhanced the isolation of the various sand and gravel formations. All wells completed in bedrock or the lower part of the Pleistocene aquifer were grouted with a mixture of Portland cement and bentonite mud. Shallow wells were only grouted near the surface. All wells were completed with a concrete pad at the surface.

Organic drilling mud was tried on a few holes, but, owing to the high unit material cost, the extra attention to water maintenance, and the expense of purification chemicals, this product was abandoned. The primary benefit, simplified well development, was outweighed by the above factors. Exclusive use of bentonite mud alleviates these problems, but requires more attention to development of the well in order to clean the gravel pack.

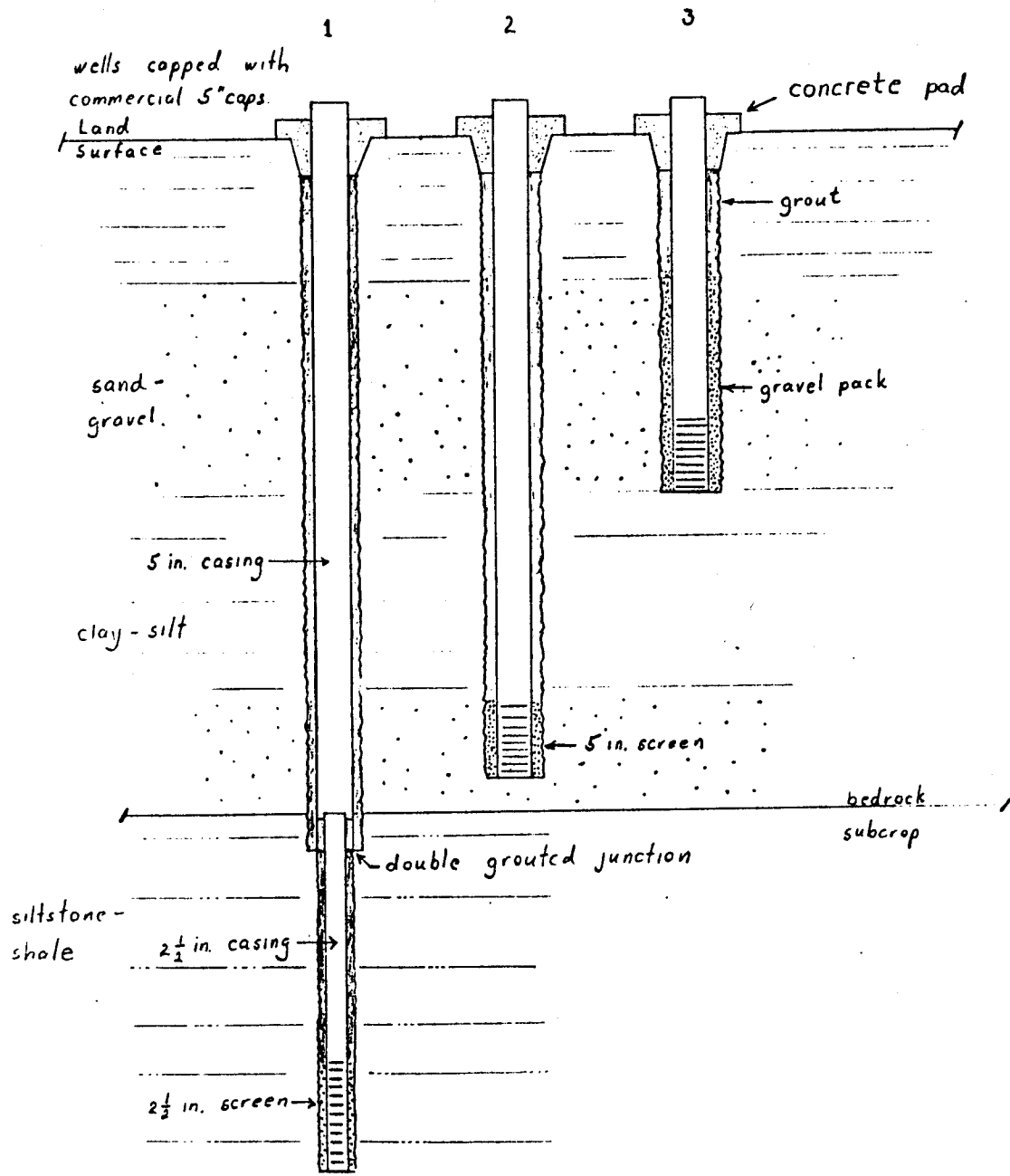
In the 1979 drilling season 10 and 12 inch test holes were drilled. Drilling proceeded by boring a 4-3/4 inch pilot hole and reaming to final size with a 10 or 12 inch drag bit. Sample logs tended to be more accurate with the small pilot hole since the return fluid velocity up the hole is increased. The travel time from drill bit to mud pit is reduced. The larger diameter hole also speeded up the installation of the well casing since the effects of caving sand and clay collapse around the hole are minimized. Gravel packing and grouting are more easily performed in the larger annular space.

Wells completed in the bedrock were originally completed in one continuous operation, namely drilling a single hole to the desired depth in bedrock and then casing and screening the total depth. Several problems made this approach undesirable. First, drilling in the bedrock must be carried out with sufficiently weighted mud to bring up the heavy gravel which continues to sluff into the hole from the unconsolidated material above. Consequently, a mud cake tends to build up on the wall of the well, reducing an already low permeability. Second, the likelihood of placing the screen at the desired location is reduced by the possibility that sand will bridge on the casing and cause the screen to be improperly placed. Third, the difficulty of placing a grout seal in the bedrock hole is increased because of the difficulty of placing a tremie pipe at the bedrock subcrop. The low permeability of the bedrock requires a good grout seal in order to avoid leakage from the unconsolidated aquifer when the well is pumped, as well as discharge to the unconsolidated aquifer when the latter is pumped.

In order to circumvent these problems, it has subsequently been found advantageous to complete the bedrock wells in two operations.

First, a hole is drilled and cased a few feet into bedrock and then grouted. Drilling then proceeds through the five-inch casing with a 4-3/4 inch shale bit. This drilling may be done with a light mud which avoids building a thick cake on the bedrock wall. No gravel may enter the hole since the unconsolidated material is now cased out. Thus, the hole stays clean and the logs are more accurate. The bedrock hole is screened and cased with 2½-inch PVC pipe which extends back up into the five-inch casing (see Fig. III-1). This feeder pipe is centered as well as possible to insure a uniform annular space for a uniform gravel pack and grout seal. A tremie pipe is run down to screen level and gravel is placed to just above the screen. Fine sand is then placed above the gravel. Finally, the hole is carefully grouted with neat cement back up into the five-inch casing. After the grout is set up, the 2½-inch feeder pipe is allowed to feed into the main casing. Figure III-1 is an elevation view of a typical site with three wells completed.

Fig II-1 Schematic of Typical Observation Well Nest



Appendix IV. Well Hydrographs.  
(adjusted for pure water as a standard fluid,  
showing comparisons between wells and sites  
on a quarterly basis)

Legend

1743 = elevation above mean sea level

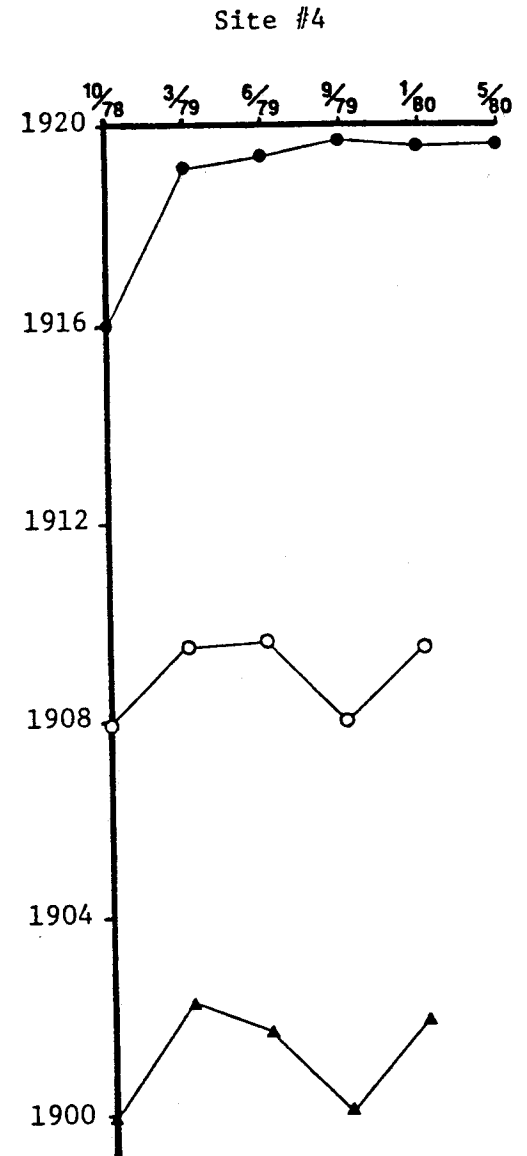
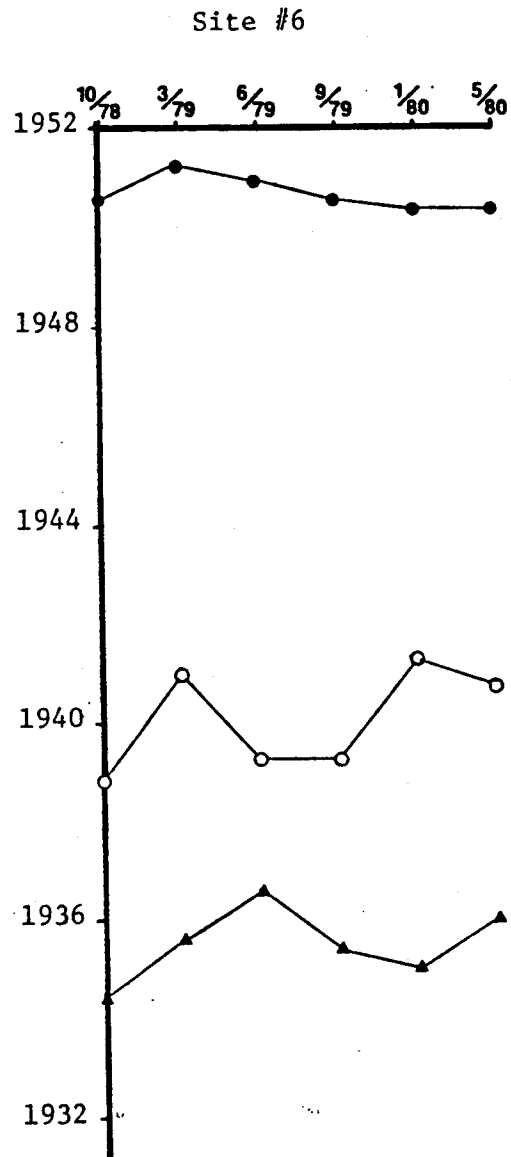
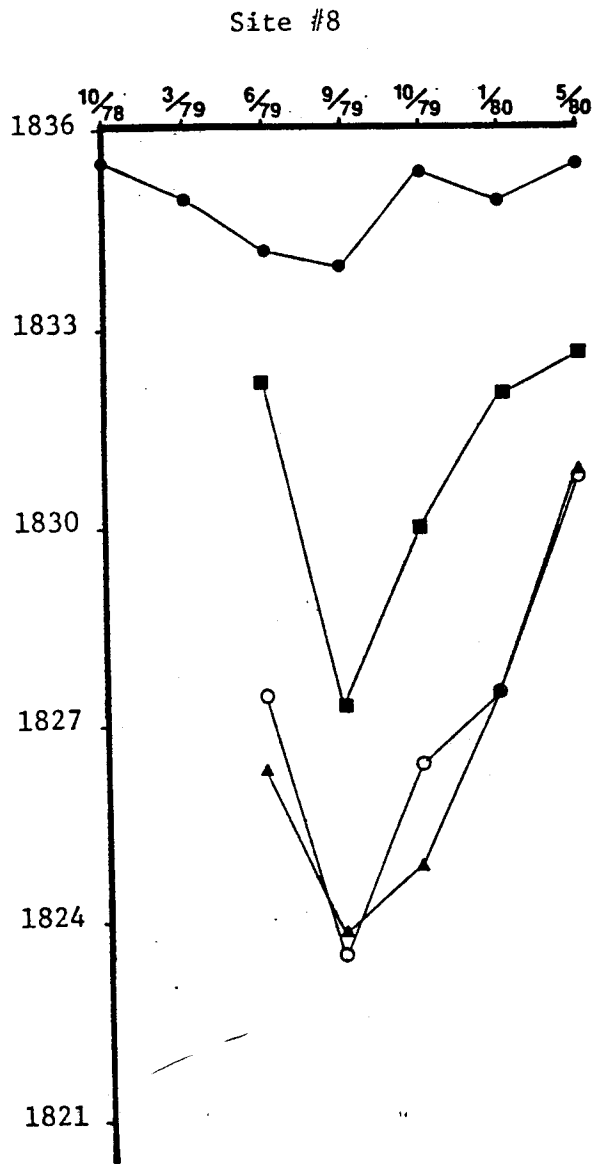
10/79 = date of measurement (month/year)

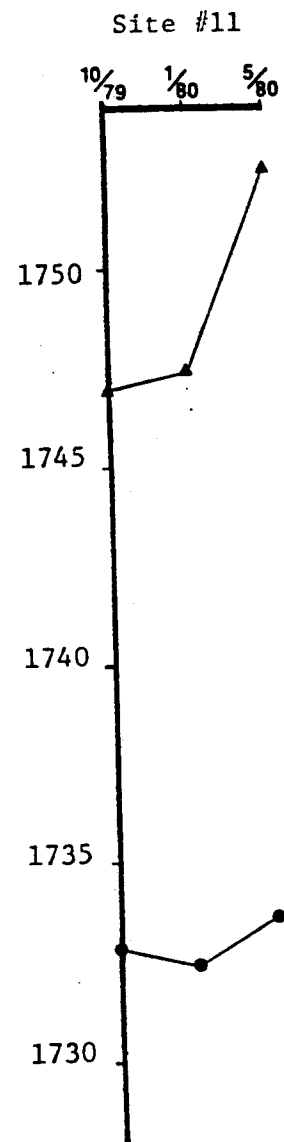
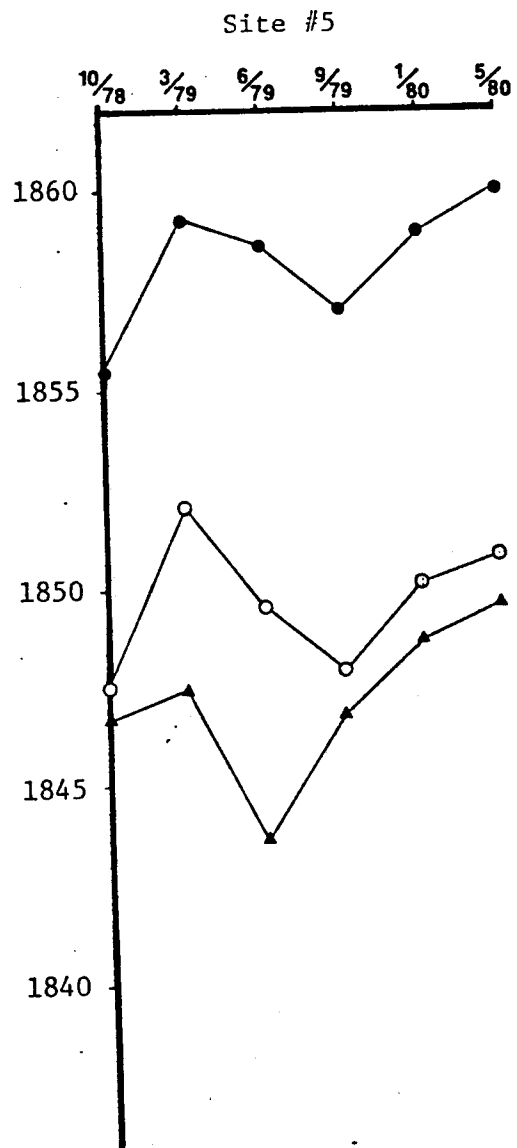
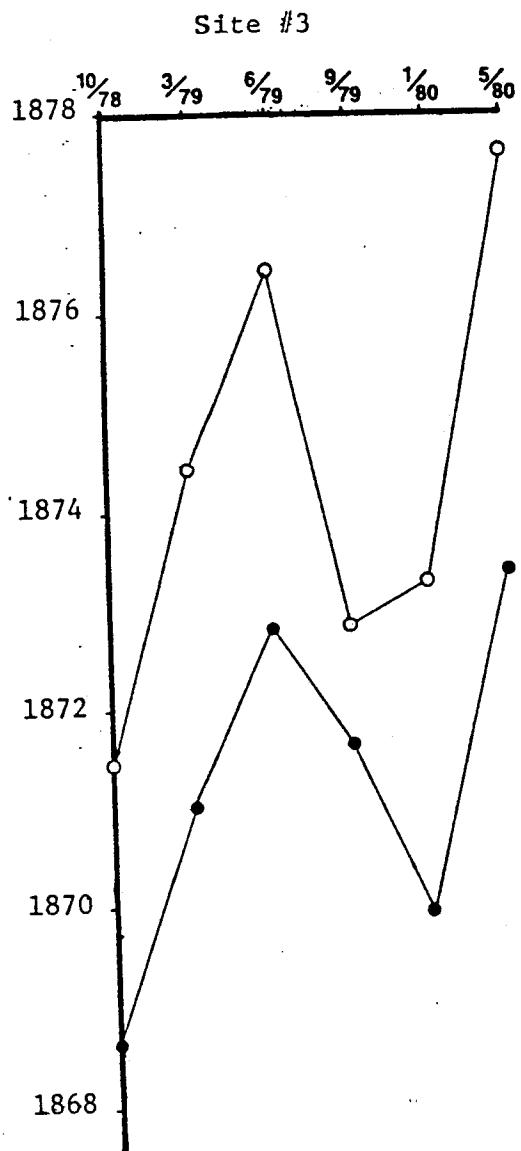
● Well #1

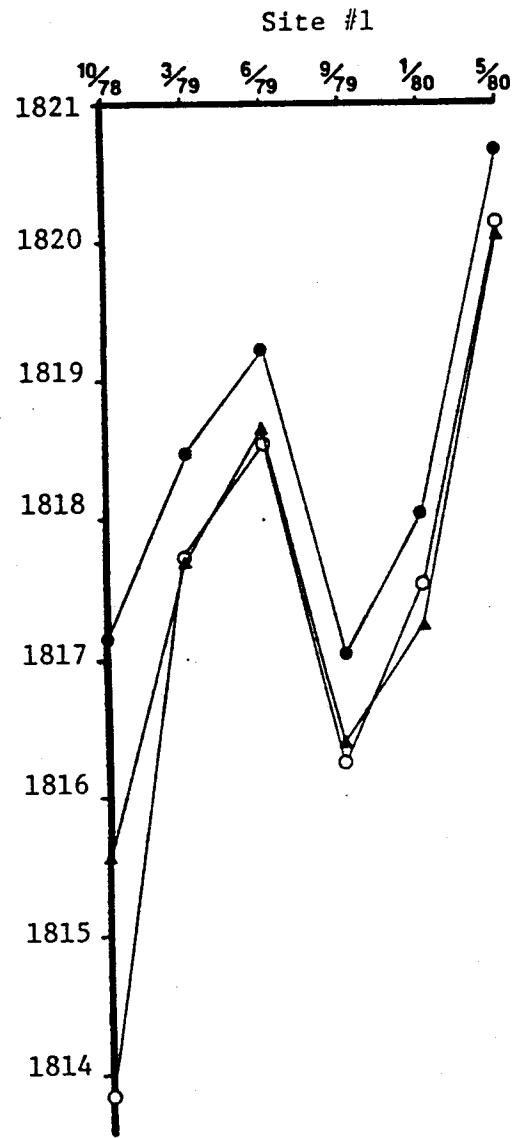
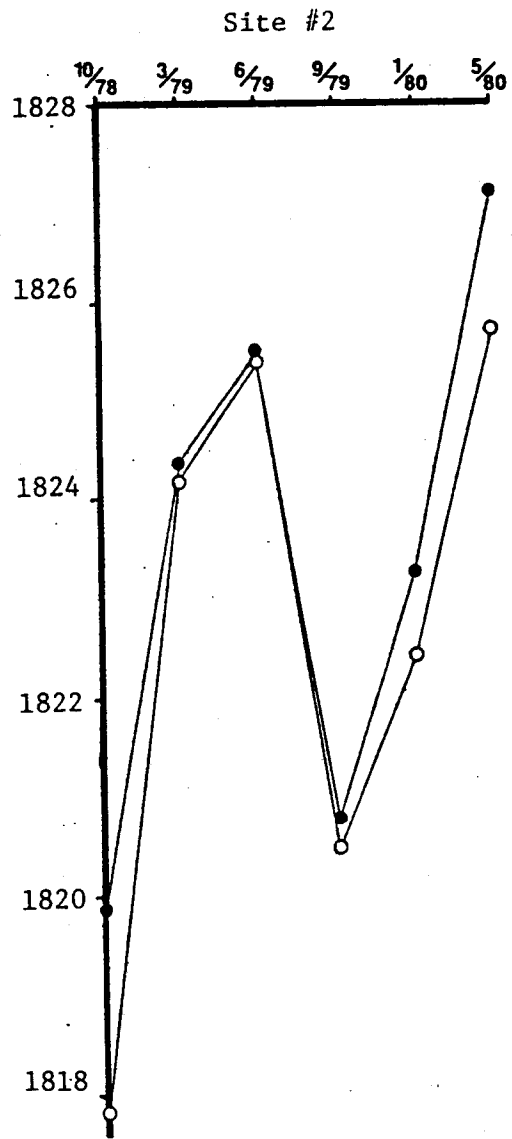
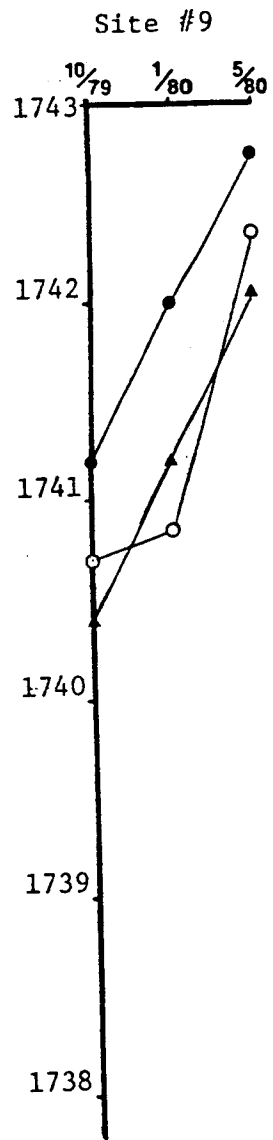
○ Well #2

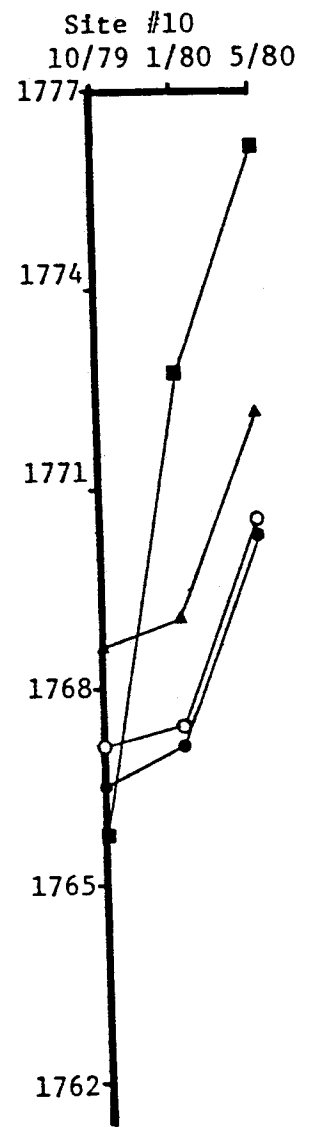
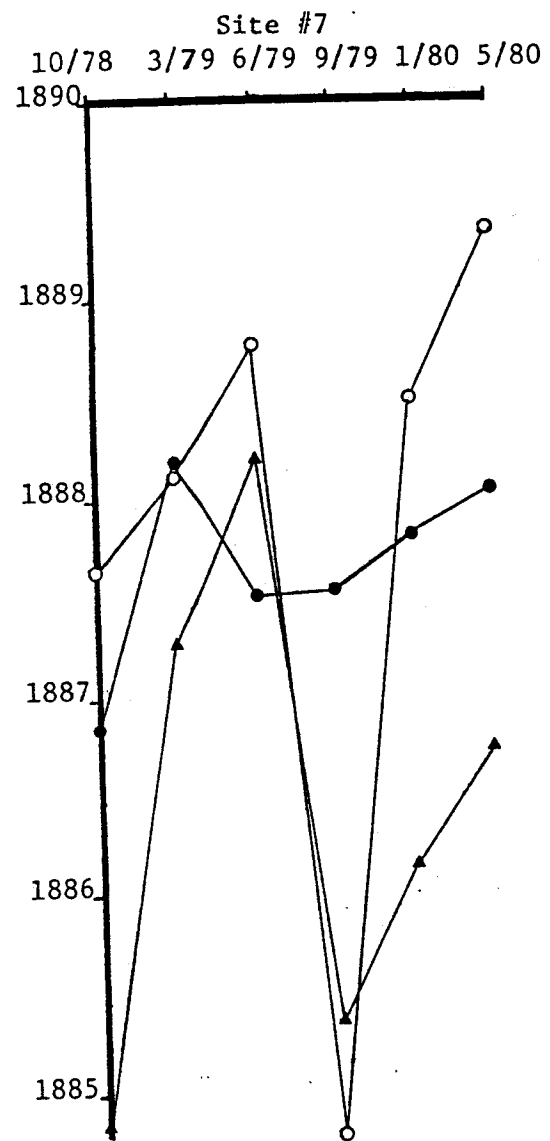
▲ Well #3

■ Well #4









Appendix V. A General Outline of the Principles of the Flow of Viscous  
Fluids in Porous Media

Darcy's Law

The basic principle describing the laminar flow of a viscous fluid through a porous material is called Darcy's Law. It was originally derived as an empirical law from experiments conducted in 1856 by Henri Darcy (see any basic groundwater text). In differential form, the law is generally stated as:

$$V-1) \quad q = -K \frac{dh}{dl}$$

where  $h$  is the hydraulic head (L)

$q$  is the specific discharge (L/T)

$K$  is the hydraulic conductivity (L/T)

$\frac{dh}{dl}$  is the hydraulic head gradient (L/T)

An alternative form which considers the porosity of the material,  $n$ , is:

$$V-2) \quad v = -\frac{K}{n} \frac{dh}{dl}$$

where  $v$  is referred to as the average linear velocity of the fluid.

This latter equation emphasizes the fact that in the Darcy equation the microscopic details of flow are ignored and only the gross, macroscopic, statistically averaged details of the flow are considered (Hubbert, 1956, derives the Darcy equation from the Navier-Stokes Equation by averaging the forces of motion over a representative elementary volume).

## Fluid Potential

Consideration of equation V-1 leads to the conclusion that the movement of a fluid is controlled by an energy gradient.

Hubbert (1940) demonstrated that the hydraulic head,  $h$ , is proportional to the hydraulic potential  $\phi$  such that

$$V-3) \quad gh = \phi$$

and has units of energy per unit mass. The term  $\phi$ , also called Hubbert's potential, has the form

$$V-4) \quad \phi = gz + \int_{P_0}^P \frac{dp}{\rho}$$

where  $g$  = acceleration due to gravity ( $L/T^2$ )

$z$  = elevation of a point above an arbitrary datum ( $L$ )

$p$  = pressure of the fluid column at a point ( $L^2/T^2$ )

$\rho$  = specific density of the fluid ( $M/T^3$ )

Thus, the driving force of the fluid is mechanical, which results from the action of gravity and fluid pressure; and the direction of flow must be in the direction of decreasing mechanical energy.

In fluid mechanics, the basic principle of fluid motion is expressed for a hypothetical nonviscous fluid as Bernoulli's law:

$$V-5) \quad \phi = gz + \int_{P_0}^P \frac{dp}{\rho} + \frac{v^2}{2} = \text{const.}$$

which states that for a frictionless motion, the mechanical energy is constant in the system and potential energy is converted entirely to

kinetic energy along the flow line. Equation V-4 differs significantly from equation V-5 in the following ways. First, the fluid is considered to have viscosity and hence experiences losses due to friction along a flow line. Second, the velocities are considered to be of such a small magnitude that the kinetic energy term  $\frac{v^2}{2}$  is negligible. Hence, the flow of groundwater results in a conversion of mechanical energy to heat energy along the flow path (Dominico, 1972).

### Hydraulic Conductivity

Thus far, the parameter K, the hydraulic conductivity, has gone unexamined. Hubbert, realizing that Darcy's law in its original form did not actually enumerate the relationship of density, viscosity, and pore geometry to the flow phenomena, gave an analysis of the parameter K based on the mechanics of flow. He derived equations describing the driving and resistive forces per unit mass of fluid

$$V-6) \quad \frac{F_d}{\rho n \cdot \Delta V} = - \frac{\partial \phi}{\partial l}$$

$$V-7) \quad \frac{F_d}{\rho n \cdot \Delta V} = - \frac{1}{N} \cdot \frac{\eta}{\rho} \cdot \frac{q}{d^2}$$

where  $\Delta V$  = a unit volume

$\eta$  = the fluid viscosity

$n$  = porosity of the unit volume

$N$  = a constant of proportionality dependent upon grain geometry

$d$  = representative grain diameter

$l$  = a length along a flow path

$\Delta V$  = a representative elementary volume

other symbols as previously defined.

A principle assumption in deriving these equations is that the flow velocity is small enough so that inertial forces are negligible. Therefore, for steady flow, equations V-6 and V-7 must sum to 0. The result of this exercise is that

$$\text{V-8) } K = Nd^2 \frac{\rho g}{\eta}$$

Thus,  $K$  is seen to be dependent upon fluid properties and the geometrical properties of the porous media. A new term may be defined, the coefficient of permeability of the medium, which is expressed as

$$\text{V-9) } k = Nd^2 \quad (L^2)$$

while the term  $\rho/\eta$  is the coefficient of permeability of the fluid.

Using equations V-1, V-3, V-8, and V-9, Darcy's law may finally be stated as

$$\text{V-10) } q = -k \frac{\rho}{\eta} \frac{d\phi}{dl} = -\sigma \frac{d\phi}{dl}$$

where  $\sigma$  is the Darcy permeability.

## Spatial Variation of Permeability

In general, a porous medium is not uniform throughout its extent. Hence, the hydraulic conductivity varies throughout the medium as the fluid moves from point to point. Furthermore, such phenomena as cementation of grains, preferential alignment of grains, or substantial changes in grain size over small distances, lead to directional differences of the hydraulic conductivity at a point. Hence, in general, the hydraulic conductivity is considered to be anisotropic and inhomogeneous over an extensive domain. Therefore, the Darcy Permeability  $\sigma$  is a second order tensor in its most general form.

$$V-11) \quad \sigma_T = \frac{K_T}{g} = \begin{bmatrix} \sigma_{xx} & \sigma_{xy} & \sigma_{xz} \\ \sigma_{yx} & \sigma_{yy} & \sigma_{yz} \\ \sigma_{zx} & \sigma_{zy} & \sigma_{zz} \end{bmatrix} = \frac{\rho}{\eta} \begin{bmatrix} k_{xx} & k_{xy} & k_{xz} \\ k_{yx} & k_{yy} & k_{yz} \\ k_{zx} & k_{zy} & k_{zz} \end{bmatrix}$$

### Generalized Darcy Flow

The generalization of  $\sigma$  makes possible a generalization of the Darcy equation of flow. If  $J$  is the hydraulic gradient with components  $J_x$ ,  $J_y$ , and  $J_z$  and  $\vec{q}$  is the specific discharge vector with components  $q_x$ ,  $q_y$ , and  $q_z$ , then the general equation for Darcian flow is

$$\vec{q} = -\sigma_T \cdot J \quad \left( J \text{ is the vector equivalent of } \frac{d\phi}{dl} \right)$$

or

$$V-12) \quad \vec{q} = - \begin{bmatrix} \sigma_{xx} & \sigma_{xy} & \sigma_{xz} \\ \sigma_{yx} & \sigma_{yy} & \sigma_{yz} \\ \sigma_{zx} & \sigma_{zy} & \sigma_{zz} \end{bmatrix} \cdot \begin{bmatrix} J_x \\ J_y \\ J_z \end{bmatrix}$$

(after Bear, 1980)

### Range of Validity of Darcy Flow

From the preceding discussion, it is obvious that Darcian flow implies a direct proportionality between the specific discharge  $\vec{q}$  and the hydraulic gradient  $J$ . The question of the range of validity of this relationship must be addressed. Hubbert (1940) summarizes the problem as follows:

for uniform rectilinear macroscopic flow of a liquid the integral over a macroscopic volume of forces due to inertia is zero, so that these can exercise no direct retarding effect upon the fluid motion. What they do, however, is produce distortion which increases the terms of the form  $\partial^2 u / \partial^2 y$ , upon which the resistivity forces depend ( $f_{ryx} = n \frac{\partial^2 u}{\partial y^2} \cdot dV$ ). Since the forces due to inertia increase as the square of the velocity, the effect is nonlinear with respect to  $q$ ; and for values of  $q$  for which the inertial forces are not negligible the resistance to flow must increase at a progressively greater rate as  $q$  is increased.

From this summary, it is seen that the Darcy law remains valid only for values of  $q$  for which inertial forces remain negligible. Hubbert points out that Darcian flow ceases to exist even before turbulence develops in the flow system. Hubbert suggests a Reynolds number of 4 as the upper limit for Darcian flow, while Bear (1972, 1980) suggests the Darcy Law is valid for a range of the Reynolds number below 1 to 10.

## The Flow of Fluids in Extensive Media

Adopting the Eulerian approach of setting up a fixed control volume  $\delta V$  in a porous medium and monitoring the movement of fluid through that volume, and specifying that no sources or sinks of matter may exist in the control volume, it can be shown (Bear, 1980) that for  $\rho = \rho(p, c)$  ( $p$  = pressure and  $c$  = a solute concentration)

$$V-13) \quad -\text{div} \rho \vec{q} = \rho S_{op} \frac{\partial p}{\partial t} + n \frac{\partial \rho}{\partial c} \frac{\partial c}{\partial t}$$

where  $\rho \vec{q}$  is the mass flux,  $S_{op}$  is the specific storativity and  $n$  is the porosity of the aquifer. This is the mass conservation equation.

A continuity equation of flow can be derived by using the Darcy flow equation for  $\vec{q}$ , by assuming incompressible flow and by assuming no solutes in the fluid. The result is:

$$V-14) \quad \text{div} (K_T \cdot \text{grad} \phi) = S_{op} \frac{\partial \phi}{\partial t}$$

where  $K_T$  is in general a symmetric tensor of rank two,  $\phi = \phi(p)$  and  $K_T = K_T(\rho, \eta)$ . For most groundwater work,  $K$  is assumed independent of changes in  $\rho$  and  $\eta$ ; and  $\rho$  is assumed to be independent of changes in pressure. This equation, the diffusion equation, describes unsteady flow within a continuous porous medium in which no sources or sinks operate. For steady flow,  $\partial \phi / \partial t = 0$ . For an isotropic, homogeneous medium  $K_T = K$ , and equation V-14 may be shown to reduce to Laplace's equation. Groundwater flow problems may be solved mathematically by applying these equations to the appropriate flow domains along with the appropriate initial and boundary conditions. Bear (1980) lists an extensive catalog of useful

boundary conditions.

The effect of the implied change in hydraulic conductivity on the exact flow path of fluid is examined by Hubbert (1940). He indicates that for  $K_1/K_2 \approx .01$ , lines of flow will refract almost 90 degrees across the boundary. If flow is directed nearly vertically out of the bedrock, then it will tend to flow parallel to the boundary on the unconsolidated side, the side with the larger K value.

### Special Considerations

#### Flow Nets and Potentiometric Surfaces

As Hubert (1940) points out, a property which can be measured over an extensive domain is termed a field. These fields may be scalar, vector, or tensor in nature and are assumed to vary continuously over the domain of interest. Hydraulic potential is a field property of a porous medium containing a fluid. If no motion occurs, then the hydraulic potential is invariant over the entire field. Conversely, if the fluid is in motion, then at every point in the flow field, there is a value of the hydraulic potential which in general will differ in a continuous fashion from the value at a neighboring point. Hence, in a three-dimensional domain, all equal valued measurements of  $\phi$  constitute a surface; the  $\phi$  values of the field being greater on one side of the surface and smaller on the other side, than the value of the surface itself. In general, these will be curvilinear surfaces.

The generalized Darcy law states that the direction of flow in a homogeneous, isotropic medium is  $-\text{grad } \phi$ . where grad is the gradient of the field, and defined as the direction of maximum rate of change of the field property. The gradient is normal to the equipotential surfaces.

Hence, generalized three-dimensional flow can be visualized as a number of stream tubes and equipotential surfaces which are mutually perpendicular and fill the entire flow domain.

In hydrologic mapping, the general purpose is to construct a series of equipotential surfaces which will allow the computation of the motion of a volume of fluid. The problems involved in creating a three-dimensional flow map are obvious. Generally, a plan view is produced in which the equipotential lines depicted are assumed to be projections of the equipotential surfaces existing in the subsurface. The equipotential lines are said to describe a potentiometric surface. This label is only rigorously true when all measurements used in constructing the map are obtained at the same elevation in the flow field. Furthermore, since generally only one elevation is available per measuring point, a potentiometric map generally results which implicitly assumes vertical equipotential surfaces, ignoring vertical components of flow. Dominico (1972) gives a good review of this topic.

#### Measuring and Comparing Hydraulic Heads in Extensive Porous Media

When a tube piezometer is installed in a porous medium the fluid which fills the tube is assumed to be the same fluid existing at the open end of the piezometer in the aquifer. The Hubbert potential for an incompressible fluid is

$$V-15a) \quad \phi = zg + p/\rho \quad (L^2/T^2, \text{ energy/unit mass})$$

or, equivalently

$$V-15b) \quad h = z + p/\gamma \quad (L, \text{ energy / unit weight})$$

The distance from a standard datum (generally mean sea level) to the lower end of the tube is the gravity head  $z$ . The height of the column of water in the tube is termed the pressure head  $p/\gamma$ . The sum of these is the total or hydraulic head. For the case of a static body of water of uniform density,  $h$  or  $\phi$  will be the same regardless of where in the porous medium the end of the tube piezometer is placed since by definition a static body of water must be equipotential at all points.

For a homogeneous body of water in motion in a homogeneous isotropic porous medium, the situation is somewhat more complicated. If flow is horizontal, the equipotential surfaces are vertical, and a piezometer intercepting a particular value of the potential surface will register the same value of  $h$  at any elevation  $z$  within the flow field. In general, however, two separate piezometers completed at different points will register different head. So long as the fluid density is uniform, the direction of fluid movement is determined directly by comparing these heads. This material is discussed in more detail by Dominico (1972).

When the density of the fluid is not constant, then determination of flow direction by observing heads directly is in general not possible. The pressure head must then be thought of as an integral of some form. A particular case in which this is not true is the case where two wells are completed at the same elevation  $z$  in water where  $\rho = \rho(z)$  alone and flow is completely horizontal. Flow direction is directly determined by measuring  $\Delta h = h_2 - h_1$ . In general, even in water where  $\rho$

is a function of  $z$  alone, such a determination is not possible because  $z_1 \neq z_2$ .

In cases where flow is not horizontal but wells are completed such that  $z_1 = z_2$ , the use of the fresh water equivalent head offers an alternative to an integrated head. Obtaining the integrated head is uncertain due to general lack of knowledge of the function dependence of  $\rho(z)$  at each well. The fresh water equivalent head comparison depends on the supposition that the pressure head in the tube just balances the vertical column of total fluid mass outside the tube. In effect, the column of fluid of density  $\rho_0$  in the tube represents the pressure due to the integrated density of a column of variable density just outside the tube. Since it is assumed for now that  $z_1 = z_2$  but  $\rho_1 \neq \rho_2$ , conversion of the respective pressure heads to a standard fluid will allow determination of the horizontal component of flow between the two wells. The standard reference fluid generally chosen is "fresh" water. The term "pure" water would seem more appropriate.

Determining the fresh water head is a simple process of maintaining a constant mass above a point in space. Hence, let  $\rho_1 = \alpha \rho_f$ , where  $\alpha \geq 1$  and  $\rho_f$  of pure water is generally assumed equal to 1.00, although in reality it may be less than 1.00. Assume the fluid height in tube 1 is  $l_1$ . Then the hydrostatic pressure at point 1 is

$$V-16a) \quad p = \rho_1 l_1 g = \alpha \rho_f l_1 g$$

From equation V-16a it is seen that

$$V-16b) \quad \frac{p}{\rho_1} = l_1 g, \quad \frac{p}{\rho_f} = \alpha l_1 g, \quad \text{and} \quad \alpha = \frac{\rho_1}{\rho_f}$$

Thus the fresh water column must be greater than the column of original water in the tube by a factor of  $\rho_1/\rho_f$ . Similar calculations can be made for tube 2, and the comparison of the fresh water heads in this special case determines the horizontal component of flow between wells 1 and 2.

For more general situations in which  $z_1 \neq z_2 \neq \dots \neq z_n$  and  $\rho(z)$  is not specifically known, the situation is much more complicated. Methods have been published which attempt to deal with the more complex cases (Hubbert, 1953; Lusczynski, 1961; Bond, 1970 and 1972). The following section is based upon Bond (1970), assuming that  $\rho(z)$  is a linear function of  $z$ ,  $\rho \propto \frac{1}{z}$  where  $z$  increases vertically upward from a datum.

#### Determination of the Direction of Vertical Flow Between Nearby Wells

The head difference between wells completed at different elevations in an aquifer whose fluid varies in density with depth along may or may not indicate fluid motion; and the direction of that flow is itself indeterminate from the observation of the head differences unless the wells are completed at the same elevation. Conversion of these heads to fresh water equivalents is not sufficient to resolve the ambiguity. A method is suggested by Bond (1970) to determine the direction of flow in a fluid of variable density.

It is based on computing the theoretical head difference due to the integrated excess mass, when compared to pure water, between the screens of two piezometers completed at different depths in an aquifer whose water varies in density with depth (Fig. V-1). This difference is compared to the actual field values which have been converted to fresh water heads. The wells being measured are assumed close together so

that

$$\frac{dh}{ds} \approx \frac{dh}{dz}$$

This method has been applied to a hypothetical aquifer assumed to have a linear increase of density with depth (McElwee and Macfarlane, personal communication, July, 1980). They solve the integral

$$\Delta H_c^0 = \int_{z_1}^{z_2} \left( \frac{\rho(z)}{\rho_{fw}} - 1 \right) dz$$

for the density relationship

$$\rho(z) = \rho_1 + (z - z_1) \left( \frac{\rho_2 - \rho_1}{z_2 - z_1} \right)$$

which yields

$$\Delta H_c^0 = z_1 + z_2 + \frac{(\rho_1 + \rho_2)(z_2 - z_1)}{2 \rho_{fw}}$$

This number was compared to the fresh water head differences of the wells measured in the field,  $\Delta H_f$ . In actuality,  $H_f^0$  is the pure water equivalent of  $H_f$ , the measured head, based upon values of  $\rho_0(t)$ , the density of pure water at temperature  $t$  (Fig. V-2). Since  $\Delta H_c^0$  is not dependent upon temperature, a slight discrepancy will exist in the comparison of  $\Delta H_c^0(z)$  and  $\Delta H_f^0(z, t)$ . When comparing the values of these quantities, for the convention  $z_2 > z_1$ , the following relations hold

$$\Delta H_f^0 - \Delta H_c^0 > 0 \quad : \quad \text{water flows from well 2 to well 1}$$

$$\Delta H_f^0 - \Delta H_c^0 = 0 \quad : \quad \text{no flow}$$

$$\Delta H_f^0 - \Delta H_c^0 < 0 \quad : \quad \text{water flows from well 1 to well 2}$$

These computations were made for all test sites in the investigation. When possible, the wells used were those completed in the bedrock (well #1), and the basal unconsolidated (well #2). Sites where this is not possible are numbers II, III, and XI, which have been reviewed in the main text. These sites were included and considered as approximate results. Figure V-3 is a table of computed values for the fresh water head contrast  $\Delta H_f^0 - \Delta H_c^0$ . This data was used to construct Figure 19 in Chapter 4.

Figure V-1. Schematic of the density corrected fresh water head difference.

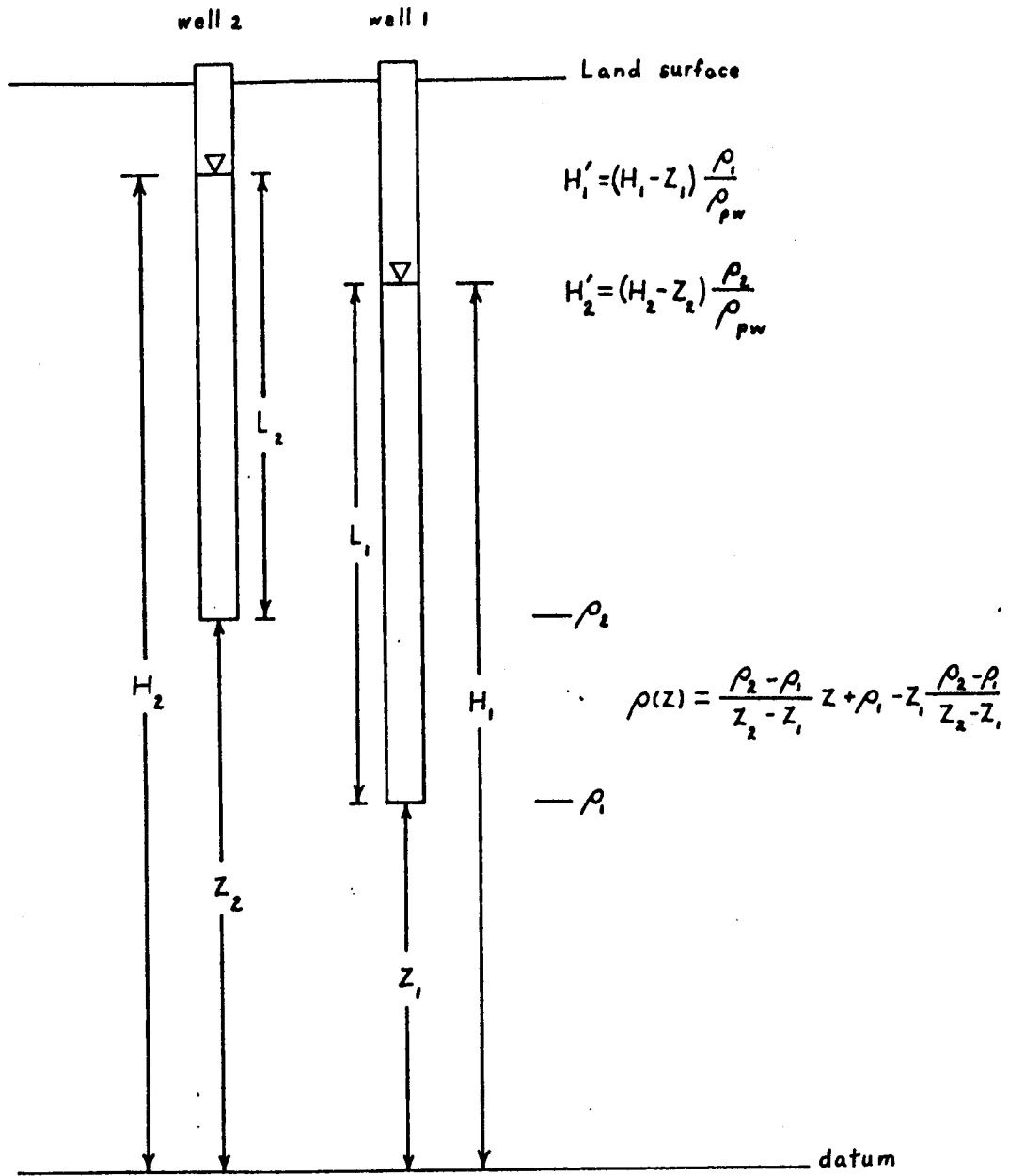
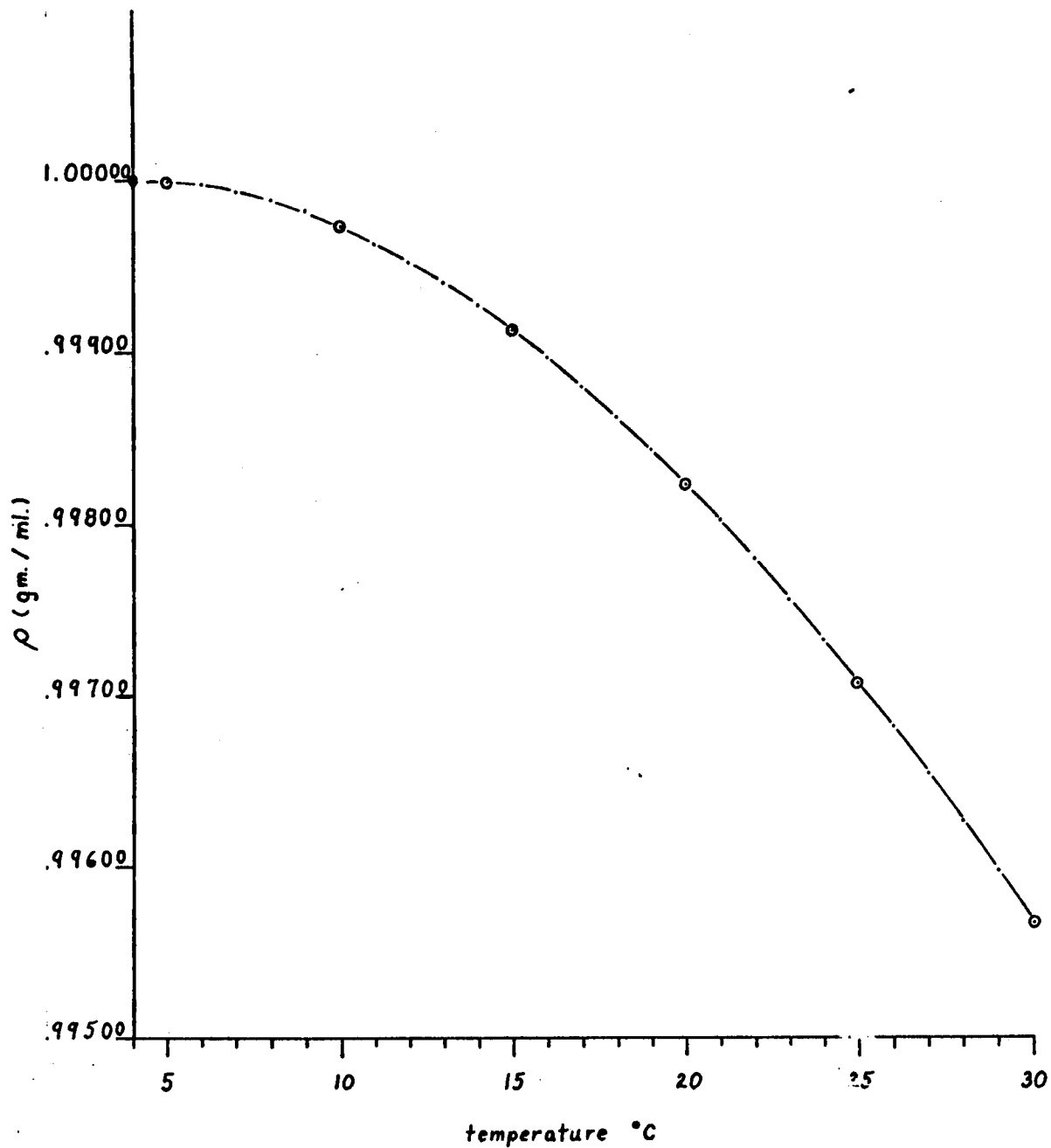


Figure V-2. Relative Density of Pure Water ( $\rho$ ).  
vs.  
Temperature ( $^{\circ}\text{C}$ )



(Data from Handbook of Physics and Chemistry, 1964)

Figure V-3. Contrast Between Calculated and Measured Pure Water Head Differences of Wells Completed at Different Elevations in Water

SITE	WELL	$Z_i$ (ft)	$\rho_i$ (g/ml)	$T_i$ (°C)	$\rho_o$ (g/ml)	$\Delta H_c^0$ (ft)	$\Delta H_f^0$ (ft)	$\Delta H_f^0 - \Delta H_c^0$ (ft)
I	1	1680.0	1.014	24.0	0.99732	.38	-.51	-.89
	2	1719.5	1.000	24.0				
II	1	1722.5	0.998	24.0	0.99732	.20	-2.09	-2.29
	2	1798.0	0.998	24.0				
III	1	1747.0	0.998	24.0	0.99732	.05	4.30	4.25
	2	1824.5	0.998	24.0				
IV	1	1688.0	1.036	24.0	0.99732	2.28	-10.5	-12.78
	2	1801.0	0.999	24.0				
V	1	1657.0	1.049	24.0	0.99732	3.94	-9.34	-13.28
	2	1755.0	1.026	24.0				
VI	1	1729.0	1.049	24.0	0.99732	2.16	-9.96	-12.12
	2	1808.5	1.000	24.0				
VII	1	1645.0	1.044	24.0	0.99732	2.64	1.33	-1.31
	2	1754.0	0.998	24.0				
VIII	1	1606.0	1.056	23.4	0.99747	3.61	-4.76	-8.36
	2	1726.0	0.999	23.4				
IX	1	1662.5	1.003	23.4	0.99747	0.08	-0.39	-0.47
	2	1681.5	1.000	23.4				
X	1	1626.5	1.001	21.8	0.99772	0.14	0.24	0.10
	2	1645.5	1.000	22.9				
XI	1	1524.0	1.008	22.9	0.99760	1.21	18.73	17.52
	2	1699.5	1.001	22.8				

$Z_i$  : elevation of screen center

$\rho_i$  : density of well water at  $T_i$

$T_i$  : temperature at which  $\rho_i$  is measured

$\rho_o$  : density of pure water at  $T_i$

$\Delta H_c^0$  : calculated pure water head difference

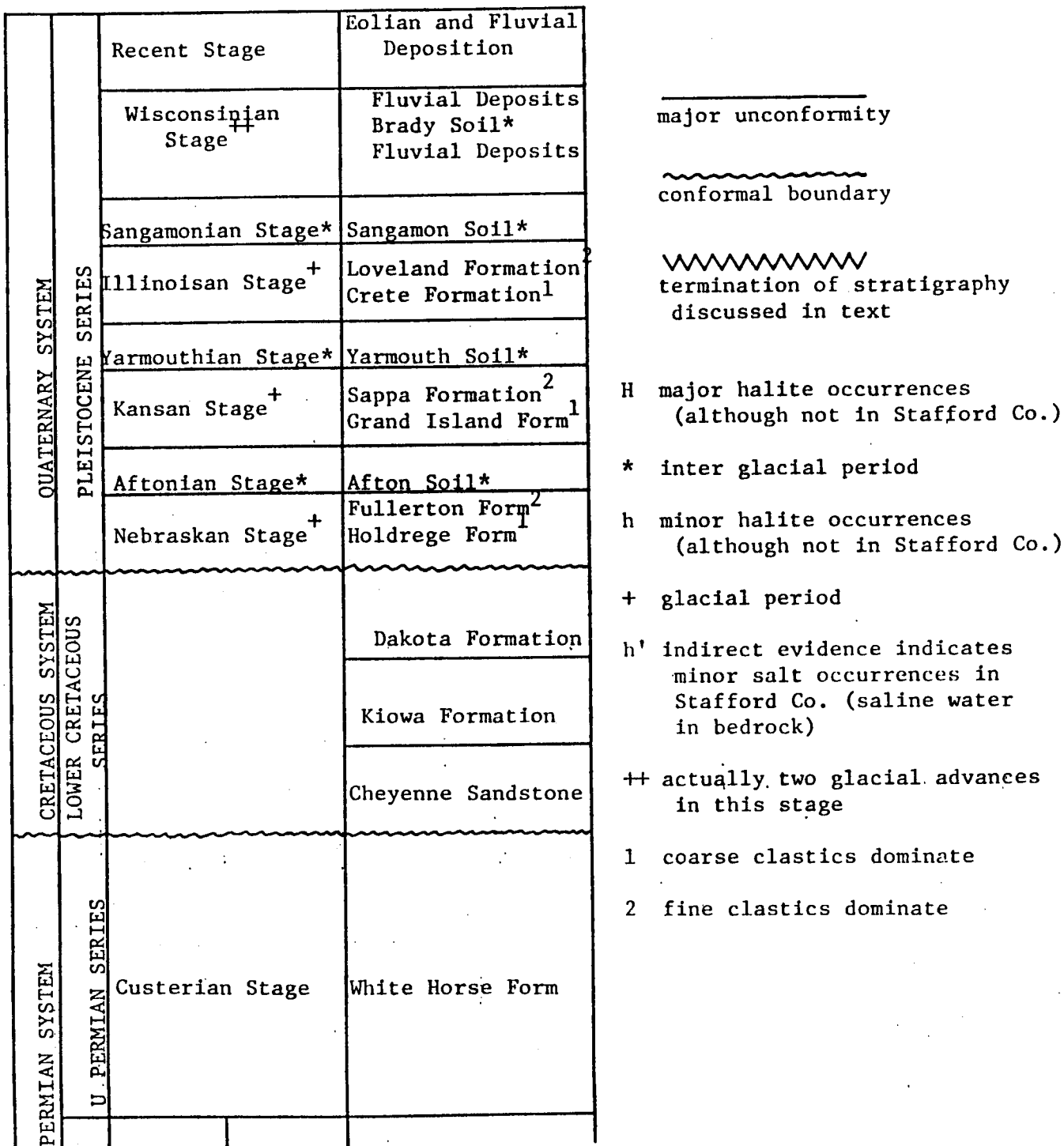
$\Delta H_f^0$  : pure water head difference based on field data

Appendix VI. A Synopsis of the Surficial and Subcropping Geology in  
Stafford County, Kansas, with a Discussion of the Occur-  
rence of Halite in the Permian "Red beds"

Introduction

Stafford County, Kansas is situated over the juncture of the Central Kansas Uplift and the Pratt Anticline, structural features which serve to divide the Cimarron Basin and the Sedgwick Basin. Stratigraphically, the area may be described in simplistic terms as consisting of a veneer of unconsolidated Pleistocene and Recent sediments unconformably overlying Cretaceous and Permian formations; the Cretaceous units being separated from the Permian units by a major unconformity. The subcropping Permian units are collectively described as part of the "red beds," and are part of a depositional unit commonly referred to as the Permian Salt Basin (Holdaway, 1977). The "red beds," while covered in Stafford County, are well exposed in Clark, Comanche, Barber, Harper, Kingman, Reno, Harvey, and McPherson counties. With the exception of a small outlier correlated with the Kiowa Formation, no Cretaceous rocks outcrop in the study area. Units of the Kiowa Formation and Cheyenne Sandstone outcrop in Kiowa, Clark, Comanche, and Rice counties (Kansas Geological Survey Map M-1, 1964). Latta (1950) places a unit of the Dakota in the subsurface of northwestern Stafford County, but the limits of the subcrop are not exactly known. Outcrops of this unit occur in neighboring Barton, Rice, and Pawnee counties (Kansas Geological Survey Map M-1, 1964). The age and stratigraphic position of the rocks discussed in this report are shown in Figure VI-1.

Figure 1. Detailed Stratigraphy Most Probably Occurring in Stafford County (to the base of the Cimarronian Stage)  
(after Zeller, 1968)



PERMIAN SYSTEM	LOWER PERMIAN SERIES	CIMARRONIAN STAGE	NIPEWALLA GROUP	h Dog Creek Form
				H Blaine Formation
H Flower-pot Shale				
h,h' Cedar Hills SS				
H,h' Salt Plain Form				
h,h' Harper SS				
SUMNER GROUP	h Stone Corral Form			
	H Ninnescah Shale			
	H Wellington Form			

## The Permian System

The Permian formations underlying Stafford County represent the entire Permian System, except for possibly the most recent units of the Upper Permian Series. The most recent classification of Permian stratigraphy (O'Connor, et al., 1968) divides the system into two series and three stages. The Gearyan and Cimarronian Stages constitute the Lower Permian Series, while the Custerian Stage constitutes the Upper Permian Series. The Gearyan Stage, not shown in Figure VI-1, is comprised generally of alternating normal marine shales and limestones exhibiting cyclical patterns similar to the underlying Pennsylvanian System (Merriam, 1963).

The Cimarronian and Custerian stages are of most concern in this work. All of the subcropping formations in Stafford County are members of these stages, which consist almost entirely of evaporites and red beds. The occurrence of these evaporites will be discussed in more detail later, since their presence has implications for the hydrologic aspects of this study. Merriam (1963) indicates that the subcropping formations in Stafford County include the Whitehorse, Dog Creek, Blaine, and Cedar Hills - Salt Plain formations. Fader and Stullken (1978) agree with the general pattern of the subcrop, if not with the exact details. Not subcropping in Stafford County are the Harper Sandstone, the Stone Corral Formation, the Ninnescah Shale, and the Wellington Formation. The subcropping Permian units are of considerable hydrological importance because they are known aquifers containing salt water.

The Nippewalla Group is comprised of the Harper, Salt Plain, Cedar Hills, Flower-pot, Blaine, and Dog Creek formations. These rocks consist principally of red beds that are primarily siltstones and fine

grained sandstone, with minor quantities of silty shale and gypsum. At outcrop, the units have the following thicknesses: Harper Sandstone (180-229 feet), Salt Plain (265 feet), Cedar Hills Sandstone (180 feet), Flower-pot Shale (180 feet), Blaine Formation (50 feet), and Dog Creek Shale (14-35 feet), for a total thickness ranging from 869 to 930 feet (Swineford, 1955).

#### Stratigraphy of the Nippewalla

Descriptions of the lithology and petrology of the Cimarronian and Custerian stages are derived from investigations of surface outcrops where they occur and from examination of cuttings from drill holes which penetrate these units. Often additional information is obtained from the correlation of geophysical logs with the cuttings. In the following discussion, the outcrop descriptions are due to Swineford (1955) and the subsurface descriptions are by other authors as noted in the text.

Harper Sandstone: In outcrop the Harper is considered to consist of two members. The lower member is termed the Chikaskia and is composed primarily of brownish-red sandy siltstones to silty shales. The overlying Kingman member is composed mainly of brownish-red, thin, slabby siltstones with occasional beds of brownish-red silty shale and light gray to white siltstones and sandy shales. The Kingman is the coarser unit. The formation at outcrop is roughly composed of 70% siltstone, 25% silty shale to shale, and 5% sandstone. About 90% of the formation is red in color.

Salt Plain Formation: The exposures of this formation consist principally of reddish brown flakey siltstones, thin sandy siltstones, and very fine grained sandstones. The lithologic analysis indicates 65% siltstone, 25% shale to silty shale and 10% sandstone. Ninety-five percent of the formation is red in color. In the subsurface, this unit is difficult to separate from the underlying Harper or the overlying Cedar Hills (Schumaker, 1966). Swineford feels that the lower stratigraphic boundary should be abolished. Merriam (1963) maps a Cedar Hills - Salt Plain - Harper unit through Stafford County. In outcrop Swineford notes considerable carbonate cement, and also some halite casts. Salt is known to exist locally in the subsurface.

Cedar Hills Sandstone: The outcrops of this formation consist generally of brownish-red, massive, very fine-grained sandstone, and sandy siltstones separated by beds of argillaceous siltstones and silty shale. The top and bottom of the formation are marked by beds of white, fine-grained sandstone. Individual beds seem to be traceable long distances in outcrop. Holdoway (1978) notes a similar traceability in subsurface beds. The most prominent features in exposure are two massive, friable, silty sandstone, separated by less resistant sandy siltstones and argillaceous siltstone. The composition of the formation outcrop is about 70% sandstone, 25% siltstone, and 5% shale and silty shale. Some carbonate cement is noted as are small amounts of crystalline calcite and some coarsely crystalline dolomite and gypsum. About 80% of the formation is red in color. In the subsurface the sandstones consist of conspicuous amber to clear, fine to coarse grained, poorly cemented, sub-rounded to rounded, frosted to well polished, quartz grains that

appear in clusters or as free grains (Schumaker, 1966). Many beds are very shaley or contain anhydrite or gypsum. Holdoway (1978) notes the presence of halite cement in western Kansas.

Flower-pot Shale: Swineford indicates that in outcrop, the formation is composed primarily of reddish-brown gypsiferous shale and silty shale with a few thin sandstone and siltstone units. Some of the sandstones are cemented by coarsely crystalline gypsum. Little calcareous material is noted. The Flower-pot Shale is 80% shale and silty shale, 20% sandstone and siltstone, and traces of limestone-dolomite and gypsum-anhydrite. The formation is 90% red in color. Schumaker (1963) notes that the Flower-pot is a distinct lithologic unit in the subsurface; typically a reddish-brown anhydritic shale. Holdoway (1978) discusses the halite content in detail.

Blaine Formation: The Blaine is the principal evaporite unit in the Nippewalla group. Swineford notes that in outcrop it consists of massive gypsum, thin dolomite, and brownish-red shale beds. The outcropping unit probably correlates with the subsurface Medicine Lodge member (Malone, 1962). At outcrop, the formation is 65% anhydrite or gypsum, 30% shale to silty shale, and 5% carbonates. It is only 25% red in color. In the subsurface the Blaine is typically anhydrite (Holdoway, 1978; Schumaker, 1966; Campbell, 1968; Malone, 1962). Locally it also contains salt, gypsum, and shale units. Schumaker (1966) notes its absence in several areas in Edwards, Hodgeman, and Ford counties, as well as in southern Lane and northeastern Finney counties. These absences may be due to non-deposition or removal. It is traceable for a

distance in Stafford County, but only with difficulty as the subcrop is approached. In the subsurface there are as many as four distinct anhydrite beds, but these feather out to the northeast and many authors feel that they correlate with the Dog Creek Shale as a facies change (Malone, 1962; Campbell, 1963; Schumaker, 1966; Swineford, 1955).

Dog Creek Shale: As described in outcrop by Swineford, this formation is composed of thin beds of dark-red silty shale, brownish-red and greenish-gray siltstones, and very fine-grained sandstone, dolomite, gypsum, and dolomite and gypsiferous sandstone. Large crystals of gypsum are common. Halite casts up to 9 mm in diameter are noted locally in outcrop. The units are 75% shale to silty shale, 15% siltstone, and only 5% sandstone. Evaporites constitute less than 5% of the formation. The formation is 85% red in color. In the subsurface, the Dog Creek consists of reddishbrown, silty, gypsiferous, and anhydritic shales (Schumaker, 1966).

Whitehorse Sandstone (Custerian Stage): This formation is the basal unit of the Upper Permian Series, and is probably present in the subsurface of Stafford County generally as a thin sandstone, bounded unconformably above by Cretaceous units and conformably below by the Dog Creek Shale. The outcrop described by Swineford is composed of red friable sandstone, siltstone, and shale, with minor quantities of white to buff sandstone and dolomite. The sandstones range from resistant, calcareous cemented units, to relatively uncemented sandstone. In the subsurface, Schumaker (1963) notes undifferentiated reddish-brown silty

shale, slightly gypsiferous, to sandy and gypsiferous. Some sandstone units may be present locally. Where not eroded, a fairly uniform sub-surface thickness of 300 feet is maintained.

#### Pre-Nippewalla Halite Deposition

The Sumner Group of the Cimarronian Stage contains two important salt units: the Hutchinson Salt Member of the Wellington Formation and the Lower Cimarron Salt, the latter being a lithofacies of the Ninnescah Shale, near the base of the Stone Corral Anhydrite (Schumaker, 1966). Prevalent geological information (Campbell, 1963; Merriam, 1963, 1972) indicates a continuity of the Stone Corral Anhydrite which would appear to isolate these salt units from circulating groundwater in the study area. Therefore, these units are not considered likely sources of low quality water.

#### The Occurrence of Halite in the Nippewalla Group

This section on halite is based principally on work done by Holdaway (1978). She analyzed and described the core known as A.E.C. #5 drilled in Wichita County in 1972. Other work done on this core includes James (1972).

The ubiquity of halite in the Nippewalla Group is quickly grasped, even in the most cursory review of pertinent literature. In some cases, the halite is present as cement or as discrete crystals distributed randomly through a formation at least on a local scale. Large bedded halite units are also known to occur at several horizons over portions of the Cimarronian depositional basin (Schumaker, 1966). Schumaker describes in great detail the depositional environment which could

account for the relatively great thicknesses of salt deposited in the western half of Kansas in Permian time. Malone (1962) describes the eastern part of the Nippewalla as being dominated by clastic deposition, while evaporite deposition is more pervasive in the western end. Holdoway (1978) modifies this view to an extent in noting that the Flower-pot salt in west-central Kansas is not the massive unit as was supposed, but rather was an intermixture of red silt (5-15%) and crystalline halite (85-95%).

The extent of the red beds and evaporites were controlled throughout Permian depositional history by geologic structure and supply of materials. Evaporite survival after deposition depended upon tectonic movements and groundwater circulation. Climate has had an important role in both deposition and dissolution of evaporites (Merriam, 1963; Malone, 1962; Campbell, 1963; Holdoway, 1978).

Halite is known to occur in the Nippewalla Group as individual crystals, cement, as well as bedded salt, now interpreted as lithofacies of the formations in which they occur (Swineford, 1955; Malone, 1962; Merriam, 1963; Campbell, 1963; Schumaker, 1966; Holdoway, 1978).

Bedded salt units of the latter type are associated with the Harper - Salt Plain, the Flower-pot Shale, and the Blaine Formation. Significant halite deposition is not presently recognized in the Custerian Stage. Units formerly correlated with the Cedar Hills Sandstone (Malone, 1962), are most recently associated with the Flower-pot Shale (Schumaker, 1966; Holdoway, 1978).

Harper - Salt Plain Halite: The earliest occurrence of an extensive bedded halite unit in the Nippewalla is in western Kansas, in an

area located within portions of Stanton, Grant, Kearny, Finney, and Scott counties. Malone (1962) correlated this unit with the Harper - Salt Plain depositional sequence. Campbell (1963) also discusses this unit, indicating that crystalline halite may be traced into the basal Harper and the Stone Corral. Schumaker (1966) discusses this unit, but does not map it, feeling that its character and extent are not well enough documented.

The Flower-Pot Salt Units: The most extensive deposition of halite in the Nippewalla Group occurs in two units known collectively as the Flower-pot Salt. Malone (1962) has termed these units the Eastern Salt Platform and the Western Salt Platform (although he correlated the salt with the Cedar Hills Sandstone). The Western Platform is the more extensive of the two, covering all or parts of ten counties in west-central Kansas (Schumaker, 1966). Thicknesses of 300 feet, which appear to be the maximum, appear in Finney County, while the average thickness is about 225 feet. Schumaker outlines the Eastern Salt Platform as occurring in south-central Kansas, specifically in all or parts of Clark, Commanche, Edwards, Ford, Gray, Haskell, Kiowa, and Meade counties. Maximum thicknesses of about 350 feet occur in Clark and Meade counties, with the average formation thickness about 200 feet. The character of the salt in the Eastern Salt Platform is not well known, due to the oil field practice of not core drilling the red beds. The nature of the Western Salt Platform has recently been discussed in detail by Holdoway (1978) and will be summarized shortly.

The Blaine Salt: None of the previously mentioned authors discuss the presence of a Blaine Salt in association with the Eastern Salt Platform. Holdoway (1978) discusses such a unit in conjunction with the Western Salt Platform, and so discussion will be included in the review of the A.E.C. #5 core which follows.

#### Atomic Energy Commission Test Core #5

The Atomic Energy Commission, in the process of evaluating the suitability of salt units for nuclear waste disposal in Kansas, financed several test cores. One such core, commonly referred to as A.E.C. #5, was drilled in Wichita County in 1972. Salt saturated drilling mud was used in order to preserve the halite units encountered. Holdoway (1978) has discussed this core, and its geologic implications in detail. The following discussion is a synopsis of her examination of the core lithology.

The Harper - Salt Plain - Cedar Hills Interval: The Harper - Salt Plain interval was logged between 2044 and 2366 feet (or a thickness of 322 feet), but only the upper 14 feet were cored. The uncored interval shows indications of salt according to the geologists log. No crystalline salt is noted in the cored section, nor is there evidence of halite cement. The boundaries between the Harper, the Salt Plain, and the Cedar Hills are gradational. The Cedar Hills was picked between 1977 feet and 2044 feet ( or a thickness of 67 feet). Examination of the core showed a generally massive, but occasionally cross-bedded sandstone, having a bimodal distribution in grain size. The cement is generally halite, but nodules of anhydrite occur at several levels.

The Flower-Pot Interval: The Flower-Pot interval was picked between 1977 and 1701.5 feet, for a thickness of 275.5 feet. The boundary was picked on the basis of a shift from halite cement to discrete halite crystals. The Flower-Pot Salt consists of fine to coarse crystalline halite, intimately associated with varying amounts of anhydritic, red, silty mudstone. The halite is not bedded, but thin beds of mudstone and anhydrite are encountered. The crystals range in size from 0.5 - 15.0 cm diameter. In the upper Flower-Pot interval, some of the halite is finely crystalline, with fluid inclusions.

The Blaine Interval: The Blaine Formation was picked between 1587 and 170.5 feet, for a thickness of 114.5 feet. The major portion of the halite is similar to that in the Flower-Pot salt. An exception is a unit occurring between 1627.5 and 1623 feet; a thickness of 4.5 feet. The composition is fine cloudy crystalline halite, and coarse clear crystalline halite. No intimate association or interbedding or red mudstone occurs, but laminated layers of anhydrite are seen. Less than 20 feet of the Dog Creek Shale was penetrated and it consisted of reddish-brown anhydritic shale. No salt was apparently detected.

James (1972) performed x-ray diffraction analysis of the crystalline salts which indicated virtually pure  $\text{NaCl}$  (halite), although minor occurrences of gypsum were noted. Examination of the insoluble residual showed a high concentration of swelling chloride. James felt the material should be termed claystone or mudstone, rather than siltstone or shale.

As a final word on this discussion, it should be emphasized here that the general distribution of salt through the Nippewalla Group is

not well documented, except for the major depositions discussed herein and the one detailed core discussed above. Questions such as the distribution of halite cement, or discrete crystalline halite, or even small local bodies can only be answered in expensive bedrock cores drilled on an extensive scale. Such a program is economically unfeasible. Thus, the minor distribution, or non-massive distribution of halite must be inferred from natural discharges of salt water (Campbell, 1963).

### The Cretaceous System

Pre-Cretaceous erosion removed any Triassic and Jurassic formation which may have been deposited in Stafford County. Large portions of the Permian red beds were also removed. Upon this major unconformity, rocks of the Cretaceous System were deposited (O'Connor, 1968). Post-Cretaceous erosion has removed all but the lower three formations of Cretaceous age from Stafford County.

The most recent interpretation of the Permian - Cretaceous contact in the Great Bend Prairie region, and Stafford County in particular, is described by Fader and Stullken (1978). At least four other interpretations exist in the literature: Latta (1950, Merriam (1963), Zeller (1968), and Keene and Bayne (1977). The principal points of difference concern the location of the eastern extent of the main body of the Cretaceous formations and the presence or absence of outliers east of the main body. Possible reasons for these differences include: 1) quantity and quality of data available to the respective authors, 2) interpretive differences in the sample and geophysical logs, 3) the difficulty in distinguishing reworked material from the in situ formation.

The Cretaceous formations underlying Stafford County are designated as members of the Lower Cretaceous Series (O'Connor, 1968). These units are considered to represent the Cheyenne Sandstone, the Kiowa Formation, and the Dakota Formation. Only the lower portion of the Dakota is actually in place, the remainder having been removed by post-Cretaceous erosion (Latta, 1950).

The Cheyenne Sandstone: According to Merriam (1963), the Cheyenne Sandstone is a massive cross-bedded, friable, light colored, fine to medium grained sandstone, containing lenses of sandy shale and conglomerate. O'Connor (1968) notes a basal unit of pebbles and an upper zone of dark shale and plant fossils. This unit is not exposed in Stafford County, but subsurface occurrence is noted on well logs. Latta (1950) states that material correlated with the Cheyenne in Stafford and Barton counties was principally variegated light gray to light green, friable to tightly cemented, very fine to medium grained sandstone. Lenses of light colored sandy clay are encountered whereas calcareous and pyritic material are not common. O'Connor indicates that these deposits represent non-marine and littoral deposits laid down as the sea advanced northward.

The Kiowa Formation: The Kiowa Formation is distributed over a slightly larger area than the Cheyenne Sandstone. The general character is predominantly that of a medium to dark gray, micaceous, silty, carbonaceous, soft to hard marine shale, probably representing a transgressive sequence (Merriam, 1963). O'Connor (1968) points out that sandstone occurs as lenses throughout the sequence, especially in the

upper parts, and that the top of the formation is often marked in outcrop by a bench forming sandstone showing stratifications and ripple marks. Latta (1950) indicates that the sandstone lenses are fine to medium grained, white to gray and yellow-brown. He describes beds of gray to gray-white sandy limestone, some of which was too difficult to drill. Lignite is rarely encountered. An isolated outcrop occurs in northeastern Stafford County in T22, R11W (Fader and Stullken, 1978).

The Dakota Formation: The Dakota and the Kiowa are conformable formations sharing a gradational boundary along which lithologic similarities render the formation boundary unrecognizable (Latta, 1950). In Stafford and Barton counties, Latta continues, the Dakota is composed of alternating vari-colored, clay, shale, siltstone, and sandstone. Lignite and "ironstone" are common. A portion of residual Dakota extends a few miles into northwestern Stafford County.

Post-Cretaceous erosion removed much of the thick Cretaceous deposits and probably additional Permian deposits from Stafford County and the region. Thus, a major unconformity crossing two systems served as the depositional surface for the Pleistocene Series (Latta, 1950; Merrima, 1963; O'Connor, 1968).

#### The Quaternary System

The Quaternary System consists of a single series, the Pleistocene, in Kansas and, hence, in Stafford County. O'Connor and Bayne (1968) outline the most recent interpretation of the time and rock stratigraphy for the southcentral region of Kansas. They indicate that the Pleistocene deposits consist of sequential, gradational beds of fine, medium,

and coarse clastic materials, and distinct geosols (weathering profiles). Clastic deposition, generally of fluvial origin is correlated with events of continental glaciation, while the geosols are associated with the interglacial periods. Eolian deposits of sand and fluvial clastic deposits along major drainages constitute the Recent Stage of the Pleistocene Series. Latta (1950) believes that the dune sands represent several depositional ages. The older deposits have a more mature topography, higher clay content, better developed soils and are stabilized by vegetation. The younger dune deposits tend to be clean, loose and locally are subject to wind erosion if vegetative cover fails to develop or is removed. Fader and Stullken (1978) indicate that the maximum thickness of the unconsolidated Pleistocene deposits is about 250 feet in Stafford County, while the average thickness is in the range of 125 to 150 feet.

Deposition during Pleistocene glacial stages was controlled by the prevailing drainage patterns during each cycle. O.S. Fent (1950) considers most of the early Pleistocene deposition to be confined to existing drainage. The material is mostly derived from older clastic, and non-clastic sedimentary rocks to the west of Stafford County. Southern Stafford County also underwent blanket deposition of materials derived in the Rocky Mountains and laid down by laterally shifting streams. The later events of Pleistocene glacial stages was dominated by blanket deposition.

The lithology, grade sizes, and the degree of sorting in each particular stratigraphic unit is related to the ability of the depositing stream to carry a load and the availability of material for the load. Typically, early in each depositional cycle, the streams had

sufficient energy and available material to deposit considerable thicknesses of coarse material, with or without a matrix of finer sizes. Late in each cycle, however, stream energy became lower so that only the finer materials were deposited.

The the present time (late Pleistocene, Recent Stage), the dominate depositional processes, streams and wind, are being significantly modified by man's activities and the present landscape is being modified by land leveling, land treatment, and changes in land use and agricultural practices.

### Introduction

The subject of this appendix is the detailed development of the closed form of the head distribution about a drain in a confined system (equation 6-1 in the text). The basis of this work is a letter (April 18, 1980) from Dr. David B. McWhorter, Colorado State University, outlining the methodology of developing his published approximation (McWhorter, 1972). This appendix supplies the details of the development. Drs. Carl McElwee and Manoutchehr Heidari, both of the Kansas Geological Survey, guided this work through some difficult steps.

Boundary conditions are also applied to equation 6-1; thus, deriving equations 6-2 and 6-3. Equation 6-4 is also justified.

### Development of the Infinite Series Solution

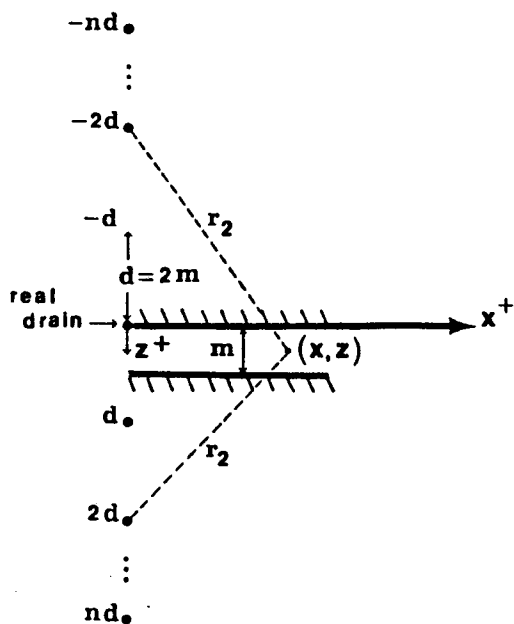
Consider now the infinite sequence of equally spaced sinks as shown below (Fig. VII-1). This infinite pattern of image drains, spaced  $d=2m$  apart, is the one which satisfies the condition of no flux across the impermeable boundaries.

The discharge per unit length of the above drain is given by the boundary condition (see Fig. VII-2).

$$Q = 2\pi r_a K_f \left. \frac{\partial H}{\partial r} \right|_{r_a}$$

For steady state radial flow in an isotropic homogeneous medium

$$\frac{1}{r} \frac{\partial}{\partial r} \left( r \frac{\partial H}{\partial r} \right) = 0$$



$$r_0^2 = [x^2 + z^2]$$

$$r_1^2 = [x^2 + (d \pm z)^2]$$

$$r_2^2 = [x^2 + (2d \pm z)^2]$$

$$\vdots$$

$$r_n^2 = [x^2 + (nd \pm z)^2]$$

it can be shown that  
 $(nd \pm z)^2 = (z \pm nd)^2: -\infty \leq n \leq +\infty$

Figure VII-1. Schematic for image well approximation in a half plane.

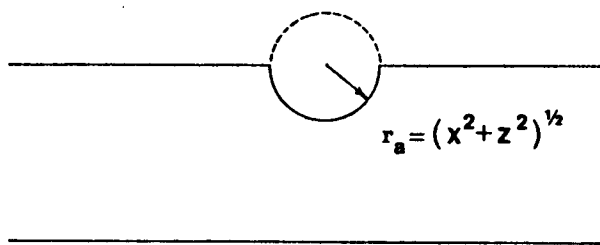


Figure VII-2. Boundary of a drain of radius a.

Integrating once:

$$r \frac{\partial H}{\partial r} = C_1 \rightarrow \frac{\partial H}{\partial r} \Big|_{r_a} = \frac{Q}{2\pi r_a K_f} = \frac{C_1}{r_a} \rightarrow C_1 = \frac{Q}{2\pi K_f}$$

Integrating twice:

$$\begin{aligned} H &= C_1 \ln r + C_2 \\ &= \frac{Q}{2\pi K_f} \ln r + C_2 \end{aligned}$$

We will slightly modify the equation to accommodate  $\ln(r^2)$ . Since  $\ln r = \ln(r^2)^{1/2} = \frac{1}{2} \ln r^2$  we transform the preceding equation:

$$H = \frac{Q}{4\pi K_f} \ln r^2 + C_2$$

For the present, let  $C_2 = 0$ .

By the theory of superposition of potentials:

$$H(x, z) = \sum_{i=-\infty}^{\infty} H_i = \sum_{i=-\infty}^{\infty} \frac{Q}{4\pi K_f} \ln r_i^2 = \frac{Q}{4\pi K_f} \sum_{i=-\infty}^{\infty} \ln r_i^2$$

$$\begin{aligned} H(x, z) &= \frac{Q}{4\pi K_f} \left( \dots + \ln r_{-n}^2 \dots + \ln r_{-1}^2 + \ln r_0^2 + \ln r_1^2 \dots + \ln r_n^2 \dots \right) \\ &= \frac{Q}{4\pi K_f} \ln \left( \dots (r_{-n}^2) \dots (r_{-1}^2) (r_0^2) (r_1^2) \dots (r_n^2) \dots \right) \\ &= \frac{Q}{4\pi K_f} \ln \left( \dots [x^2 + (nd - z)^2] \dots [x^2 + (d - z)^2] [x^2 + z^2] [x^2 + (d + z)^2] \dots \right. \\ &\quad \left. [x^2 + (nd + z)^2] \dots \right) \end{aligned}$$

and finally in most general form

$$\text{VII-1) } H(x, z) = \frac{Q}{4\pi K_f} \ln \prod_{n=-\infty}^{\infty} [x^2 + (z - nd)^2] + C$$



Superposition yields the following product series:

$$\text{VII-2)} \quad H = \frac{Q}{2\pi K_f} \ln \prod_{n=-\infty}^{\infty} [w - nd]$$

In order to obtain the closed form solution to this infinite product series, we invoke the expression

$$\sin \pi u = \pi u \prod_{n=1}^{\infty} \left(1 - \frac{u}{n}\right) \left(1 + \frac{u}{n}\right) \quad (\text{see Brand, 1958})$$

Expand VII-2 in the following manner:

$$\begin{aligned} H &= \frac{Q}{2\pi K_f} \ln \left[ \prod_{n=-\infty}^{-1} (w - nd) \prod_{n=0}^{\infty} (w - nd) \prod_{n=1}^{\infty} (w - nd) \right] \\ &= \frac{Q}{2\pi K_f} \ln \left[ (w) \prod_{n=1}^{\infty} (w + nd) \prod_{n=1}^{\infty} (w - nd) \right] \\ &= \frac{Q}{2\pi K_f} \ln \left[ (w) \prod_{n=1}^{\infty} nd \left(1 + \frac{w}{nd}\right) (-nd) \left(1 - \frac{w}{nd}\right) \right] \end{aligned}$$

and finally:

$$\text{VII-3)} \quad H = \frac{Q}{2\pi K_f} \ln \left[ w \frac{\pi}{d} \prod_{n=1}^{\infty} \left(1 + \frac{w}{nd}\right) \left(1 - \frac{w}{nd}\right) \right] + \frac{Q}{2\pi K_f} \ln \left[ \frac{d}{\pi} \prod_{n=1}^{\infty} -(nd)^2 \right].$$

We can justify the inclusion of the  $\frac{\pi}{d}$  since it will contribute to the additive constant which is at present arbitrary. Since the second term, RHS of VII-2, is independent of the spatial variables, it may also be relegated to the arbitrary constant and ignored. Hence we may now take  $U=W/d$  and write

$$\text{VII-4)} \quad H = \frac{Q}{2\pi K_f} \ln \left( \sin \frac{\pi w}{d} \right).$$

The closed form solution we seek is the real part of the complex potential given by VII-4. Using the identity

$$\sin(z + ix) = \sin z \cosh x + i \cos z \sinh x$$

we can write

$$\text{VII-5)} \quad \sin \left( \frac{\pi w}{d} \right) = \sin \frac{\pi z}{d} \cosh \frac{\pi x}{d} + i \cos \frac{\pi z}{d} \sinh \frac{\pi x}{d}$$

Using the identities

$$\sin^2 \theta + \cos^2 \theta = 1$$

and

$$\cosh^2 x - \sinh^2 x = 1$$

and Eulers formula

$$z = r e^{i\theta}$$

The real part of VII-5 can be extracted:

$$\sin \frac{\pi w}{d} = \left( \sin^2 \frac{\pi z}{d} \left( 1 + \sinh^2 \frac{\pi x}{d} \right) + \sinh^2 \frac{\pi x}{d} \left( 1 - \sin^2 \frac{\pi z}{d} \right) \right)^{1/2} e^{i\theta}$$

$$r = \left( \sin^2 \frac{\pi z}{d} + \sinh^2 \frac{\pi x}{d} \right)^{1/2}$$

so that the real, closed form solution is

$$\text{VII-6) } H(x, z) = \frac{Q}{2\pi K_f} \ln \left( \sin^2 \frac{\pi z}{d} + \sinh^2 \frac{\pi x}{d} \right)^{1/2}$$

Using the identities

$$\text{a) } \sin^2 \frac{\pi z}{d} = 1/2 \left( 1 - \cos \frac{2\pi z}{d} \right)$$

$$\text{b) } \sinh^2 \frac{\pi x}{d} = 1/2 \left( \cosh \frac{2\pi x}{d} - 1 \right)$$

which transforms VII-6 to (recall that  $d=2m$ )

$$\text{VII-7) } H(x, z) = \frac{Q}{4\pi K_f} \ln 1/2 \left( \cosh \frac{\pi x}{m} - \cos \frac{\pi z}{m} \right)$$

Since the log of a product is equal to the sum of the logs,

$$\ln 1/2$$

can be included in the arbitrary constant, which gives

$$\text{VII-8) } H(x, z) = \frac{Q}{4\pi K_f} \ln \left( \cosh \frac{\pi x}{m} - \cos \frac{\pi z}{m} \right) + C$$

The solution to this problem has been derived in an infinite aquifer and the boundaries are flow boundaries generated by the infinite series of image wells. Hence, the  $Q$  in VII-8 is due to removal of water from both sides of  $x=0$ , and so is twice the  $Q$  that a drain would actually remove

(Fig. VII-2). Substituting  $2Q$  in place of  $Q$  and canceling gives

$$\text{VII-9) } H(x, z) = \frac{Q}{2\pi K_f} \ln \left( \cosh \frac{\pi x}{m} - \cos \frac{\pi z}{m} \right) + C$$

which is equation 29 in McWhorter's paper, and equation 6-1 in this paper.

#### Application of Boundary Conditions

The head distribution for an infinite confined aquifer being drained by a line sink under steady conditions is described to an additive constant by VII-9 under conditions  $H=m$  at  $x=L$  and  $H=d$  at  $x^2+z^2=a^2$

$$\text{VII-10) } H(a, 0) = \frac{Q}{2\pi K_f} \ln \left( \cosh \frac{\pi a}{m} \cos 0 \right) + C = d$$

$$\text{VII-11) } H(L, 0) = \frac{Q}{2\pi K_f} \ln \left( \cosh \frac{\pi L}{m} \cos 0 \right) + C = m$$

Elimination of the constant between VII-10 and VII-11 yields

$$\text{VII-12) } d - \frac{Q}{2\pi K_f} \ln \left( \cosh \frac{\pi a}{m} - 1 \right) = m - \frac{Q}{2\pi K_f} \ln \left( \cosh \frac{\pi L}{m} - 1 \right)$$

with some algebra VII-12 reduces to

$$\text{VII-13) } Q = 2\pi K_f (m-d) / \left[ \ln \left( \cosh \frac{\pi L}{m} - 1 \right) - \ln \left( \cosh \frac{\pi a}{m} - 1 \right) \right]$$

which is the discharge to the drain from both sides of the  $x=0$  line.

The result indicates that the sign of a gaining drain is positive. Consider the general Darcy equation

$$Q = -KA \nabla h$$

which indicates that flow is in opposition to increasing head. Since

$$m > d$$

$$Q = -KA \frac{d-m}{l}$$

$$Q = KA \frac{m-d}{l}$$

indicating that VII-13 is in correct form and of correct sign for Q.

We now derive the head distribution for steady state

$$\text{VII-14) } H_f(x, z) = \frac{Q}{2\pi K_f} \ln \left( \cosh \frac{\pi x}{m} - \cos \frac{\pi z}{m} \right) + C,$$

under the boundary condition

$$H_f(L, 0) = m :$$

$$\text{VII-15) } H_f(L, 0) = \frac{Q}{2\pi K_f} \ln \left( \cosh \frac{\pi L}{m} - 1 \right) + C = m.$$

This implies that

$$\text{VII-16) } C = m - \frac{Q}{2\pi K_f} \ln \left( \cosh \frac{\pi L}{m} - 1 \right) ;$$

combining VII-15 and VII-16 yields

$$\text{VII-16') } H_f(x, z) = \frac{Q}{2\pi K_f} \left[ \ln \left( \cosh \frac{\pi x}{m} - \cos \frac{\pi z}{m} \right) - \ln \left( \cosh \frac{\pi L}{m} - 1 \right) \right]$$

which is the general expression for the two-dimensional head distribution between the drain and a hypothetical constant head boundary. This approximation improves with increasing L values.

#### Interface Position

The actual position of the interface is to be computed under the assumption that the upconed material surface does not effect  $H_f(x,z)$  in the vicinity of the cone. We began by stating the fluid potentials for each noncompressible fluid at the interface.

$$\text{VII-17} \quad H_f^I = p_f / \gamma_f + z$$

$$\text{VII-18) } H_s^I = p_s / \gamma_s + z$$

From McWhorter's diagram we see that

$$z = m - \xi$$

Since physical continuity dictates that pressure must be a single valued scalar as we approach the interface, we rewrite VII-17 and VII-18

$$\text{VII-17') } H_f^I = p_f / \gamma_f + m - \xi$$

$$\text{VII-18') } H_s^I = p_s / \gamma_s + m - \xi$$

and solve for  $\xi$  after eliminating  $p$  between these equations. This yields

$$\text{VII-19) } \xi = (m - H_f^i) \delta - (m - H_s^i)(1 - \delta) \quad , \quad \delta = \frac{\gamma_s}{\gamma_f - \gamma_s}$$

The final form of the equation for locating the position of the interface involves the following assumption which parallels the work of Muskat (1937). We assume that at large distances from the drain, the system approximates hydrostatic equilibrium and that the fresh water head in the static salt water is equal to  $m$ . Since no flow is assumed to occur in the salt water, the implication is that  $H_S = m$  in the entire salt water volume and hence also at the interface so that  $H_S^i = m$ . This implies that the second term, RHS of VII-19 is zero, which yields the final form for the location of the interface:

$$\text{VII-20) } \xi = (m - H_f^i) \delta.$$

## Bibliography

- Bayne, C.K., 1956, Geology and ground-water resources of Reno County, Kansas: State Geological Survey of Kansas Bulletin 120, 130 p.
- Bayne, Charles K. and O'Connor, Howard G., 1968, Quaternary system in Zeller, Doris, ed., The stratigraphic succession in Kansas: Kansas Geological Survey Bulletin 189, p. 59-67.
- Bayne, Charles K. and Ward, John R., 1974, Geology and hydrology of Rice County, central Kansas: Kansas Geological Survey Bulletin 206, part 3, 17 p.
- Bear, Jacob, 1972, Dynamics of fluids in porous media: American Elsevier Publishing Company, Inc: New York, 764 p.
- Bear, Jacob, 1979, Hydraulics of groundwater: McGraw-Hill International Book Company, New York, 567 p.
- Bond, D.C. and Cartwright, Keros, 1970, Pressure observations and water densities in aquifers and their relation to problems in gas storage: Journal Petroleum Technology, V. XXII, p. 1492-1498.
- Bond, D.C., 1972, Hydrodynamics in deep aquifers of the Illinois Basin: Illinois State Geological Survey Circular 470, 51 p. plus appendices.
- Brand, L., 1958, Advanced Calculus: John Wiley, New York, p. 527.
- Campbell, C.L., 1963, Permian evaporites between the Blaine and Stone Coral Formations: Unpublished M.S. thesis, University of Kansas, 73 p.
- Cobb, Patrick M., 1979, Description and analysis of aquifer tests conducted by the Kansas Geological Survey in Stafford and Pawnee counties, Kansas: Kansas Geological Survey Open File Report, pages unnumbered.
- Cooper, H.H., Jr., Bredehoeft, J.D., and Papadopoulos, 1967, Response of a finite diameter well to an instantaneous charge of water: Water Resources Research, v. 3, no. 1, p. 263-269.
- Domenico, Patrick A., 1972, Concepts and models in groundwater hydrology: McGraw-Hill Book Company: New York, 405 p.
- Fader, Stuart W. and Stullken, Lloyd E., 1978, Geohydrology of the Great Bend Prairie, south-central Kansas: Kansas Geological Survey Irrigation Series 4, 19 p.
- Fent, O.S., 1950, Geology and groundwater resources of Rice County, Kansas: Kansas Geological Survey Bulletin 85, 142 p.
- Fent, O.S., 1950b, Pleistocene drainage history of central Kansas: Transactions Kansas Academy Science, v. 53, no. 1, p. 81-90.

- Ferris, J.G. and Knowles, D.B., 1954, The slug test for estimating transmissibility: U.S. Geological Survey Ground Water Note 26, p. 1-7.
- Freeze, R. Allan and Cherry, John A., 1979, Groundwater: Prentice-Hall, Inc., Englewood Cliffs, New Jersey, 604 p.
- Hathaway, L.R., Galle, O.K., Waugh, T.C., and Dickey, H.P., 1978, Chemical quality of irrigation waters in Ford County and the Great Bend Prairie of Kansas: Kansas Geological Survey Chemical Quality Series 7, 41 p.
- Hathaway, Larry, Whittemore, Don, and Cobb, Pat, 1980, Quality analysis of samples obtained in 1978 and 1979 from the cooperative observation well network in Groundwater Management District #5: Kansas Geological Survey Open File Report, p.
- Hathaway, Lawrence, R. (Senior Scientist), Kansas Geological Survey), 1978, personal communication.
- Holdaway, Katrine A., 1978, Deposition of evaporites and red beds of the Nippewalla Group, Permian, western Kansas: Kansas Geological Survey Bulletin 215, 43 p.
- Hubbert, M. King, 1940, The theory of ground-water motion: The Journal of Geology, v. 48, no. 8, pt. 1, p. 785-944. Reprinted and corrected in Hubbert, M. King, 1969, The theory of ground-water motion and related papers: Hafner Publishing Company, New York, p. 25-184.
- Hubbert, M. King, 1953, Entrapment of petroleum under hydrodynamic conditions: Bulletin of the American Association of Petroleum Geologists, v. 37, no. 8, p. 1954-2026. Reprinted and corrected in Hubbert, M. King, 1969, The theory of ground-water motion and related papers: Hafner Publishing Company, New York, p. 185-260.
- Hubbert, M. King, 1957, Darcy's law and the field equations of the flow of underground fluids: Bulletin de l'Association Internationale d'Hydrologic Scientifique no. 5. Reprinted in Hubbert, M. King, 1969, The Theory of ground-water motion and related papers: Hafner Publishing Company, New York.
- James, G.W., 1972, Mineralogy and distribution of water - insoluble residues from AEC Test Hole 5 in Bayne, C.K. and Brinkley, D., eds., Geology, hydrology, thickness and quality of salt at three alternative sites for disposal of radioactive waste in Kansas: University of Kansas, Center for Research, Inc., p. 50-57.
- Keene, Katherine M. and Bayne, Charles K., 1977, Ground water from Lower Cretaceous rocks in Kansas: Kansas Geological Survey Chemical Quality Series 5, 18 p.
- Latta, Bruce F., 1948, Geology and ground-water resources of Kiowa County, Kansas: State Geological Survey of Kansas Bulletin 65, 151 p.

- Latta, Bruce F., 1950, Geology and ground-water resources of Barton and Stafford counties, Kansas: State Geological Survey of Kansas Bulletin 88, 228 p.
- Layton, Donald W. and Berry, Delmar W., 1973, Geology and ground-water resources of Pratt County, south-central Kansas: Kansas Geological Survey Bulletin 205, 33 p.
- Linsley, Ray K., Jr., Kohler, Max A., and Paulhus, Joseph L.H., 1975, Hydrology for engineers, second edition: McGraw-Hill Book Company, New York, 482 p.
- Luszczynski, Norbert J., 1961, Head and flow of ground water of variable density: Journal of Geophysical Research, v. 66, no. 12, p. 4247-4256.
- Malone, D.J., 1962, Stratigraphic relations and structural significance of the Blaine Formation in the subsurface of southwestern Kansas: Unpublished M.S. thesis, University of Wichita, 72 p.
- McElwee, Carl D., 1980, Theis parameter evaluation from pumping tests by sensitivity analysis: Ground Water, v. 18, no. 1, p. 56-60.
- McElwee, Carl D. and Macfarlane, P. Allan (Associate Scientist and Research Associate, Kansas Geological Survey), 1980, personal communication.
- McLaughlin, Thad G., 1949, Geology and ground-water resources of Pawnee and Edwards counties, Kansas: State Geological Survey of Kansas Bulletin 80, 189 p.
- McWhorter, David B., 1972, Steady and unsteady flow of fresh water in saline aquifers: Colorado State University, Water Management Technical Report No. 20, 49 p.
- Mercer, James W., Larson, Steven P., and Faust, Charles R., 1980, Simulation of salt-water interface motion: Ground Water, v. 18, no. 4, p. 374-385.
- Merriam, Daniel F., 1963, The geologic history of Kansas: Kansas Geological Survey Bulletin 162, 317 p.
- Merriam, D.F., 1972, Preliminary regional structural contour map of the Stone Corral Formation (Permian) in Kansas: State Geological Survey of Kansas, Oil and Gas Investigations no. 17, Map.
- Moore, Raymond C., 1940, Ground-water resources of Kansas: State Geological Survey of Kansas Bulletin 27, 112 p.
- Muskat, M., 1937, The flow of homogeneous fluids through porous media: McGraw-Hill, New York, 763 p.
- Muskat, M. and Wyckoff, R.D., 1935, A.I.M.E., 114, Pet. Dev. Techn. 144.

- O'Connor, Howard G. (Senior Scientist, Kansas Geological Survey), 1978, personal communication.
- O'Connor, Howard G., Zeller, Doris E., Bayne, Charles K. Jewett, John Mark, and Swineford, Ada, 1968, Permian System, in Zeller, Doris E., ed., The stratigraphic succession in Kansas: Kansas Geological Survey Bulletin 189, p. 43-53.
- Papadopulos, Stavros, Bredehoeft, John D., and Cooper, Hilton H., Jr., 1973, On the analysis of 'slug test' data: Water Resources Research, v. 9, no. 4, p. 1087-1089.
- Schumaker, Robert D., 1966, Regional study of Kansas Permian evaporite formations: Unpublished M.S. thesis, Wichita State University, 87 p.
- Shamir, U. and Dagan, G., 1970, Motion of the sea water interface in a coastal aquifer: Hydraulic Lab., Technion, Haifa.
- Stramel, G.J., 1967, Rattlesnake Creek study: Unpublished study by Wichita Water Department, 31 p.
- Stullken, Lloyd E. and Fader, Stuart W., 1976, Hydrogeologic data from the Great Bend Prairie, south-central Kansas: Kansas Geological Survey Basic Data Series, Ground-Water Release No. 5, 50 p.
- Swineford, Ada, 1955, Petrograph of Upper Permian rocks in south-central Kansas: Kansas Geological Survey Bulletin 111, 179 p.
- Todd, David Keith, 1959, Ground water hydrology: John Wiley and Sons, Inc.: New York, 336 p.
- Toth, J., 1963, A theoretical analysis of groundwater flow in small drainage basins, Journal of Geophysical Research, v. 68, no. 16, p. 4795-4812.
- Turcan, A.N., Jr., 1966, Calculation of water quality from electrical logs: theory and practice: Department of Conservation, Louisiana Geological Survey and Louisiana Department of Public Works, Water Resources Pamphlet No. 19, 23 p.
- Ubal, Don (District Geologist, Oil Field Section, Dodge City, Kansas Department of Health and Environment), 1979, personal communication.
- U.S. Geological Survey, 1973 through 1978 (annual), Water resources data for Kansas, Water Year 1973, 1974, 1975, 1976, 1977, 1978. (annual publication): U.S. Geological Survey Water-Data Reports.
- Verruijt, Arnold, 1980, The rotation of a vertical interface in a porous medium: Water Resources Research, v. 16, no. 1, p. 239-240.
- Whittemore, Donald O. (Associate Scientist, Kansas Geological Survey), 1978, personal communication.

Whittemore, Donald O., 1978b, Factors controlling variations in river water quality in Kansas: Kansas Water Resources Research Institute, 46 p.

Whittemore, Donal O. and Pollock, Livia M., 1979, Determination of salinity sources in water resources of Kansas by minor alkali metal and halide chemistry: Kansas Water Resources Research Institute Contribution No. 208.

Zeller, D.E., ed., 1968, The stratigraphic succession in Kansas: Kansas Geological Survey Bulletin 189, 81 p.

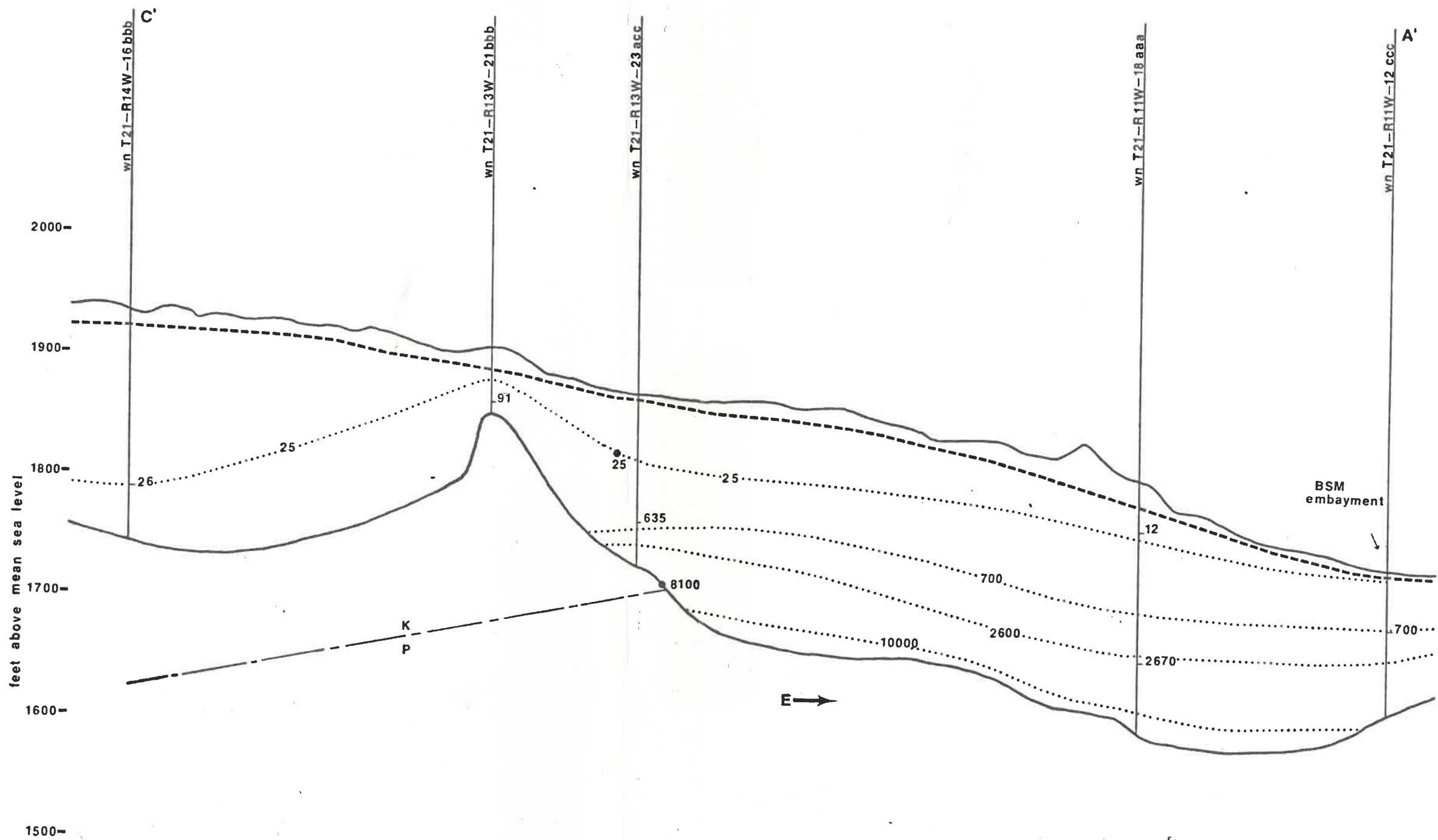


FIGURE 10. CROSS SECTION C'-A', SHOWING THE POSITION OF THE DECEMBER 1973 FREE SURFACE AND THE INFERRED DISTRIBUTION OF CHLORIDE IONS IN THE MAJOR STREAMS AND AQUIFERS.

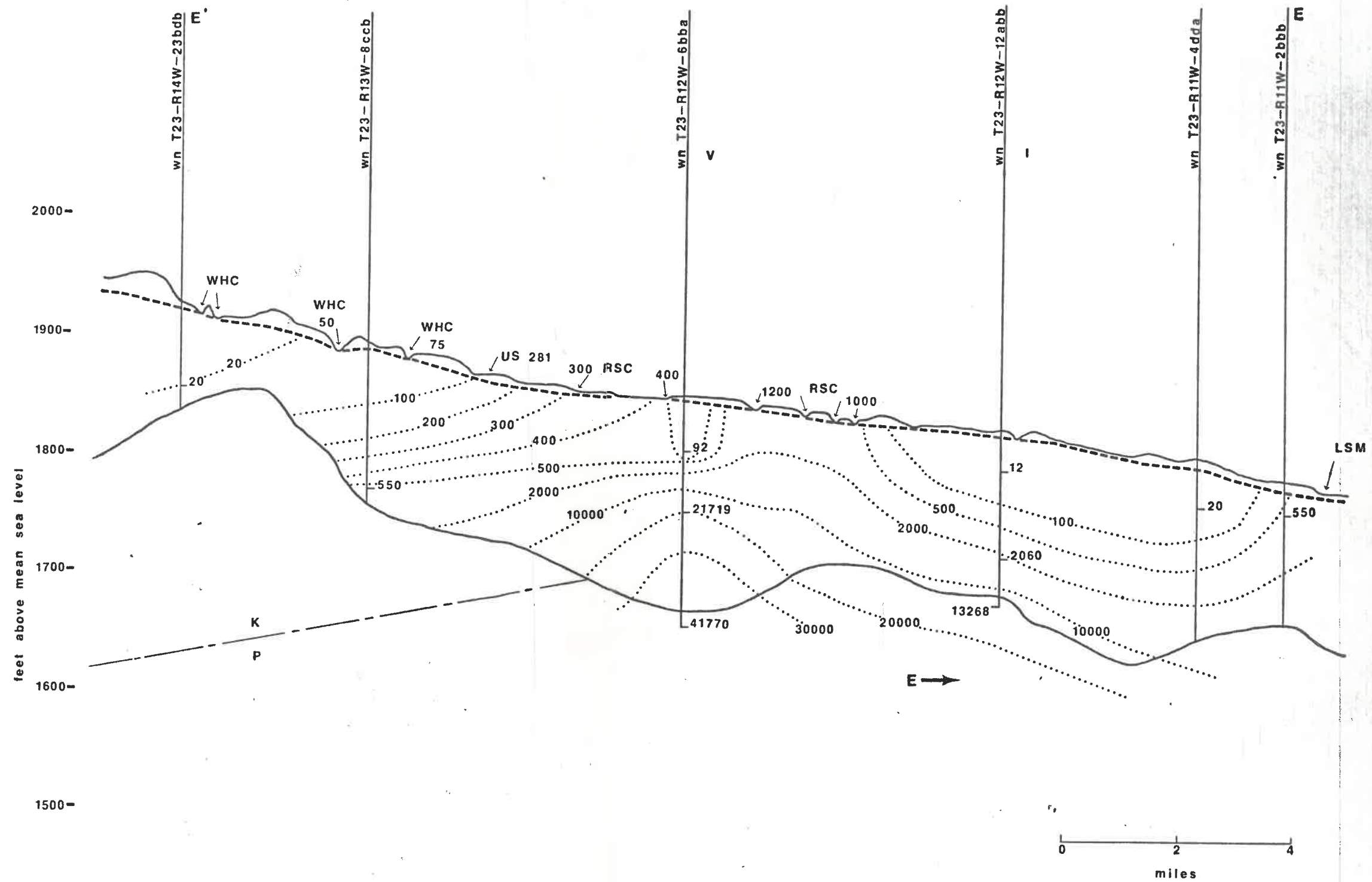


FIGURE 11. CROSS SECTION E'-E, SHOWING THE POSITION OF THE DECEMBER 1973 FREE SURFACE AND THE INFERRED DISTRIBUTION OF CHLORIDE IONS IN THE MAJOR STREAMS AND AQUIFERS.

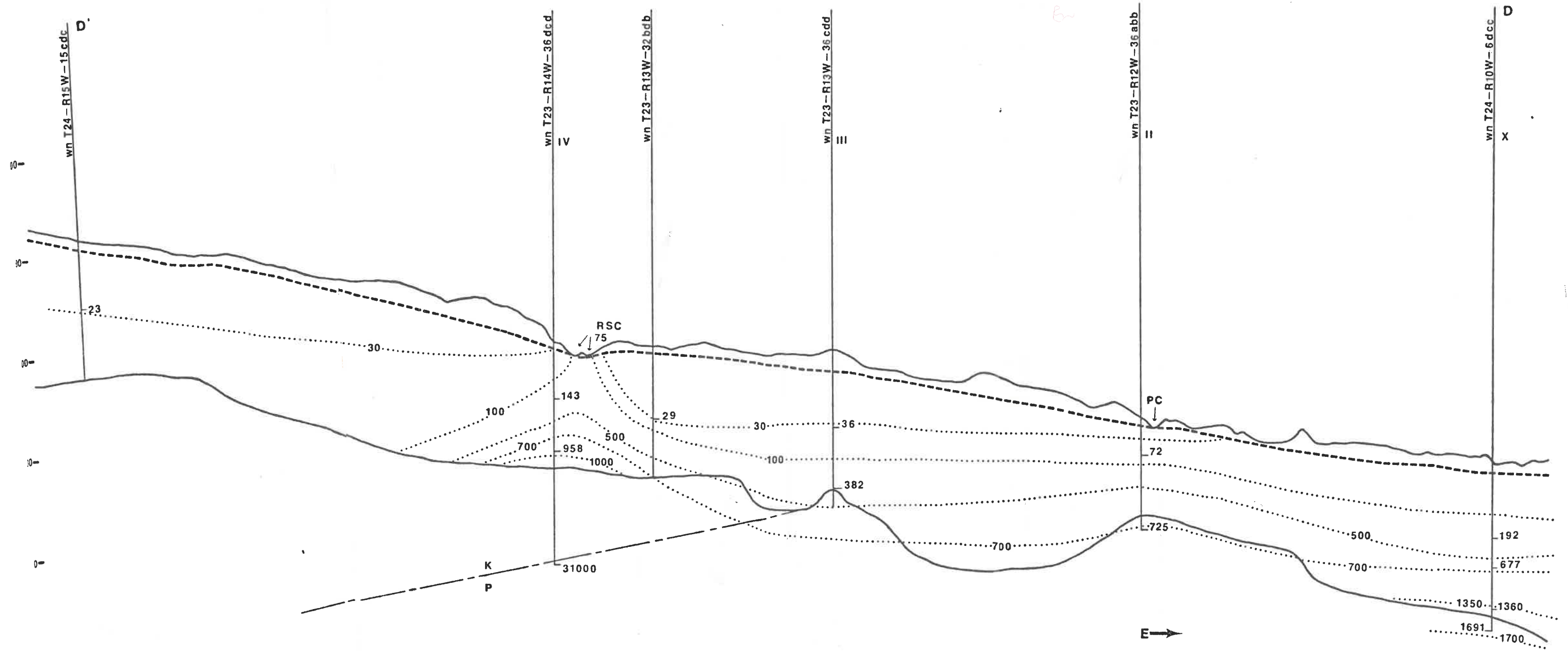


FIGURE 12. CROSS SECTION D'-D, SHOWING THE POSITION OF THE DECEMBER 1973 FREE SURFACE AND THE INFERRED DISTRIBUTION OF CHLORIDE IONS IN THE MAJOR STREAMS AND AQUIFERS.

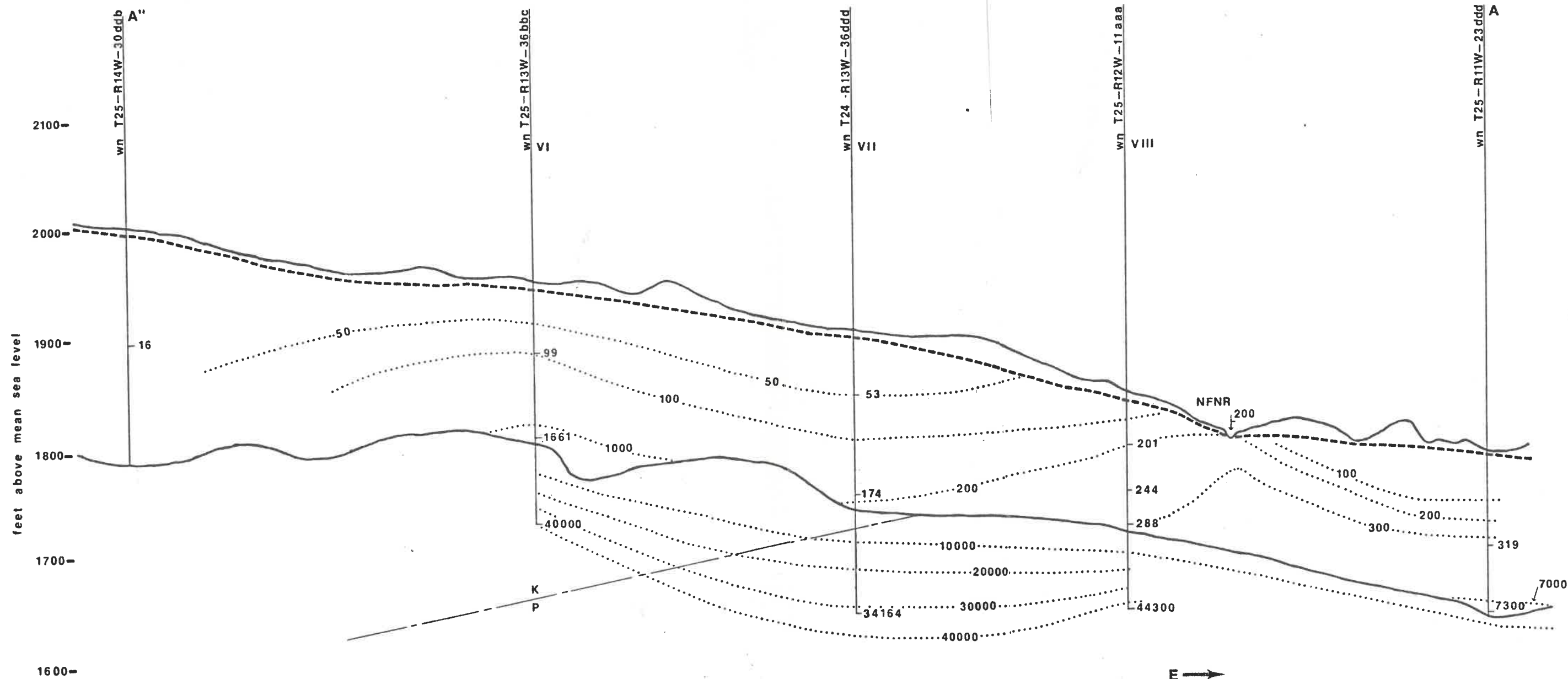


FIGURE 13. CROSS SECTION A''-A, SHOWING THE POSITION OF THE DECEMBER 1973 FREE SURFACE AND THE INFERRED DISTRIBUTION OF CHLORIDE IONS IN THE MAJOR STREAMS AND AQUIFERS.

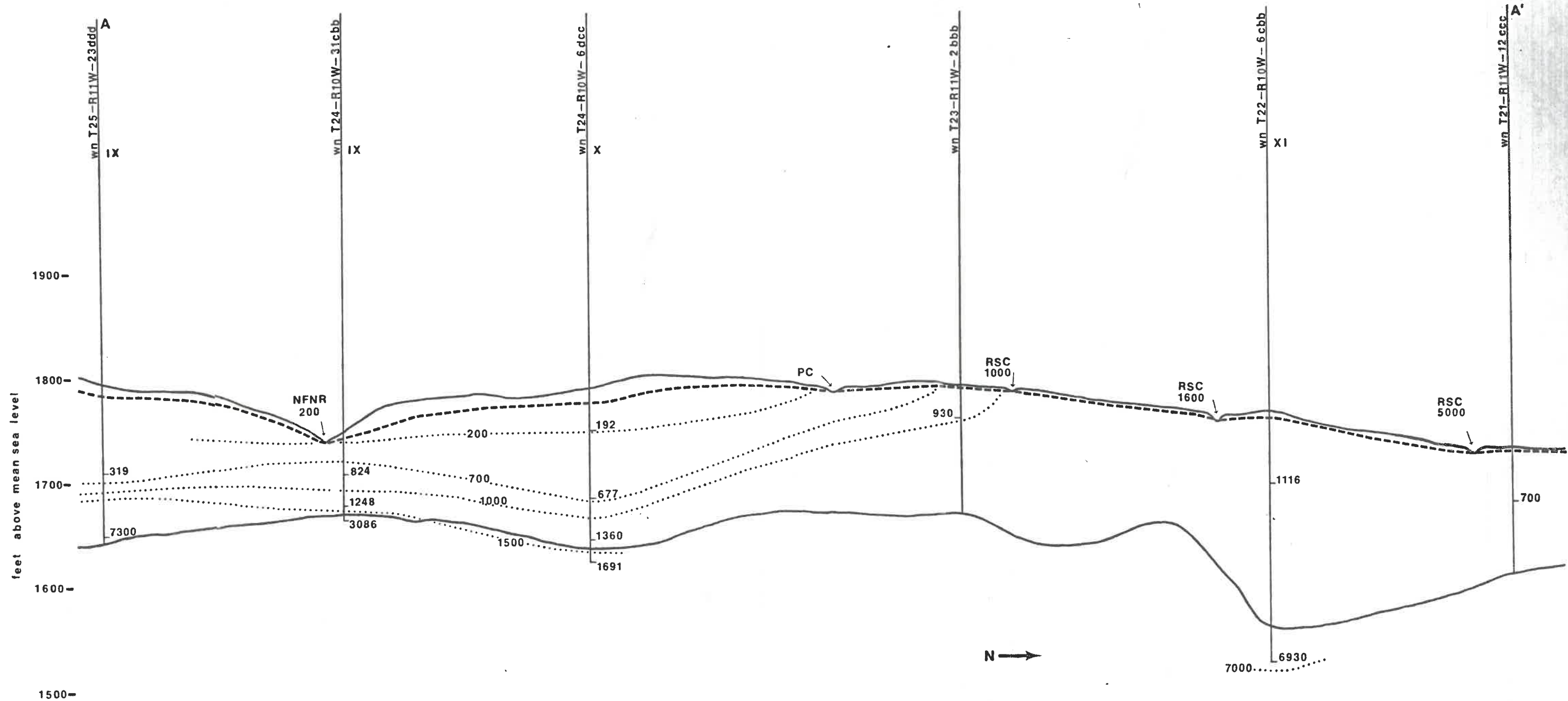


FIGURE 14. CROSS SECTION A-A', SHOWING THE POSITION OF THE DECEMBER 1973 FREE SURFACE AND THE INFERRED DISTRIBUTION OF CHLORIDE IONS IN THE MAJOR STREAMS AND AQUIFERS.

0 2 4  
miles

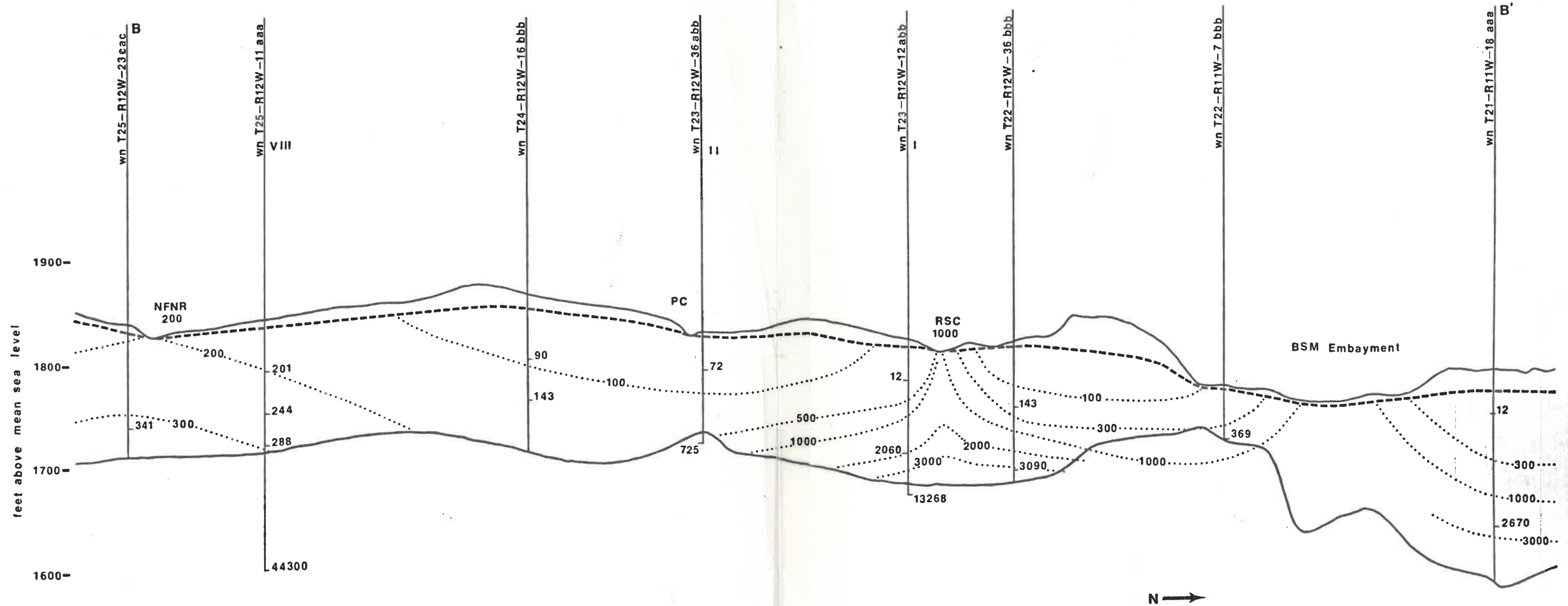


FIGURE 15. CROSS SECTION B-B', SHOWING THE POSITION OF THE DECEMBER 1973 FREE SURFACE AND THE INFERRED DISTRIBUTION OF CHLORIDE IONS IN THE MAJOR STREAMS AND AQUIFERS.

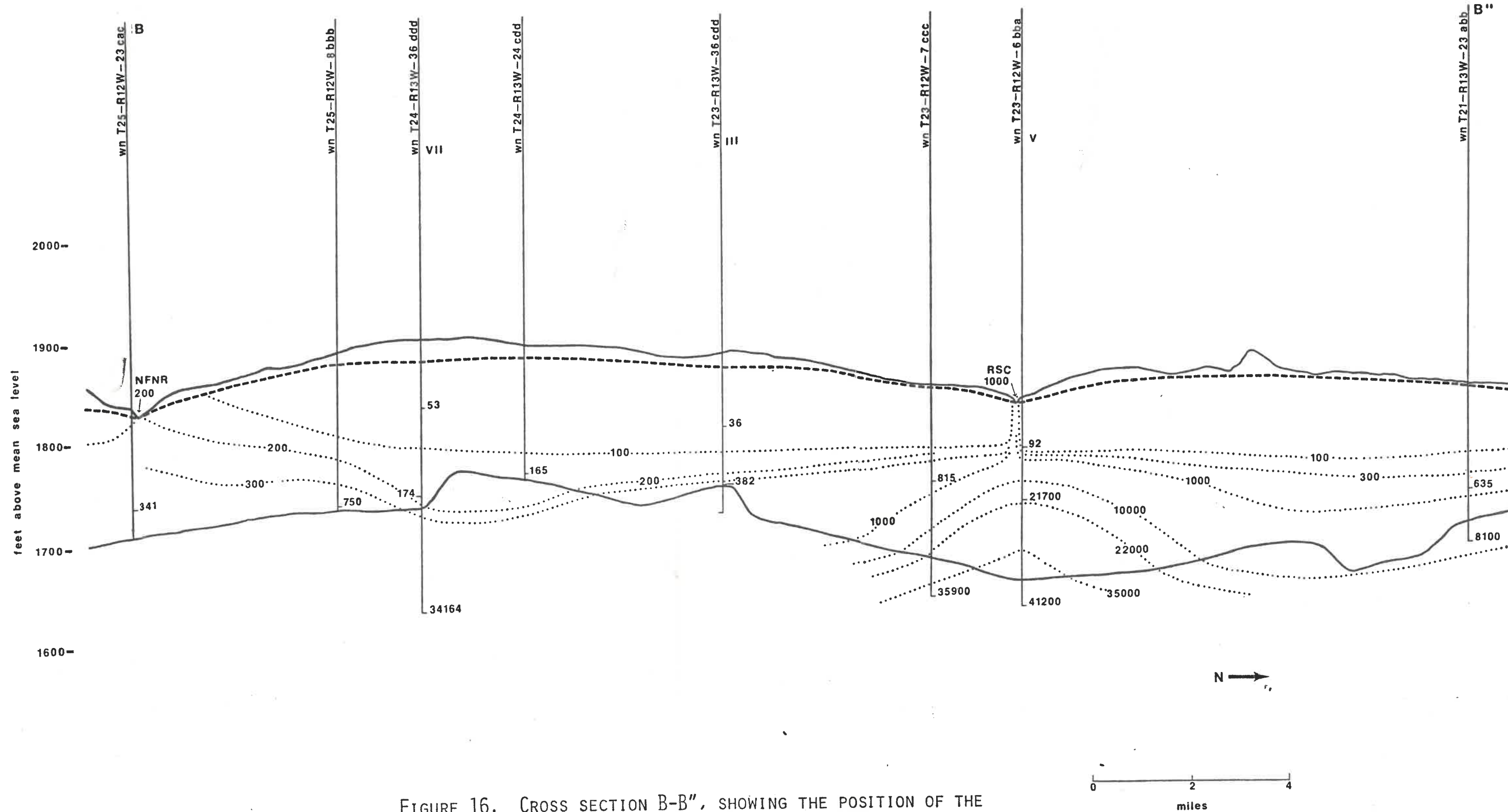


FIGURE 16. CROSS SECTION B-B'', SHOWING THE POSITION OF THE DECEMBER 1973 FREE SURFACE AND THE INFERRED DISTRIBUTION OF CHLORIDE IONS IN THE MAJOR STREAMS AND AQUIFERS.

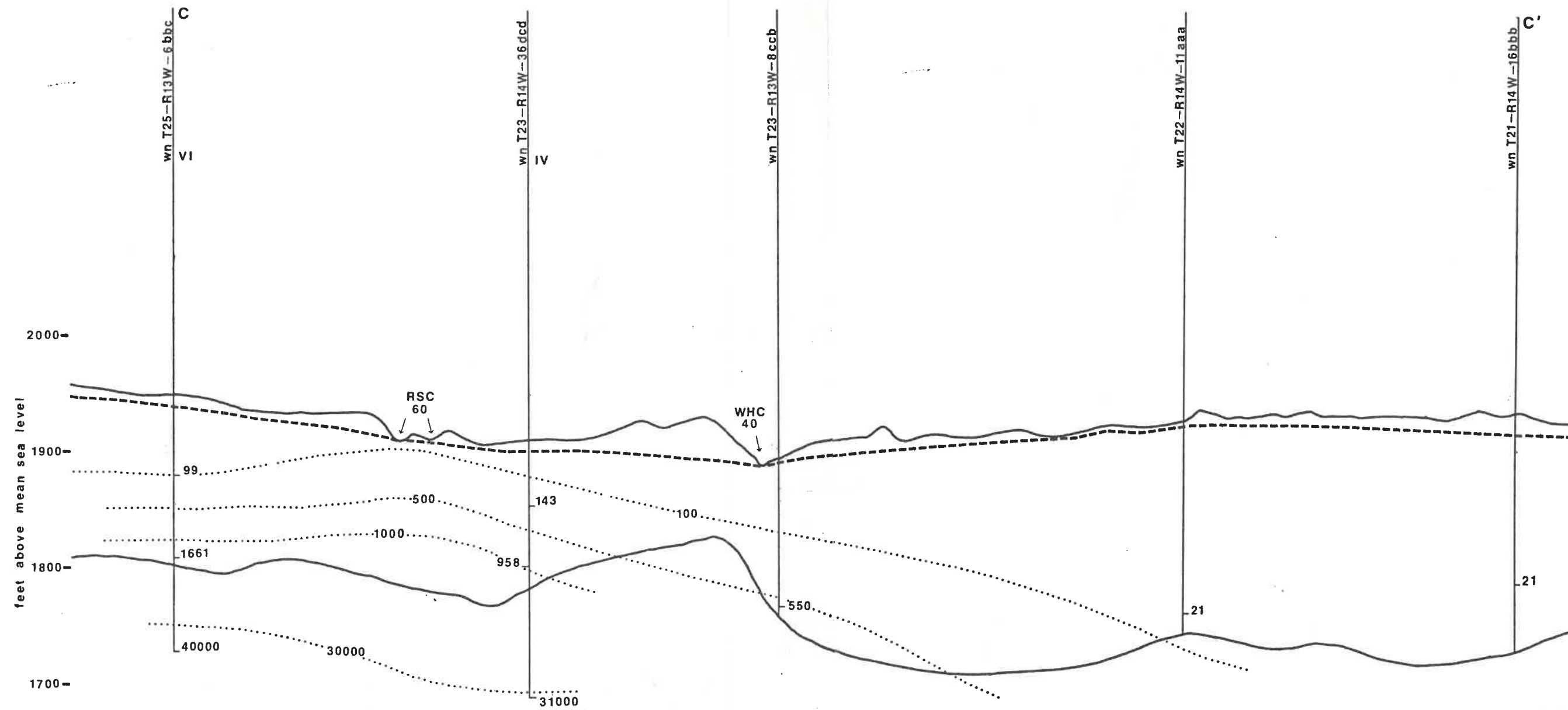


FIGURE 17. CROSS SECTION C-C', SHOWING THE POSITION OF THE DECEMBER 1973 FREE SURFACE AND THE INFERRED DISTRIBUTION OF CHLORIDE IONS IN THE MAJOR STREAMS AND AQUIFERS.

